NOTE TO USERS

DISSERTATION

HYPERTHERMIA INDUCED INTERLEUKIN-12 GENE THERAPY

Submitted by:
Farzan Siddiqui
Department of Environmental and Radiological Health Sciences

In partial fulfillment of the requirements
For the degree of Doctor of Philosophy
Colorado State University
Fort Collins, Colorado
Summer 2005

COLORADO STATE UNIVERSITY

May 13, 2005

WE HEREBY RECOMMEND THAT THE DISSERTATION PREPARED UNDER OUR SUPERVISION BY FARZAN SIDDIQUI ENTITLED HYPERTHERMIA INDUCED INTERLEUKIN-12 GENE THERAPY BE ACCEPTED AS FULFILLING IN PART REQUIREMENTS FOR THE DEGREE OF DOCTOR OF PHILOSOPHY.

Committee on Graduate Work

Mark Dewhirst

Adviser

Susan M Lakue

Co- adviser

Department Chair

ABSTRACT OF DISSERTATION

HYPERTHERMIA INDUCED INTERLEUKIN-12 GENE THERAPY

Cytokine genes are the most widely and extensively studied immunostimulatory agents in cancer gene therapy. In several studies, interleukin-12 (IL-12) was found to be the most effective cytokine in inducing the eradication of experimental tumors, preventing development of metastases and eliciting long-term antitumor immunity. Local and systemic administration of IL-12 protein has been studied in murine models and in Phase I/II human trials. However, IL-12 protein therapy has been limited by dose-dependent toxicity. Local and efficient expression of IL-12 and other cytokine genes in tumors represents an alternative immunotherapeutic approach that may avoid systemic toxicity of recombinant cytokines. To achieve this goal of localizing gene expression, a heat-inducible adenoviral gene therapy vector with feline IL-12 being placed under the control of a heat inducible promoter was developed. The rationale for using this heat shock promoter (hsp70B) is that hyperthermia is most likely to be used as an adjuvant therapy with radiation and chemotherapy in the treatment of cancers. Heating the tumor leads to activation of the *hsp* promoter and subsequent local IL12 production.

In this project the "adenovirus heat shock promoter feline interleukin-12" (AdhspfIL-12) gene construct was studied. *In vitro* studies were done to characterize the construct. Following that a phase I dose escalation trial was conducted in thirteen cats with spontaneously arising soft tissue sarcomas. The cats underwent radiation therapy to a

total dose of 48 Gy in 16 fractions. Four- five days later the gene construct was injected intratumorally. Twenty- four hours post- injection the tumor was heated to a target temperature of 41°C for 60 minutes using a microwave applicator. Cats were treated at increasing dose levels of viral construct. Tumor expression of cytokines IL-12 and IFN- γ was quantitatively determined using real time PCR. The cats were monitored for hematologic and hepatic toxicity. In this trial, it was concluded that it is possible to limit the toxicity of interleukin- 12 using the hyperthermia induced gene- therapy approach.

The anti- angiogenic properties of IL-12 were quantitatively assessed using computerized image analysis in a mouse tumor model. A significant reduction in tumor vasculature was seen in the treated group of mice with limited systemic toxicity.

Farzan Siddiqui
Department of Environmental and
Radiological Health Sciences
Colorado State University
Fort Collins, CO 80523
Summer 2005

ACKNOWLEDGEMENTS

To my parents who were my first teachers in life.

To my exceptional teachers whose dedication, enthusiasm and creativity helped make the acquisition, application and sharing of knowledge more fun than hard work.

I am very grateful to my adviser Dr Robert Ullrich for having accepted me into the Radiation Biology program at CSU and given me the opportunity to work under his tutelage. I admire him for his humility despite his magnificent professional achievements. My acknowledgments are also due to Dr Susan LaRue who helped me with all things big and small during the clinical trial. Dr Mark Dewhirst, another stalwart and giant in the field of radiation biology and hyperthermia research, is also an excellent teacher and patient listener. I would like to thank him for giving me the opportunity of working on this exciting project. I have learnt a lot from him and his methods. Dr Paul Avery was always available for me to throw ideas back and forth with. It was in his lab that I learnt how to do real- time PCR. He possesses an outstanding experimental mind and he helped me out with fresh ideas whenever I was stuck at parts of my projects. I am also very grateful to him for having taken time out of his schedule to read my manuscripts and provide valuable suggestions. Dr Chuan- Yuan Li designed the construct used in this project and was always able to provide it to me whenever needed. All the immunohistochemistry work was done in Dr EJ Ehrhart's lab. I want to thank him for spending time with me teaching me histologic pathology and analyzing the slides.

Apart from my committee members I would also like to thank all those who taught me the various techniques I have used in my project. I had come to CSU without any significant laboratory experience but it was thanks to them that I was able to learn things quickly. Special thanks to my colleagues without whose help these projects would never have been completed on time: Laura Chubb, Brad Charles, Lila Ramaiah and Kinga Krobl. A very special thanks is due to the most helpful and hard- working radiation therapists I have ever seen, Chana Fuller and Frank Conway. They always went out of their way to help me with the clinical trial and were extremely patient with my demands on their time. They also seem to have excellent suggestions whenever faced with a complicated practical problem. Their love and compassion for their patients is an inspiration. Bob Scott heads the bioinstrumentation department and designed and fabricated the equipment used in the mouse hyperthermia study.

Dr Scott Pearson, my office- mate, is our lab in-charge and it was because of him that I never had to wait an extra day for lack of a particular reagent or chemical.

Professionally, there are too many people who helped me with my projects. I have tried to mention by name all those I could remember. I would like to deeply and humbly apologize for any omissions.

A special thanks to Colorado, this has been one of the most fascinating and memorable experiences of my life.

In the end I would like to thank my brother and my wife Rana for all their help and support. Rana has been working in Detroit and we have stayed apart more than we have stayed together during our four years of marriage. Words cannot express the thanks I owe for her selflessness and sacrifices while I pursued my dream.

PREFACE

This dissertation has been arranged so that each chapter covers a different aspect and a different set of experiments all centered around the same theme of hyperthermia induced interleukin-12 gene therapy. Chapter 1 is an introductory chapter forming the background for the other chapters. Chapters 2 and 3 are based on the *in vitro* experiments done to characterize the adenoviral construct used in this project. Chapter 4 deals with the phase I clinical trial conducted in feline soft tissue sarcomas. In chapter 5 the anti- angiogenesis study performed in mice has been described.

This dissertation has been written so that each chapter forms a stand- alone manuscript suitable for submission for publication. This has resulted in a repetition of some of the material in each chapter especially in the introduction and materials and methods sections. This was unavoidable as the basic underlying theme remained the same. However, this has made each section self- contained and complete for publication.

TABLE OF CONTENTS

Chapter 1

HYPERTHERMIA INDUCED INTERLEUKIN-12 GENE- THERAPY

INTRODUCTION

Cancer is the second most common chronic killer disease in the United States. It is estimated that 50% of men and 33% of women will eventually develop some type of cancer over their lifetimes. Effective eradication of established tumors, preventing the development of micrometastasis and metastasis and establishing long- term anti- tumor immunity with a simple gene delivery system are important goals for cancer gene immunotherapy.

Cytokines are a class of molecules known to possess such properties. The cytokines that have been most widely studied are interleukin-12 and interleukin-2.

Interleukin-12 (IL-12) is a 70kDa heterodimeric protein composed of 35kDa and 40kDa subunits. The p35 subunit encodes on human chromosome 3p12-q13.2 and the p40 subunit encodes on human chromosome 5q31-q33. The expression of the two genes is regulated independently of each other.

Interlerleukin-12 is a pro-inflammatory cytokine that has been extensively studied *in vitro* and in pre- clinical and clinical settings[1,2]. Its efficacy has been proven beyond any reasonable doubt. However, its progressive march into the clinics was halted when the recombinant IL-12 protein found to be too toxic[3-5] in mice and humans.

This resulted in a paradigm shift in the approach for IL-12 delivery. Local and efficient expression of IL-12 and other cytokine genes in tumors represented an alternative immunotherapeutic approach that could potentially avoid systemic toxicity of recombinant cytokines[6-10].

Interleukin- 12 can exert anti- tumor activities via T cells [6,8,11-13], NK cells [14-18], or NKT cells [19]. Induction of cytokines, such as IFN-γ [11,20-23] and IFN-inducible protein-l0 [24], has also been implicated as a mechanism of antitumor activity of IL-12.

In addition to its immunostimulatory properties, IL-12 possesses anti- angiogenic effects, thus inhibiting tumor formation and metastases [14,25]. Angiogenesis, the process leading to the formation of new vessels from a preexisting vascular network, is essential for the growth, invasion and metastasis of solid tumors. Tumor microvessel density (MVD), a measure of the intensity of angiogenesis, has been evaluated in several neoplasms and the use of antibodies like anti- CD105, which preferentially reacts with angiogenic tissues, has been proposed to study anti- angiogenesis[26]. Various mechanisms have been postulated to explain the anti-angiogenic action of IL-12 (Figure 1) [14,27-31].

Our approach to interleukin-12 delivery involved placing the gene encoding IL-12 under control of a human heat shock promoter 70B (hsp 70B) and using a replication deficient adenovirus type 5 as the vector for gene transfer. The rationale for this approach were (1) intratumoral delivery of this construct combined with local hyperthermia would allow us to have spatial and temporal control over IL-12 expression (2) hyperthermia is a well-accepted modality employed in cancer therapy.

Studies done in mice using a murine IL-12 construct had proved the efficacy of this approach[32,33]. A further step in the direction of advancing this approach was to use it in an animal clinical trial. For this purpose the construct was modified to have a feline IL-12 gene replace the murine IL-12 gene.

This is the 'Adenovirus heat shock promoter feline interleukin-12' (Ad*hsp*flIL-12) construct being investigated in this dissertation.

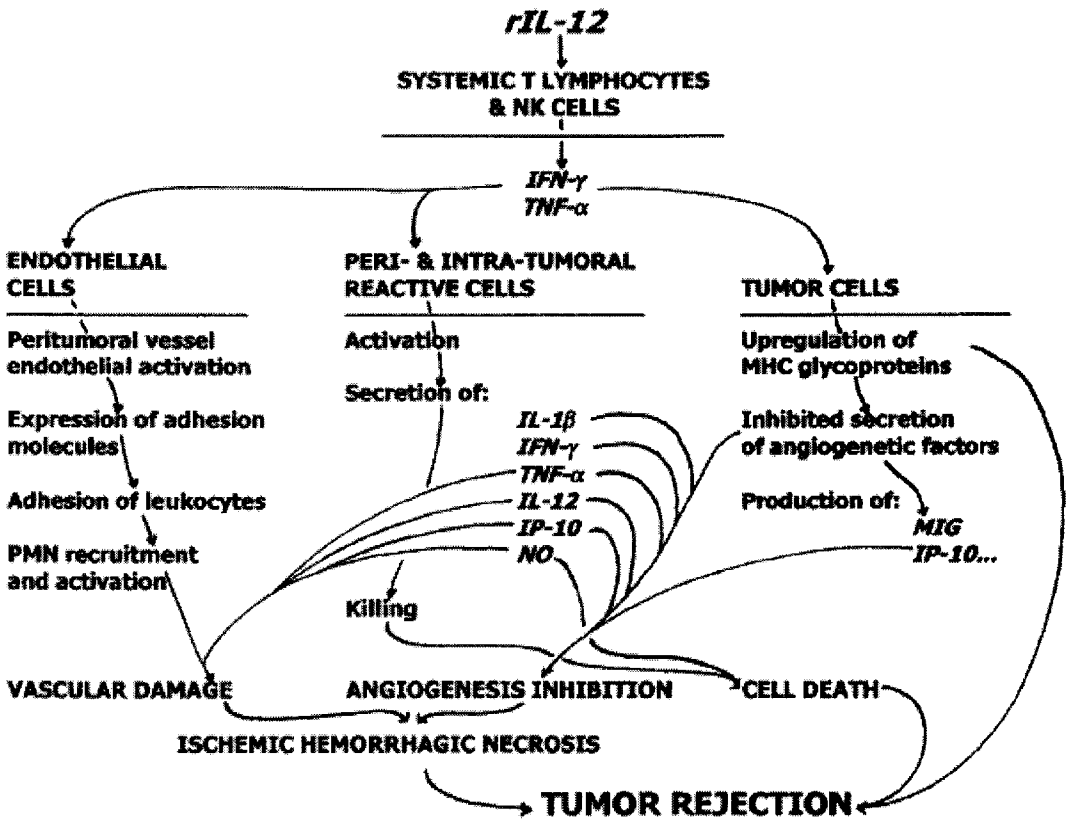

Figure 1- A figure showing the complex network of pathways postulated to be responsible for the anti- angiogenic actions of IL-12[31].

ADENOVIRUSES

Adenoviruses were isolated in 1954 and have been extensively used as gene therapy vectors for treating human diseases, especially cancer. Wild type adenoviruses cause minor human diseases like upper respiratory tract infections, keratoconjunctivitis and gastroenteritis.

Adenoviruses offer unique advantages when used in gene therapy. Early clinical vaccination with wild-type (wt) live adenovirus showed no significant side effects, demonstrating the relative safety of adenoviruses as vectors for *in vivo* gene therapy. Harvey *et al*[34] did an extensive study on the administration of adenoviruses in humans with various comorbid conditions and found adenoviral vectors to be well tolerated up to doses of 10^{11} particle units. About 80% of the general population has been found to have antibodies against adenoviruses including serotype 5[35]. Adenoviruses efficiently infect and transfer genes in a wide variety of cell types including dividing and non-dividing cells. Unlike retroviruses, they do not integrate into the host genome thus reducing risks of virus induced cancers or mutations. Also the main goal of cancer gene therapy is to eliminate rather than rectify malignant cells and there is generally little need for integration. The strong inflammatory and immunological responses to adenoviruses may enhance tumor cell killing in cancer gene therapy. In the laboratory, adenoviruses are easy to manipulate by classical recombinant DNA techniques and can be produced in large quantities in cell culture.

All adenovirus particles are non-enveloped and 60-90nm diameter. They possess an icosahedral symmetry composed of 252 capsomers divided into 240 hexons and 12 pentons at vertices of icosahedron (Figure 2). The adenoviral genome is composed of two

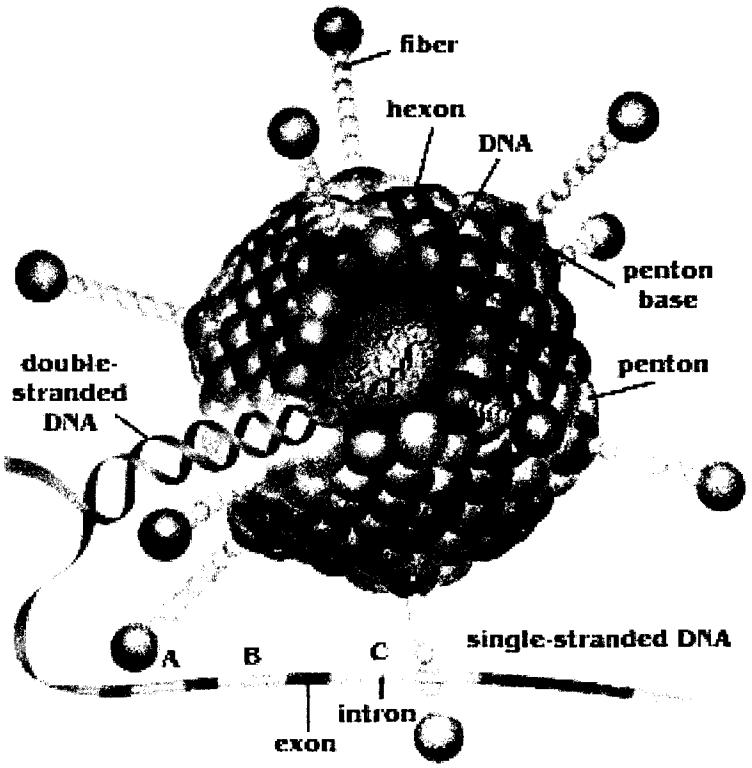

Figure 2- Structure of the adenovirus (Image courtesy http://www.nobelprize.org/).

origins of replication, five early transcription units (E1A, E1B, E2, E3, E4), two 'delayed early' (IVa2 and IX) and late genes (Figure 3). The E1A and E1B proteins are the first viral early proteins to be produced from early region 1 (El) after the viral DNA enters the nucleus. These proteins are essential for viral replication. The late gene products are mainly viral structural proteins such as hexon, penton base and fiber.

There are three types of receptors for adenoviruses on cells- the coxsackievirus group B and adenovirus receptor (CAR), the MHC-I α2 subunit and sialic acid saccharides on glycoproteins. The transfection efficiency of adenoviral vectors has been found to highly dependent on the CAR receptor status in different types of tumors[36]. Viral DNA replication begins approximately 7 hours after infection, after which late proteins expressed from the late regions are synthesized. Viral assembly begins in the cell nucleus at 20 to 24 hours after infection, and after 2 to 3 days the cells lyse and release virus particles.

Adenoviruses can accommodate up to 8 kb of foreign DNA. The removal of various genes from the adenoviral genome to accommodate foreign DNA has led to the development of various "generations" of the virus.

The "first generation adenoviral vectors" have the El and/ or E3 regions deleted. The purpose of the El deletion is to abolish the potential oncogenicity of adenovirus vectors, and to make vector *replication deficient*. As the El proteins are essential for viral replication, the propagation of El-deleted adenovirus vectors requires complement cell lines to provide *in trans* the El protein. Cells lines commonly used for this purpose include HEK 293, 911 and PER.C6. For gene delivery, the deleted El or E3 region is replaced by a transgene driven by a promoter and enhancer elements. A major drawback

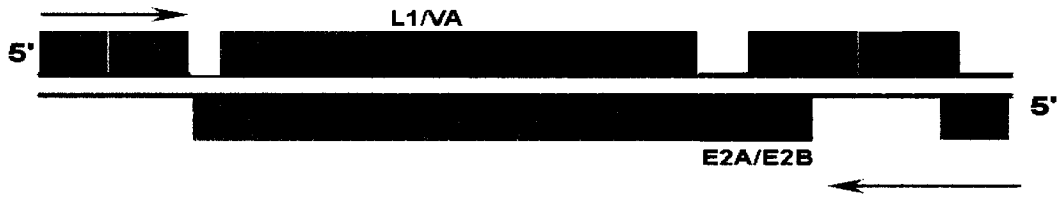

Figure 3a

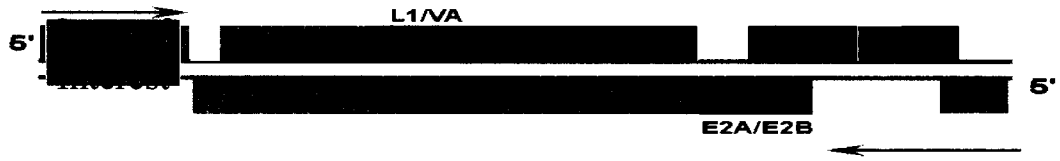

Figre 3b

Figure 3- ADENOVIRAL GENOME (Image courtesy www.fda.gov)
Figure 3a- The adenoviral genome showing the early (E) and late (L) genes.
Figure 3b- First generation adenoviral vector with the gene of interest replacing the E1A region.

of first generation adenoviral vectors is their ability to elicit strong immune responses against the viral vector capsid proteins and infected cells expressing viral antigens. This may, however, be a potential advantage when the infected cells in question are tumor cells.

HEAT SHOCK RESPONSE

The heat shock response is an evolutionarily conserved protective mechanism first described in *Drosophila melanogaster* salivary glands in response to heat[37]. The production of heat shock proteins is also seen in response to various types of cellular stresses including environmental stresses (amino acid analogues, transition heavy metals, inhibitors of energy metabolism), pathophysiological states (fever, oxidant injury, ischemia, aging) and even during normal physiological states like cell division and growth and differentiation[38]. The heat shock proteins function as "molecular chaperones"[39]. In this, they bind to the cellular proteins and prevent their degradation when acted upon by cellular stressors. Heat shock proteins also serve to enhance the immune response by presenting the tumor antigens or microbial antigens to the dendritic cells[40,41].

The human heat shock promoter hsp 70b is a highly inducible promoter and has been employed to control the expression of genes of interest in experimental and clinical settings in several systems[32,33,42-47]. Using this promoter in cancer gene immunotherapy allows the combination of hyperthermia, a well- established modality for cancer therapy, and targeted inducible gene- expression. The HSP70 promoter is tightly regulated but

highly inducible following heat shock. Temperatures needed to induce this response are in a clinically relevant temperature range (eg between 39^0C and 42^0C) and repeated heat treatments can maintain elevated levels of gene expression for extended periods of time[44].

REAL- TIME PCR

Real- time PCR is a relatively recent development for quantitative estimation of DNA or cDNA in samples. It has found applications in viral quantitation, quantitation of gene expression, array verification, drug therapy efficacy, DNA damage measurement, pathogen detection and genotyping. Some of the currently available instrumentation is shown in Table 1.

There were two important findings that led to the development of this technique (1) the finding that *Taq* polymerase possesses 5' →3'-exonuclease activity (2) construction of dual-labeled oligonucleotide probes, which emit a fluorescence signal only on cleavage, based on the fluorescence resonance energy transfer (FRET) principle. FRET is the non-radiative transfer of photon energy from an excited fluorophore (the donor) to another fluorophore (the acceptor) when both are located within close proximity (1-10 nm). The criteria that need to be satisfied are (1) donor and acceptor molecules must be in close proximity (typically 1-10nm) (2) absorption spectrum of the acceptor must overlap fluorescence emission spectrum of the donor (3) donor and acceptor transition dipole orientations must be approximately parallel.

Real time PCR instruments			
Company	PCR system	Sample format	Max. sample number
Applied Biosystems	ABI Prism 7700	Microplate	96
		Tubes	
	ABI Prism 7000/ 7300/7500	Microplate	96
	GeneAmp 5700	Microplate	96
	ABI Prism 7900	Tubes	96, 384
		Microplate	
Bio-Rad	iCycler iQ	Microplate	96
		Tubes	96
Cepheid	Smart Cycler	Tubes	16
Corbett Research	Rotor Gene	Tubes	32
		Strip tubes	72
Roche Molecular Biochemicals	LightCycler	Capillaries	32
Stratagene	Mx4000 Multiplex	Microplate	96

Table 1- Some currently available instrumentation for real- time PCR. Based on a table in Giulietti *et al*[48].

Dyes that are commonly used as reporters are FAM, TET, JOE and HEX. Quencher dyes are TAMRA and DABCYL.

The TaqMan detection works as follows (Figure 4) (courtesy Applied Biosystems).

"Step Process

1. An oligonucleotide probe is constructed containing a reporter fluorescent dye on the 5′ end and a quencher dye on the 3′ end. While the probe is intact, the proximity of the quencher dye greatly reduces the fluorescence emitted by the reporter dye by fluorescence resonance energy transfer (FRET) through space.

2. If the target sequence is present, the probe anneals downstream from one of the primer sites and is cleaved by the 5′ nuclease activity of Taq DNA polymerase as this primer is extended.

3. This cleavage of the probe:

- Separates the reporter dye from the quencher dye, increasing the reporter dye signal.
- Removes the probe from the target strand, allowing primer extension to continue to the end of the template strand. Thus, inclusion of the probe does not inhibit the overall PCR process.

4. Additional reporter dye molecules are cleaved from their respective probes with each cycle, resulting in an increase in fluorescence intensity proportional to the amount of amplicon produced."

More details are available at http://docs.appliedbiosystems.com/pebiodocs/00105622.pdf.

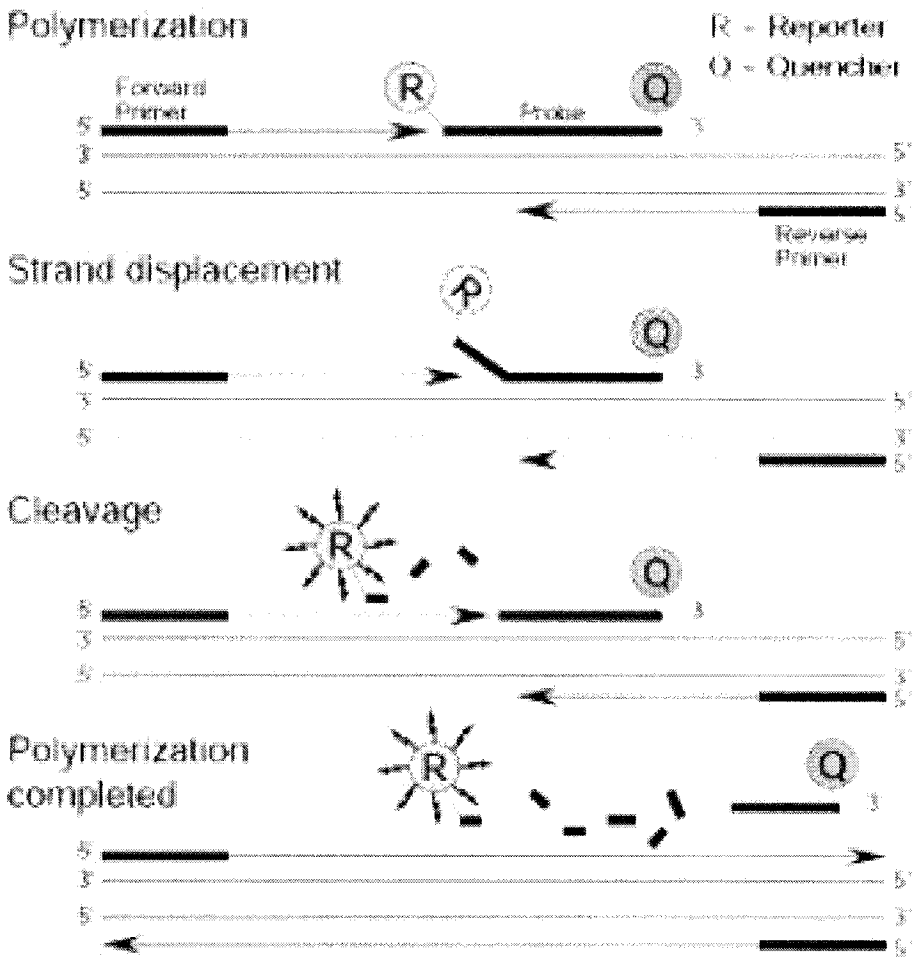

Figure 4- The TaqMan detection chemistry. R- reported dye. Q- quencher dye. Proximity of the reporter dye to the quencher prevents the fluorescence from reaching the detector. When cleaved, the reported dye moves away for the quencher. Its fluorescence cannot be absorbed by the quencher and is then detected by the detector in the instrument. (Image courtesy Applied Biosystems).

An amplification curve for real- time PCR has the following phases (Figure 5);

Exponential: Exact doubling of product is accumulating at every cycle (assuming 100% reaction efficiency). The reaction is very specific and precise.

Linear (High Variability): The reaction components are being consumed, the reaction is slowing, and products are starting to degrade.

Plateau (End-Point: Gel detection for traditional methods): The reaction has stopped, no more products are being made and if left long enough, the PCR products will begin to degrade.

The graph obtained is converted to a log- linear scale and a threshold set manually in the middle one- third of the exponential phase of the curve. The software then automatically outputs the cycle threshold (Ct) value for each curve on the plot. These values can be exported to a spreadsheet program such as Microsoft Excel for further calculations.

Primers and probes

Sequence for primers and probes can usually be obtained from literature. The advantage is that, in most cases, the sequences and PCR conditions have been validated. This saves on primer and probe development costs and time.

If sequences are not available from literature they can easily be designed using primer and probe design software. An example of one such program is the Primer Express® software. Details are available online at http://www.appliedbiosystems.com/support/tutorials/pdf/taqman_mgb_primersprobes_for_gene_expression.pdf.

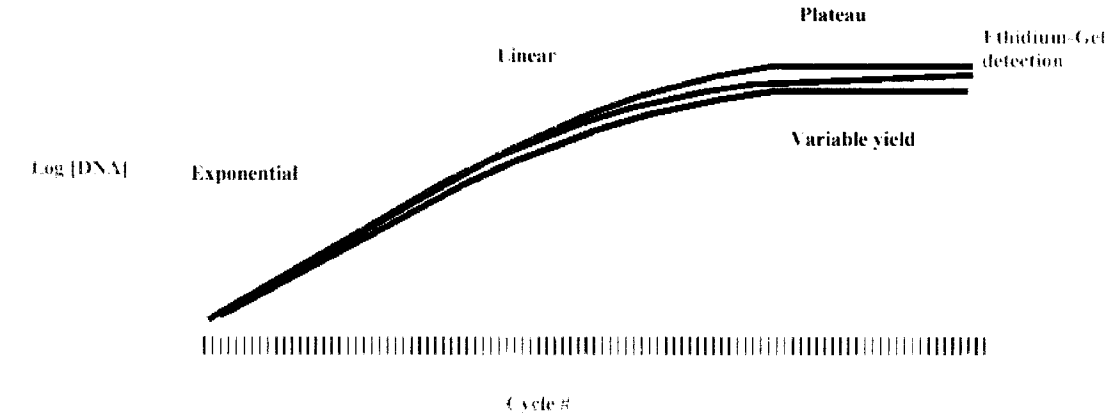

Figure 5a

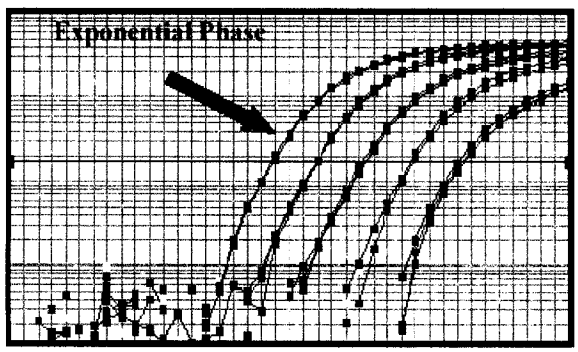

Figure 5b

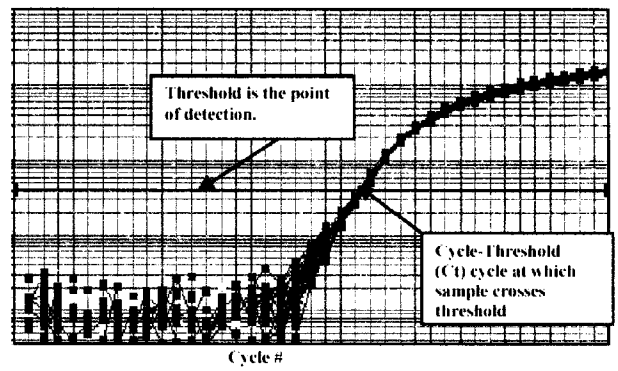

Figure 5c

Figure 5- PCR AMPLIFICATION CURVE
Figure 5a- Phases of the curve.
Figure 5b- The exponential phase is the only one used for analysis.
Figure5c- A threshold line is set at the middle one- third of the exponential line and the cycle threshold (Ct) value is the cycle number (x- axis) on which the curve crosses the threshold. This value is calculated automatically by the software and presented as such.

Once the sequence has been determined, the reporter dye (eg. FAM) and quencher dye (eg. TAMRA) can be decided upon and ordered commercially. For this project all primers and probes were obtained from MWG Biotech, High Point, NC.

The "Relative Quantification" method

Arithmetic formulas are used to calculate relative expression levels, compared with a calibrator, which can be, for instance, a control (non-treated) sample[49]. The amount of target, normalized to an endogenous housekeeping gene and relative to the calibrator, is then given by $2^{-\Delta\Delta Ct}$, where $\Delta\Delta Ct = \Delta Ct$ (sample)- ΔCt (calibrator), ΔCt is the Ct of the target gene subtracted from the Ct of the housekeeping gene. The equation thus represents the normalized expression of the target gene in the unknown sample, relative to the normalized expression of the calibrator sample. The advantages of this method are that no standards have to be constructed and that 96 wells can be fully applied for unknown samples, saving time and money. The disadvantage is that efficiencies of amplification of housekeeping and target gene have to be similar to obtain reliable results.

Efficiency of Amplification

Various methods have been described to assess the amplification efficiencies for the primer and probe sequences and PCR protocol being used[49,50]. In this procedure the target cDNA is serially diluted and real time PCR performed (Figure 6). Cycle threshold values for the serially diluted samples are plotted on a graph with the log dilution on the X- axis and cycle threshold values on the Y- axis. The slope of the line is used to obtain the

efficiency of PCR amplification using the formula- Efficiency = $10^{(-1/slope)}$-1 (Figure 6). For 100% efficiency the ideal slope is -3.3213. Another method is to do pairwise comparisons between the gene of interest and the housekeeping gene. The differences in cycle threshold values are plotted and the slope of the line obtained. A slope of zero signifies equal amplification efficiencies for both genes (Figure 7).

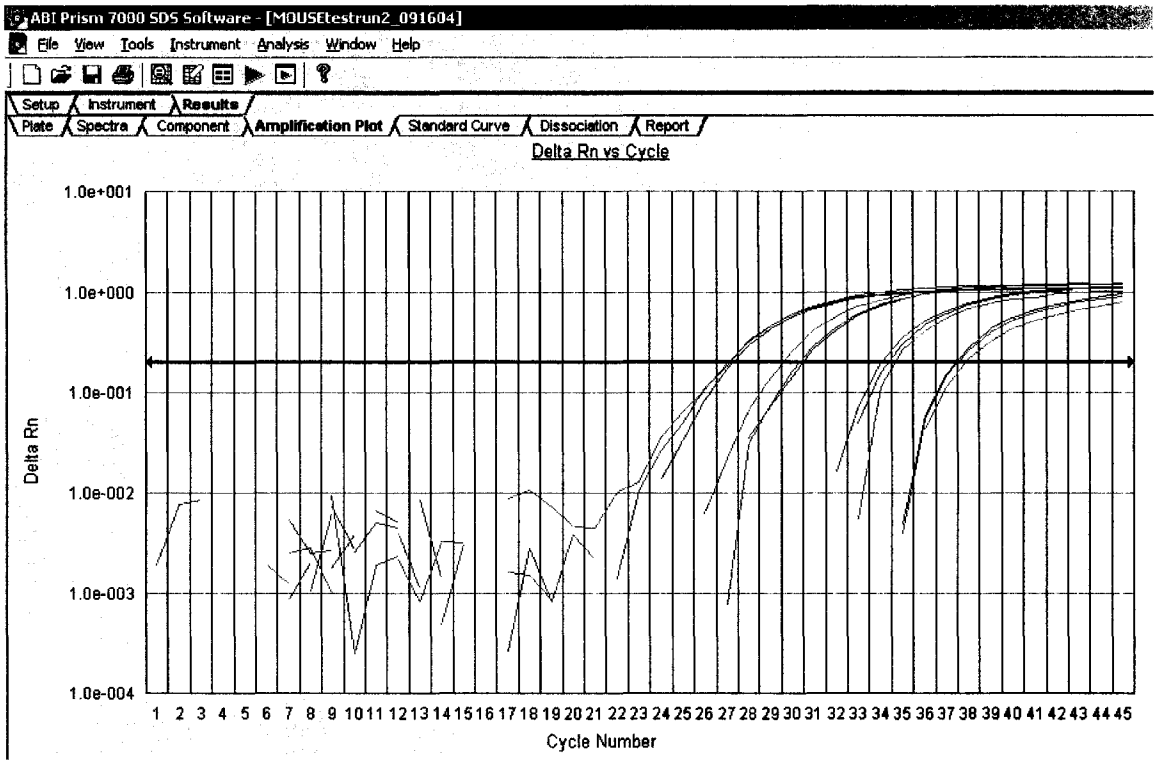

Figure 6- EXAMPLE OF A PCR RUN TO ASSESS AMPLIFICATION EFFICIENCY Serially diluted samples were run in triplicate and the cycle threshold values obtained were used to calculate amplification efficiency.

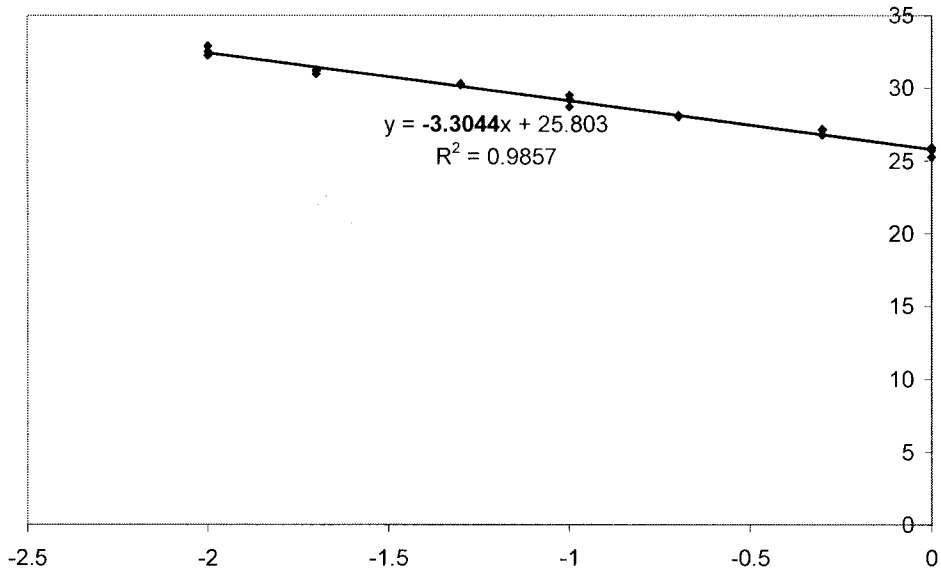

Figure 7a

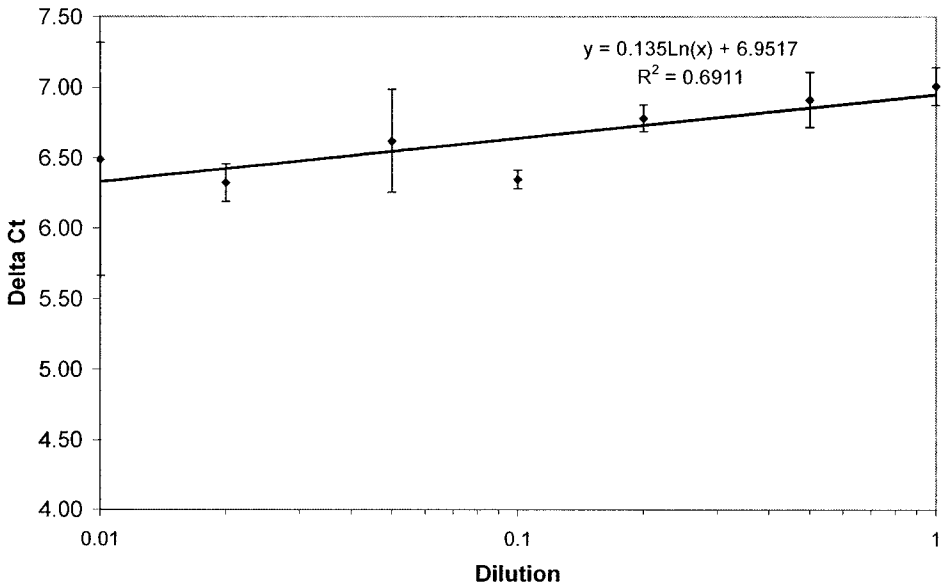

Figure 7b

Figure 7- REAL- TIME PCR AMPLIFICATION EFFICIENCY
Figure 7a- The slope obtained for the gene of interest is -3.3044, suggesting almost 100% efficiency.
Figure 7b- The slope of the line for difference in Ct values is close to zero hence this pair can be used for quantification by the $2^{-\Delta\Delta Ct}$ method.

THE TUMOR MODEL

Feline soft tissue sarcomas are a unique clinical entity. They have been found to arise at injection sites in cats after vaccination[51,52]. These spontaneously arising soft tissue sarcomas provided us with an excellent model to study the construct in a clinical trial. Client- owned cats presenting for treatment to the Colorado State University (CSU) and North Carolina State University (NCSU) Veterinary Teaching Hospitals were recruited into the trial. A phase I dose- escalation trial was conducted to assess the maximum tolerated dose of the virus plaque forming units (pfu). The trial was designed as per guidelines suggested by Stewart *et al*[35].

The distinct advantage of using this spontaneously arising tumor model is that it closely mimics solid tumors in humans, unlike the more artificial tumor microenvironment in transplanted tumors in mice.

THE STUDIES

In vitro studies on the construct were done prior to its use in the trial. Crandell Feline Kidney (CrFK) cells are fibroblast- like cells that grow attached to the tissue- culture plates. These cells were infected with Ad*hsp*fIL-12 and experiments were done to assess the transfection efficiency, response to being heated at various temperatures and effect of multiplicity of infection.

An unexpected finding was the induction of the *hsp* even in cells that had not been heated. Further investigation into this phenomenon led to the conclusion that cellular nutritional deficiency could also lead to *hsp* induction. Results and implications of these findings are discussed in chapters 2 and 3.

Chapter 4 deals with the clinical trial. A total of 13 cats were treated between the two institutes. Eight cats received treatment at CSU and five at NCSU. Based on the results of the study we were able to establish the maximally tolerated safe dose.

Anti- angiogenic properties of IL-12 were studied in a mouse tumor model. Originally we had planned this as an end- point in the clinical trial. However, it was not always possible to acquire satisfactory tumor tissue samples for this study from the cats. Hence, the study was carried- out in mice (Chapter 5). 4T1 tumors were grown in mice and then treated with Ad*hsp*mIL-12 + hyperthermia. Differences in vasculature were quantitatively assessed using a computerized image analysis system (CIAS). A significant reduction in tumor vasculature was seen in the treated group with no evidence of systemic toxicity.

CONCLUSIONS

The results of these studies and experiments support the conclusion that interleukin-12 can be safely delivered intratumorally using the hyperthermia- induced gene- therapy approach with acceptable systemic toxicity. The heat shock promoter, while being highly inducible, allows sufficient control over IL-12 expression.

REFERENCES

1 Colombo MP, Trinchieri G. Interleukin-12 in anti-tumor immunity and immunotherapy. *Cytokine Growth Factor Rev* 2002; **13:** 155-168.

2 Golab J, Zagozdzon R. Antitumor effects of interleukin-12 in pre-clinical and early clinical studies (Review). *Int J Mol Med* 1999; **3:** 537-544.

3 Car B *et al.* Role of interferon-gamma in interleukin 12-induced pathology in mice. *Am J Pathol* 1995; **147:** 1693-1707.

4 Car BD, Eng VM, Lipman JM, Anderson TD. The toxicology of interleukin-12: a review. *Toxicol Pathol* 1999; **27:** 58-63.

5 Atkins MB *et al.* Phase I evaluation of intravenous recombinant human interleukin 12 in patients with advanced malignancies. *Clin Cancer Res* 1997; **3:** 409-417.

6 Saffran DC *et al.* Immunotherapy of established tumors in mice by intratumoral injection of interleukin-2 plasmid DNA: induction of CD8+ T-cell immunity. *Cancer Gene Ther* 1998; **5:** 321-330.

7 Rakhmilevich AL *et al.* Cytokine gene therapy of cancer using gene gun technology: superior antitumor activity of interleukin-12. *Hum Gene Ther* 1997; **8:** 1303-1311.

8 Rakhmilevich AL *et al.* Gene gun-mediated skin transfection with interleukin 12 gene results in regression of established primary and metastatic murine tumors. *Proc Natl Acad Sci U S A* 1996; **93:** 6291-6296.

9 Shi F *et al.* Intratumoral injection of interleukin-12 plasmid DNA, either naked or in complex with cationic lipid, results in similar tumor regression in a murine model. *Mol Cancer Ther* 2002; **1:** 949-957.

10 Colombo MP *et al.* Amount of interleukin 12 available at the tumor site is critical for tumor regression. *Cancer Res* 1996; **56:** 2531-2534.

11 Nastala CL *et al.* Recombinant IL-12 administration induces tumor regression in association with IFN-gamma production. *J Immunol* 1994; **153:** 1697-1706.

12 Fernandez NC *et al.* High frequency of specific CD8+ T cells in the tumor and blood is associated with efficient local IL-12 gene therapy of cancer. *J Immunol* 1999; **162:** 609-617.

13 Lode HN *et al.* Gene therapy with a single chain interleukin 12 fusion protein induces T cell-dependent protective immunity in a syngeneic model of murine neuroblastoma. *Proc Natl Acad Sci U S A* 1998; **95:** 2475-2480.

14 Yao L *et al.* Contribution of natural killer cells to inhibition of angiogenesis by interleukin-12. *Blood* 1999; **93:** 1612-1621.

15 Pham-Nguyen KB *et al.* Role of NK and T cells in IL-12-induced anti-tumor response against hepatic colon carcinoma. *Int J Cancer* 1999; **81:** 813-819.

16 Kodama T *et al.* Perforin-dependent NK cell cytotoxicity is sufficient for anti-metastatic effect of IL-12. *Eur J Immunol* 1999; **29:** 1390-1396.

17 Watanabe M *et al.* Intradermal delivery of IL-12 naked DNA induces systemic NK cell activation and Th1 response in vivo that is independent of endogenous IL-12 production. *J Immunol* 1999; **163:** 1943-1950.

18 Rakhmilevich AL *et al.* Interleukin-12 gene therapy of a weakly immunogenic mouse mammary carcinoma results in reduction of spontaneous lung metastases via a T-cell-independent mechanism. *Cancer Gene Ther* 2000; **7:** 826-838.

19 Cui J *et al.* Requirement for Valpha14 NKT cells in IL-12-mediated rejection of tumors. *Science* 1997; **278:** 1623-1626.

20 Brunda MJ *et al.* Role of interferon-gamma in mediating the antitumor efficacy of interleukin-12. *J Immunother Emphasis Tumor Immunol* 1995; **17:** 71-77.

21 Manetti R *et al.* Interleukin 12 induces stable priming for interferon gamma (IFN-gamma) production during differentiation of human T helper (Th) cells and transient IFN-gamma production in established Th2 cell clones. *J Exp Med* 1994; **179:** 1273-1283.

22 Gately MK *et al.* Administration of recombinant IL-12 to normal mice enhances cytolytic lymphocyte activity and induces production of IFN-gamma in vivo. *Int Immunol* 1994; **6:** 157-167.

23 Tannenbaum CS *et al.* Cytokine and chemokine expression in tumors of mice receiving systemic therapy with IL-12. *J Immunol* 1996; **156:** 693-699.

24 Tannenbaum CS *et al.* The CXC chemokines IP-10 and Mig are necessary for IL-12-mediated regression of the mouse RENCA tumor. *J Immunol* 1998; **161:** 927-932.

25 Voest EE *et al.* Inhibition of angiogenesis in vivo by interleukin 12. *J Natl Cancer Inst* 1995; **87:** 581-586.

26 Kumar S *et al.* Breast carcinoma: vascular density determined using CD105 antibody correlates with tumor prognosis. *Cancer Res* 1999; **59:** 856-861.

27 Strasly M *et al.* IL-12 inhibition of endothelial cell functions and angiogenesis depends on lymphocyte-endothelial cell cross-talk. *J Immunol* 2001; **166:** 3890-3899.

28 Coughlin CM *et al.* Interleukin-12 and interleukin-18 synergistically induce murine tumor regression which involves inhibition of angiogenesis. *J Clin Invest* 1998; **101:** 1441-1452.

29 Gee MS *et al.* Hypoxia-mediated apoptosis from angiogenesis inhibition underlies tumor control by recombinant interleukin 12. *Cancer Res* 1999; **59:** 4882-4889.

30 Duda DG *et al.* Direct in vitro evidence and in vivo analysis of the antiangiogenesis effects of interleukin 12. *Cancer Res* 2000; **60:** 1111-1116.

31 Cavallo F *et al.* Immune events associated with the cure of established tumors and spontaneous metastases by local and systemic interleukin 12. *Cancer Res* 1999; **59:** 414-421.

32 Huang Q *et al.* Heat-induced gene expression as a novel targeted cancer gene therapy strategy. *Cancer Res* 2000; **60:** 3435-3439.

33 Lohr F *et al.* Enhancement of radiotherapy by hyperthermia-regulated gene therapy. *Int J Radiat Oncol Biol Phys* 2000; **48:** 1513-1518.

34 Harvey BG *et al.* Safety of local delivery of low- and intermediate-dose adenovirus gene transfer vectors to individuals with a spectrum of morbid conditions. *Hum Gene Ther* 2002; **13:** 15-63.

35 Stewart AK *et al.* A phase I study of adenovirus mediated gene transfer of interleukin 2 cDNA into metastatic breast cancer or melanoma. *Hum Gene Ther* 1997; **8:** 1403-1414.

36 Gu W *et al.* High-level expression of the coxsackievirus and adenovirus receptor messenger RNA in osteosarcoma, Ewing's sarcoma, and benign neurogenic tumors among musculoskeletal tumors. *Clin Cancer Res* 2004; **10:** 3831-3838.

37 Ritossa F. Discovery of the heat shock response. *Cell Stress Chaperones* 1996; **1:** 97-98.

38 Morimoto RI, Tissiáeres A, Georgopoulos C. *The Biology of heat shock proteins and molecular chaperones*. Cold Spring Harbor Laboratory Press: Plainview , N.Y., 1994.

39 Hightower LE. Heat shock, stress proteins, chaperones, and proteotoxicity. *Cell* 1991; **66:** 191-197.

40 Li Z, Menoret A, Srivastava P. Roles of heat-shock proteins in antigen presentation and cross-presentation. *Curr Opin Immunol* 2002; **14:** 45-51.

41 Srivastava P. Interaction of heat shock proteins with peptides and antigen presenting cells: chaperoning of the innate and adaptive immune responses. *Annu Rev Immunol* 2002; **20:** 395-425.

42 Blackburn RV, Galoforo SS, Corry PM, Lee YJ. Adenoviral-mediated transfer of a heat-inducible double suicide gene into prostate carcinoma cells. *Cancer Res* 1998; **58:** 1358-1362.

43 Braiden V *et al.* Eradication of breast cancer xenografts by hyperthermic suicide gene therapy under the control of the heat shock protein promoter. *Hum Gene Ther* 2000; **11:** 2453-2463.

44 Borrelli MJ *et al.* Heat-activated transgene expression from adenovirus vectors infected into human prostate cancer cells. *Cancer Res* 2001; **61:** 1113-1121.

45 Lee YJ *et al.* Replicating adenoviral vector-mediated transfer of a heat-inducible double suicide gene for gene therapy. *Cancer Gene Ther* 2001; **8:** 397-404.

46 Lohr F *et al.* Systemic vector leakage and transgene expression by intratumorally injected recombinant adenovirus vectors. *Clin Cancer Res* 2001; **7:** 3625-3628.

47 Li GC *et al.* Adenovirus-mediated heat-activated antisense Ku70 expression radiosensitizes tumor cells in vitro and in vivo. *Cancer Res* 2003; **63:** 3268-3274.

48 Giulietti A *et al.* An overview of real-time quantitative PCR: applications to quantify cytokine gene expression. *Methods* 2001; **25:** 386-401.

49 Livak KJ, Schmittgen TD. Analysis of relative gene expression data using real-time quantitative PCR and the 2(-Delta Delta C(T)) Method. *Methods* 2001; **25:** 402-408.

50 Pfaffl MW. A new mathematical model for relative quantification in real-time RT-PCR. *Nucleic Acids Res* 2001; **29:** e45.

51 Hendrick MJ, Goldschmidt MH. Do injection site reactions induce fibrosarcomas in cats? *J Am Vet Med Assoc* 1991; **199:** 968.

52 Hauck M. Feline injection site sarcomas. *Vet Clin North Am Small Anim Pract* 2003; **33:** 553-557, vii.

Chapter 2

CHARACTERIZATION OF A RECOMBINANT ADENOVIRUS VECTOR ENCODING HEAT INDUCIBLE FELINE INTERLEUKIN-12 FOR USE IN HYPERTHERMIA- INDUCED GENE- THERAPY

ABSTRACT

Interleukin-12 (IL-12) is a pro-inflammatory cytokine that has been extensively studied for the therapy of parasitic and viral infections and cancer. However, it is also a highly toxic molecule and for that reason has not been accepted readily into the clinic. We designed a replication deficient adenoviral vector to deliver the interleukin-12 gene into the cells. The interleukin-12 gene has been placed under control of a heat inducible promoter, *human heat shock promoter 70b.* The intent is to spatially and temporally control the expression of IL-12 thus limiting its toxicity.

We studied, *in vitro*, the transfection efficiency of the adenoviral vector, the production of IL-12 in the infected cells in response to hyperthermia, the effect of multiplicity of infection and the biologic function of IL-12 in terms of its ability to produce interferon- γ, its downstream cytokine.

The results of these *in vitro* experiments are presented in this chapter.

INTRODUCTION

The aim of cancer gene immunotherapy is the resolution of primary tumors and the development of a systemic immune response directed against metastases and micrometastases. Interleukin- 12 (IL-12) is one of the most widely studied immunoregulatory cytokines and has been found to eradicate tumors, metastases, elicit long- term anti-tumor immunity [1-6] and possess anti- angiogenic properties[7-10].The IL-12 protein is a 70 kDa heterodimer (p70) consisting of two covalently linked subunits, p35 and p40. It is produced by antigen- presenting cells, dendritic cells and macrophages in response to infection. In turn, IL-12 induces the synthesis of interferon- γ (IFN- γ) by T cells and NK cells. It also enhances cell mediated immunity (CMI) by promoting the generation and potentiation of the activity of cytotoxic T lymphocytes (CTL) and lymphokine activated killer (LAK) cells[11,12]. There is also evidence for a role of IL-12 in humoral immunity[13]. Interleukin- 12 is postulated to exert its anti- tumor effect through NK cells [7,14-17], NKT cells [18,19] and T cells [20-23]. IFN- γ, a downstream product of IL-12 action, is also thought to play a major role in the anti- tumor actions of IL-12 [1,24-29].

Various methods of IL-12 administration have been studied and described in literature including systemic administration[25,30-32], intratumoral injection of IL-12 plasmid DNA[5], genetic engineering approaches[33,34] and gene therapy techniques[6,17,35-39].The role of interleukin-12 in the anti-cancer arsenal has been limited due to its toxicities. In mice daily administration of 0.1-10μg of recombinant murine IL-12 for up to 2 weeks resulted in liver function abnormalities, muscle degeneration, gastrointestinal toxicity and hematopoietic changes including anemia, neutropenia, lymphopenia and thrombocytopenia[40]. In humans, the toxic effects are mostly IFN- γ dependent and

include fever, chills, fatigue, headache, nausea, vomiting, cough, myalgia, dizziness, insomnia, anemia, neutropenia, lymphocytopenia, thrombocytopenia, hyperglycemia, liver function test abnormalities, rhinitis, stomatitis and colitis[41]. In a phase II clinical trial in renal carcinoma using recombinant human IL-12, two deaths were reported[42,43]. One approach that can be used to avoid the systemic toxicity of IL-12 is to use local intratumoral IL-12 gene therapy. This approach should yield high tumoral levels of IL-12 with little or no systemic IL-12 exposure, thereby avoiding consequent toxicities.

A promising gene delivery method harnesses the heat shock response, an evolutionarily conserved response to cellular stress involving the rapid and transient increase in the cellular production of heat shock proteins, most importantly *hsp70* and *hsp90*. These proteins have protective functions in keeping other key proteins from being denatured by heat or other stresses and hence are also called *molecular chaperones*[44-46]. The heat shock promoter, hsp70, has been found to be one of the most efficient inducible regulatory sequences[47-49]. A further level of spatial specificity of IL-12 expression can be achieved if the hsp promoter containing gene construct is injected intratumorally and the expression of the construct is restricted to the tumor by delivering hyperthermia only to that area. This approach has been shown to improve selectivity of expression to the heated tumor, whereas intratumoral administration of expression constructs under control of a constitutive promoter can lead to ectopic expression of transgene in distant organs, such as the liver, spleen and lung[36].

Adenoviruses have been developed for use as gene delivery vehicles[50-52] and they offer certain advantages which make them attractive candidates for this role. Under experimental conditions, early clinical vaccination with wild-type (wt) live adenovirus

showed no significant side effects, demonstrating the relative safety of adenoviruses as vectors for *in vivo* gene therapy. They efficiently infect and transfer genes in a wide variety of cell types including dividing and non-dividing cells. Strong immunogenicity of adenoviral vectors may enhance tumor- killing in cancer gene therapy. Furthermore, adenoviruses are easy to manipulate by classical recombinant DNA techniques, and they have the added advantage that they can be produced in large quantities in cell culture. Unlike retroviruses, adenoviruses do not integrate into the host genome. This gives adenoviral vectors an important safety feature for *in vivo* gene therapy. This is important because there is no need for stable integration into the host genome in case of anti- cancer therapy, unlike diseases involving inborn errors of metabolism where a stable integration is desired.

With this background, we designed the Adenovirus heat shock promoter feline interleukin-12 construct and studied its properties *in vitro* with respect to its ability to produce IL-12 in Crandell feline kidney cells and the downstream effects of IL-12 in inducing IFN- γ production in peripheral blood mononuclear cells. This work was done in support of an immunogene therapy trial being conducted in pet cats with vaccine-associated sarcomas. This trial is being conducted as a prelude to initiation of human trials using a similar gene therapy approach.

MATERIALS AND METHODS

Cells used- Crandell Feline Kidney (CrFK) cells were cultured in DMEM supplemented with 10% fetal bovine serum (FBS) and 1% penicillin- streptomycin (CrFK media). These cells were grown in six- well tissue culture plates. It was determined that a

minimum of 3 X 10^5 cells need to be plated to allow subsequent growth. These were the primary cells infected with the adenoviral construct and exponential growth in cell number was seen over the next 2-3 days of the experiment.

Peripheral blood mononuclear cells (PBMC) were obtained from specific pathogen free cats maintained at Colorado State University and isolated by density gradient centrifugation (Histopaque 1077, Sigma). These cells were plated in six- well tissue culture plates at a density of 1 X 10^6 cells per well in RPMI 1640 medium supplemented with 20% FBS, 1% penicillin- streptomycin, 2% glutamine and 1 x 10^{-5} M 2-mercaptoethanol (LBT media). Supernatants from CrFK cells, containing the IL-12 protein, were used to stimulate production of IFN- γ in these PBMC.

Design of vector- The AdEasy system (Stratagene, La Jolla, CA) was used to construct the Ad*hsp*fIL12. The two subunits (p35 and p40) of the feline IL-12 were amplified from cDNA of CrFK cell line and sequence-verified. They were then connected into one gene expression unit by use of a flexible linker sequence (Gly4Ser). A 400-bp hsp70B promoter was then used to control the expression of the modified feline IL-12 gene. The whole hsp-fIL12 gene expression cassette was then transferred into an adenovirus shuttle plasmid. The shuttle plasmid was cotransfected into 293 cells to derive Ad*hsp*fIL12. Amplification and isolation of the virus was achieved following standard protocols[53,54]. AdCA35 expressing LacZ was kindly provided by Dr. Frank Graham, McMaster University.

An adenoviral vector with the enhanced green fluorescent protein (eGFP) under control of constitutive cytomegalovirus (CMV) promoter was used in experiments to determine transfection efficiency.

Flow Cytometry- CrFK cells were infected with an adenoviral construct with the feline IL-12 gene and enhanced green fluorescent protein (eGFP) placed under control of the constitutively expressing CMV promoter (Ad CMV fIL-12 + eGFP). This vector was used to determine the transfection efficiency of the adenoviral vector by detecting green fluorescence using the Coulter EPICS XL-MCL (Fullerton, CA) flow cytometer.

Real Time PCR- Real- time reverse transcriptase PCR was used to detect and quantitatively express the production of feline interleukin-12, interferon-γ and GAPDH mRNAs.

Sequences for the primers and probes were obtained from the literature[55] and purchased from MWG Biotech (High Point, NC).

Feline GAPDH

Forward- GAPDH.57f GCC GTG GAA TTT GCC GT

Reverse- GAPDH.138r GCC ATC AAT GAC CCC TTC AT

Probe- GAPDH.77p CTC AAC TAC ATG GTC TAC ATG TTC CAG TAT GAT TCC A

IL 12 p40

Forward- IL12.253f TGG CTT CAG TTG CAG GTT CTT

Reverse- IL12.333r TGG ACG CTA TTC ACA AGC TCA

Probe- IL12.283p CGG TTT GAT GAT GTC CCT GAT GAA GAA GCT

IFN- γ

Forward- IFN.141f TGG TGG GTC GCT TTT CGT AG

Reverse- IFN. 225r GAA GGA GAC AAT TTG GCT TTG AA

Probe- IFN. 152p CAT TTT GAA GAA CTG GAA AGA GGA GAG TGA TAA AAC AAT

The reporter dye attached covalently at the 5' end was FAM (6- carboxyfluorescin) and the quencher bound to the 3' end was TAMRA (6- carboxytetramethylrhodamine).

Real time PCR was performed using the Applied Biosystems ABI Prism 7000 (Foster City, CA). The amplification protocol was: 2 min at 50°C, 10 min at 95°C, 40 cycles of 15s at 95°C and 60s at 60°C. Cycle threshold values were obtained from the ABI software and the $2^{-\Delta\Delta Ct}$ method[56] was used to determine the relative expression of the genes of interest. Briefly, a standard housekeeping gene (eg. GAPDH, β- actin, β_2 microglobulin) is chosen as an internal control gene. This serves to normalize the amount of cDNA loaded for each reaction. An untreated control is selected as the 'calibrator'. The relative expression data is then obtained as the fold change in gene expression normalized to the chosen endogenous reference gene and relative to the untreated control.

Prior to using the $2^{-\Delta\Delta Ct}$ method for relative quantification, we validated its use for the primer and probe sequences and PCR conditions being employed in our experimental conditions. The methods and acceptable results are described in literature[56,57]. Briefly, the target cDNA was serially diluted and real time PCR performed. Cycle threshold values for the serially diluted samples are plotted on a graph with the log dilution on the X- axis and cycle threshold values on the Y- axis. The slope of the line is used to obtain the efficiency of PCR amplification using the formula- Efficiency = $10^{(-1/slope)}$-1.

Adenoviral Infection- Cells were plated in six- well plates in 2 ml of CrFK media at a density of 3 X 10^5 cells/well. Twenty- four hours later cells in one of the representative wells were trypsinized and counted using a hemocytometer. Total number of cells was thus obtained and the volume of adenoviral construct stock solution needed for the desired MOI was determined. This volume was dissolved in 300µl of sterile PBS and added to each well after drawing off the media for a period of 30 minutes at room temperature after which fresh media was added back to all wells. The plates were then placed back in the incubator at 37°C and 5% CO_2. Twenty- four hours were allowed for adenoviral infection and then the cells were subjected to hyperthermia. Cells were heated in a VWR Water Bath Model 1235PC. Heating was carried out in six – well plates that were placed in the water bath such that only the wells remained immersed in the heated water and water did not enter the plates. After placing the six- well tissue culture plates in the water bath, 8-10 minutes were allowed for temperature equilibration and then subsequently heated for 60 minutes.

PBMC stimulation- Naïve feline peripheral blood mononuclear cells (PBMC) were obtained from specific pathogen free cats, and stimulated using 5 μg/ml Concavalin A for 48 hours to upregulate the IL-12 receptor. These are the target cells for IL-12 protein *in vivo*, which leads to the production of IFN-γ. Supernatants were collected from the Ad*hsp*fIL12 infected CrFK cells at specified time- points after being heated at 41°C for 60 minutes. One hundred microliter of these supernatants, containing IL-12 protein, were then added to Concavalin A stimulated PBMCs. Twelve hours after addition of the supernatants, PBMCs were lysed and real time PCR was carried out.

To assess presence of a dose- response relationship CrFK cells infected with Ad*hsp*fIL12 were heated at 41°C for 60 minutes, supernatants were collected at 6 and 12 hours post-HT and 100μl or 200μl was added to the PMBC media. Twelve hours later PBMCs were lysed, RNA extracted and cDNA synthesized. Real- time PCR were performed for IFN-γ mRNA levels.

Cell lysis and RNA Isolation- At standardized time points after heat treatment the cells were lysed and RNA isolated using TRIzol Reagent (GibcoBRL) as per manufacturer's protocol. RNA purity was assessed spectrophotometrically.

cDNA synthesis- Total isolated RNA was treated with DNase I (Invitrogen) to remove any genomic DNA. cDNA synthesis was then carried out using Superscript II RNase H^- Reverse Transcriptase (Invitrogen, Carlsbad, CA). Each reaction mixture contained 10μl of RNA solution to which was added 4μl First strand buffer (5X), 1μl dNTP (10mM), 1μl DTT (0.1M), 0.25μl Rnase out (40U/ μl), 0.25μl SuperScript II (200 U/ μl), 2μl of

random hexamers (300ng/ µl) and 1.5µl DNase, RNase free water giving a total of 20µl per reaction mixture. This was incubated at 42°C for 50 minutes following which 30µl of DNase, RNase free water was added to the mix and the enzymes inactivated by placing the reaction tubes on a 95°C heat- block for 5 minutes. The cDNA was then stored at – 20°C till the time of RT- PCR.

RESULTS

Transfection efficiency - CrFK cells infected with the Ad CMV fIL12+eGFP construct at MOIs of 0, 5, 10, 20, 30 and 40 were split into two groups. In the first group the media containing any free- floating virus was left in the wells over all three days of the experiment. In the second group, after 24 hours of infection, the CrFK media containing any free virus was removed, the cells washed with PBS and fresh media added.

Cell counts were carried out to assess if adenoviral infection, *per se*, has any effect on cell growth. As shown in Figure 1, there appears to be no major effect of adenoviral infection on exponential cell growth.

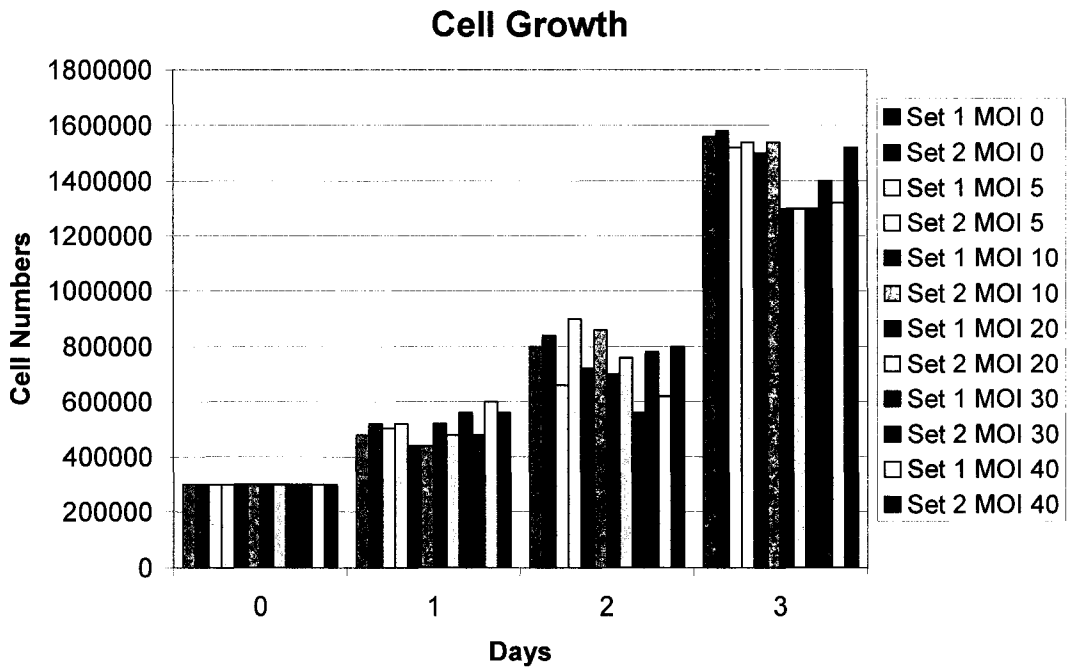

Figure 1- CELL GROWTH IN RESPONSE TO ADENOVIRAL INFECTION
Cells per well were counted in two sets of cells over a period of three days after plating. Each count is the average of three counts performed using a Coulter cell counter. In set 1, the viral construct added to the cells was left in the media over the duration of the experiment. In set 2, after 24 hours of infection, the attached CrFK cells were washed with PBS to remove any free- floating virus and fresh media replaced. No major effect of adenoviral infection was noted on exponential cell growth at various MOIs (0, 5, 10, 20, 30 and 40).

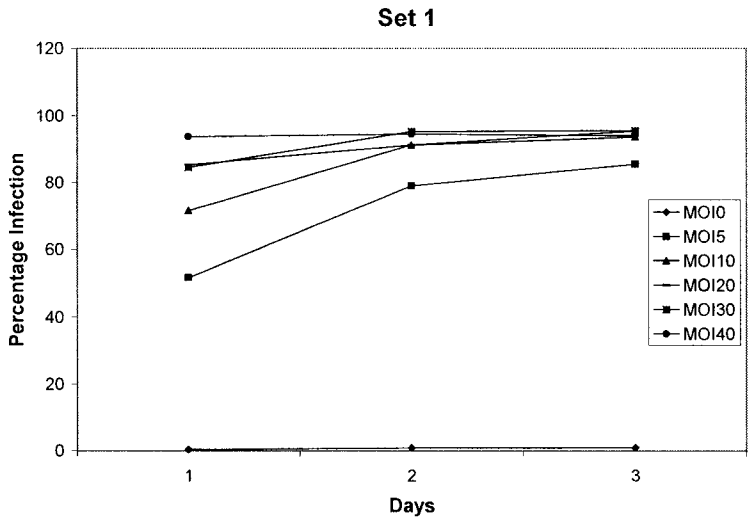

Figure 2a

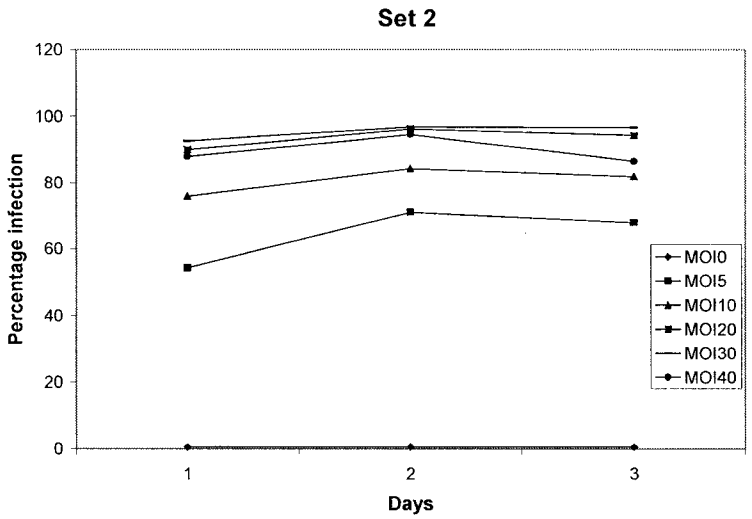

Figure 2b

Figure 2- TRANSFECTION EFFICIENCY OF ADENOVIRUSES
CrFK cells were infected with the Ad CMV fIL-12 + eGFP construct and green fluorescence detected flow cytometrically over 3 days, starting 24 hours after addition of virus (day1). A high transfection efficiency (90%- 95%) was noted at MOIs > 20. The high percentage of infected cells was maintained over the 3 days in set 1 (Fig. 2a). There was a slight decrease in percentage infection on day 3 in cells where the free- floating virus had been washed- off (Fig. 2b).

In the cells in sets 1 and 2 (Figures 2a and b), the percentage of infected cells is a reflection of the MOI on day 1. By the second day, 90%- 95% of cells in both groups are infected. By day 3, the percentage of cells infected remains constant in set 1 but decreased slightly in set 2 where the extra virus had been washed off.

These results show that the adenoviral construct is a highly efficient method of gene transfer *in vitro.* The percentage of infected cells remains high even if extra virus is washed off as might occur due to blood circulation *in vivo.*

Validation of the $2^{-\Delta\Delta Ct}$ method for relative quantification of feline cytokine mRNA- Criteria for the use of this method have been described in literature[56,57]. For the three genes of interest the following slopes were obtained IL-12= -3.1557, IFN- γ = -3.5056 and GAPDH= -3.3798 suggesting high level of PCR amplification (for 100% efficiency, ideal slope = -3.3213)[57]. Using the second method[56], pairwise comparisons were made between IL-12 – GAPDH and IFN-γ – GAPDH. For an ideal situation of slope=0, we obtained slopes of 0.097 for IL12 – GAPDH and 0.095 for IFN-γ – GAPDH. Thus, it was established that using our primer- probe sequences and PCR conditions, there was a high PCR amplification and the $2^{-\Delta\Delta Ct}$ method could be used for relative quantification.

Temperature dependent increase in IL-12 mRNA expression- CrFK cells were infected at an MOI=20. Twenty- four hours later, cells were heated in a water bath at the desired temperature. Each temperature experiment was carried out two- three times, each time in triplicate. The results are shown in Figure 3 and Table 1. Each graph shows the trends for increase and decrease in IL-12 mRNA expression in the CrFK cells infected with Ad *hsp*

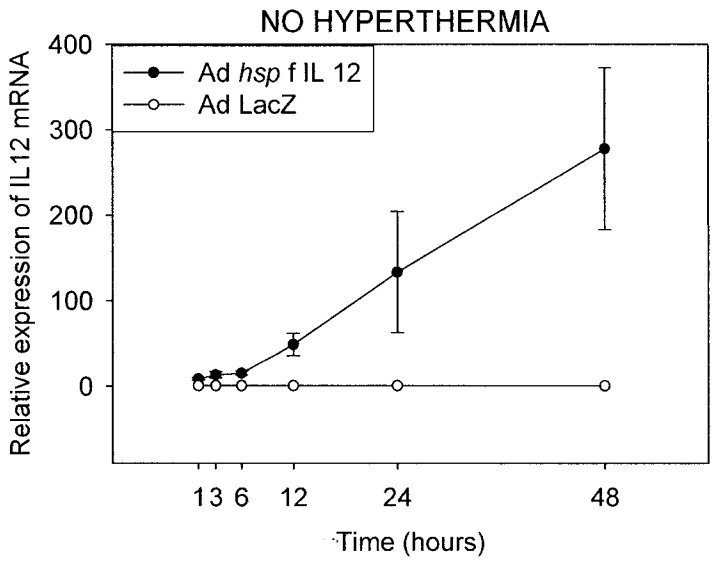

Figure 3a

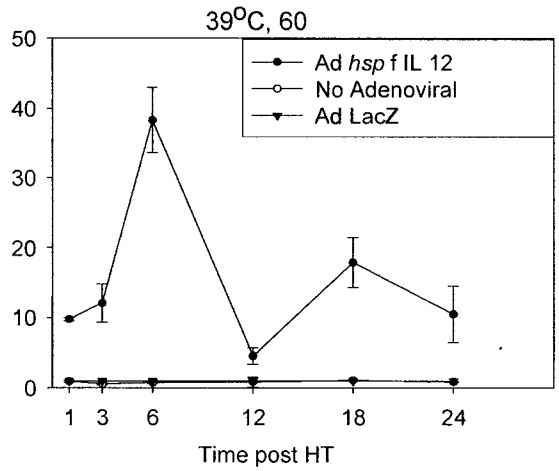

Figure 3b

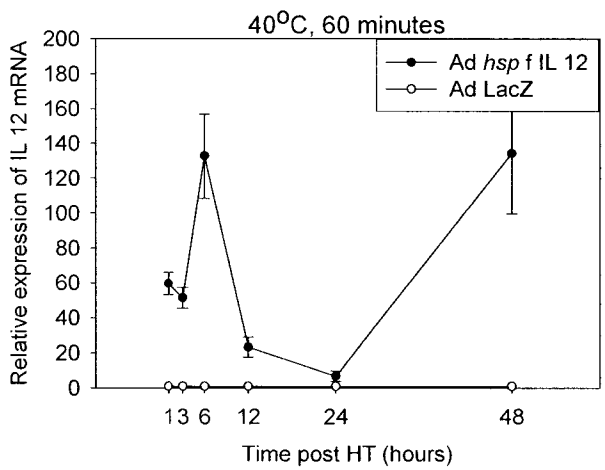

Figure 3c

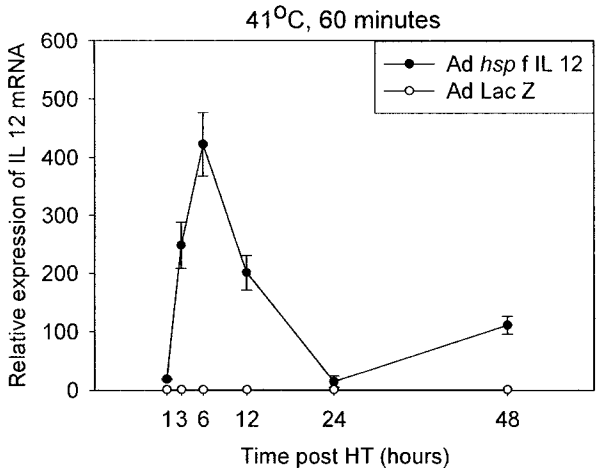

Figure 3d

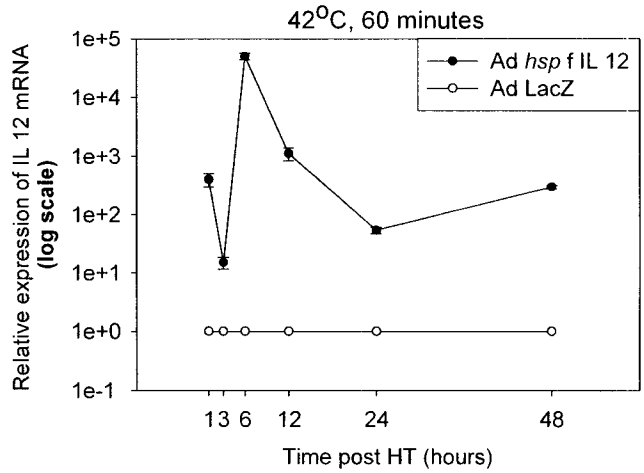

Figure 3e

Figure 3- TEMPERATURE DEPENDENT IL-12 EXPRESSION
Profiles of temperature dependent changes in IL-12 mRNA expression at specified time-points after hyperthermia. Cells were infected using the Ad *hsp* fIL-12 construct at MOI= 20. Fig 4a shows the minimal levels of expression at the early time points in unheated cells (kept in an incubator at 37°C, 5% CO_2). The relative expression increases at later times due to induction of the heat shock promoter by nutritional stress in exponentially growing cells. Figures 3 b-e show the profiles for heating at 39°C, 40°C, 41°C and 42°C for a duration of 60 minutes. Each temperature experiment was performed 2-3 times each in triplicate. The maximal expression of mRNA is seen at 6 hours post- HT in all cases with a rapid decrease and then a secondary increase at 48 hours probably due to the same phenomenon noted above, i.e. induction of the heat shock promoter by nutritional stress in exponentially growing cells. There is an approximately 3.5 fold increase in maximal expression between 39°C, 40°C and 41°C. However, a supralinear increase is seen at 42°C (Note- log scale on y- axis).

Time (hours post HT)	39^{0}C (average ± SD)	40^{0}C (average ± SD)	41^{0}C (average ± SD)	42^{0}C (average ± SD)
1	9.7 ± 0.3	59.7 ± 6.3	18.72 ± 0.9	394.7 ± 99.4
3	12.1 ± 2.8	51.4 ± 6.1	248.2 ± 39.9	14.9 ± 3.44
6	**38.3 ± 4.7**	**132.6 ± 24.3**	**422.3 ± 54.7**	**49724.4 ± 6691.8**
12	4.5 ± 1.2	23.3 ± 5.6	200.9 ± 29.7	1112.2 ± 280.8
18	17.9 ± 3.4	-	-	-
24	10.5 ± 4.1	6.8 ± 3.1	14.9 ± 9.7	53.6 ± 6.9
48	-	134.2 ± 34.7	110.9 ± 15.1	295.9 ± 20.6

Table 1- CrFK were infected at a MOI=20 with the Ad*hsp*fIL-12 gene construct and heated at various non- cytotoxic temperatures for 60 minutes. The IL-12 mRNA relative expression relative to non- infected CrFK cells is presented as average ± standard deviation. Each temperature experiment was performed 2-3 times each in triplicate.

feline IL-12 construct *relative to* IL-12 mRNA expression in cells infected with Ad LacZ or no adenoviral infection. The graph in Figure 3a is for infected cells which were not heated and Figures 3 b-e are for cells heated at various temperatures. Experiments were also done to determine the trend for the time points between 6 hours to 12 hours post-HT. The relative expression at 6, 8, 10 and 12 hours showed a decreasing trend (data not shown). The heated cells show a biphasic response, with the initial peak due to hyperthermia followed by a rapid decline and again a rising trend at later time- points. However, in the non- heated cells only a steady increase is seen in the IL-12 mRNA levels without the initial peak. The phenomenon of increasing relative expression in non-heated cells and the secondary increase in heated cells at later time points can be ascribed to *heat shock promoter* induction by nutritional stress (Chapter 3).

There was an approximately 3.5 fold increase in expression at the six- hour post- HT time point between 39^0C, 40^0C and 41^0C. However, there was a supralinear increase seen at 42^0C.

At 43 and 44^0C there is direct hyperthermia induced cytotoxicity as determined by trypan blue dye exclusion (Figure 4). This is not desirable for our purposes as cell viability is essential. Only intact cellular machinery will be able to produce IL-12.

Effect of multiplicity of infection- CrFK cells infected at MOIs of 5, 10, 20, 30 and 40 were heated at 40^0C. A dose- dependent increase in maximal relative expression was seen (Figures 5 a and b). The curve, however, tends to flatten out at high MOIs.

Production of IFN-γ from IL-12 target cells- We wanted to ascertain that the IL-12 mRNA being detected using the real time PCR was actually being translated into functional IL-12 protein. It can be seen in Figure 6 that maximal production of IFN-γ in feline PBMC occurred when they were stimulated with CrFK supernatant collected at 18

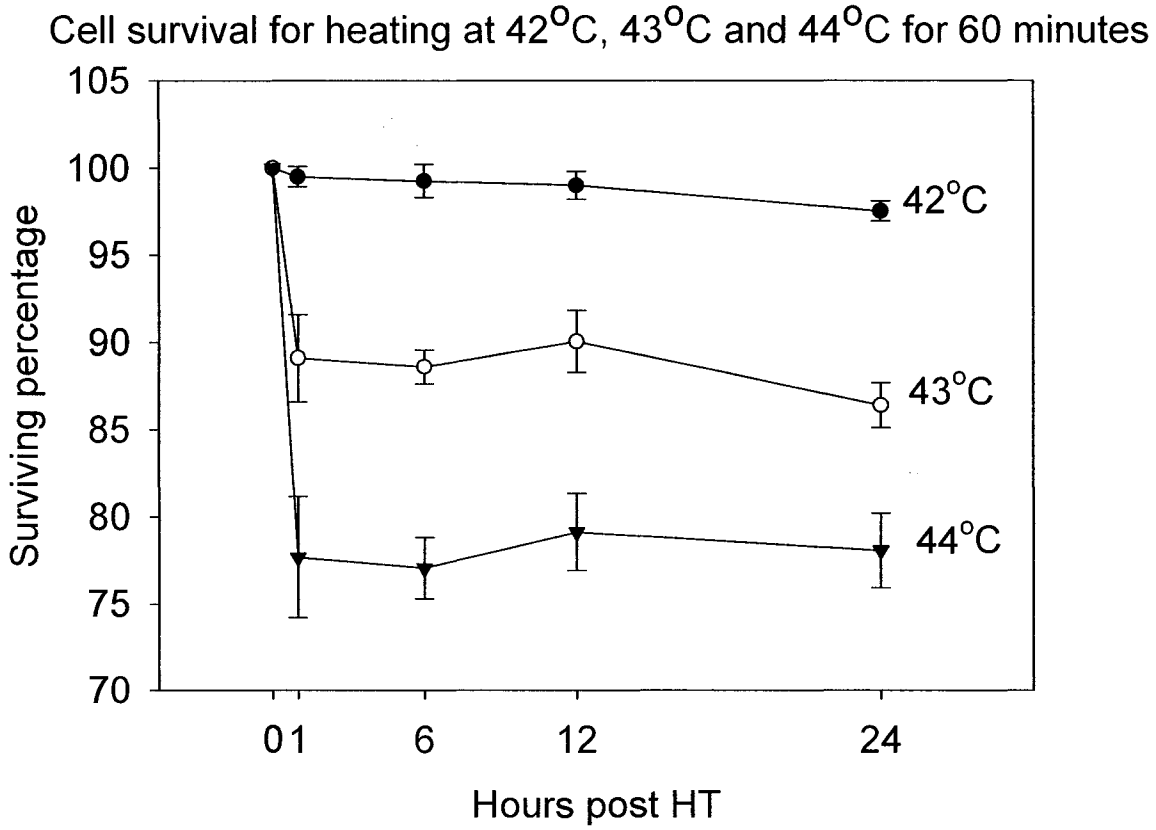

Figure 4- ASSESSMENT OF CELL VIABILITY AT HIGHER TEMPERATURES
The trypan blue dye- exclusion test was used to assess cellular viability after being heated at 43°C and 44°C for 60 minutes. Direct hyperthermia induced cytotoxicity reduced the percentage of viable cells to ~88% for 43°C and ~ 73% for 44°C as early as 1 hour post-HT and this percentage remained constant up to 24 hours post- HT.

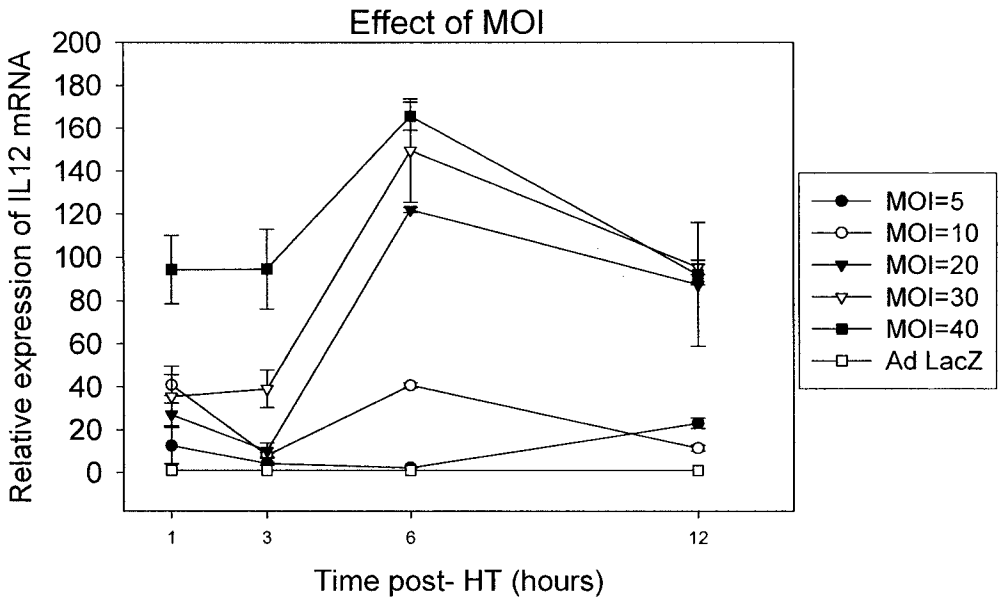

Figure 5a

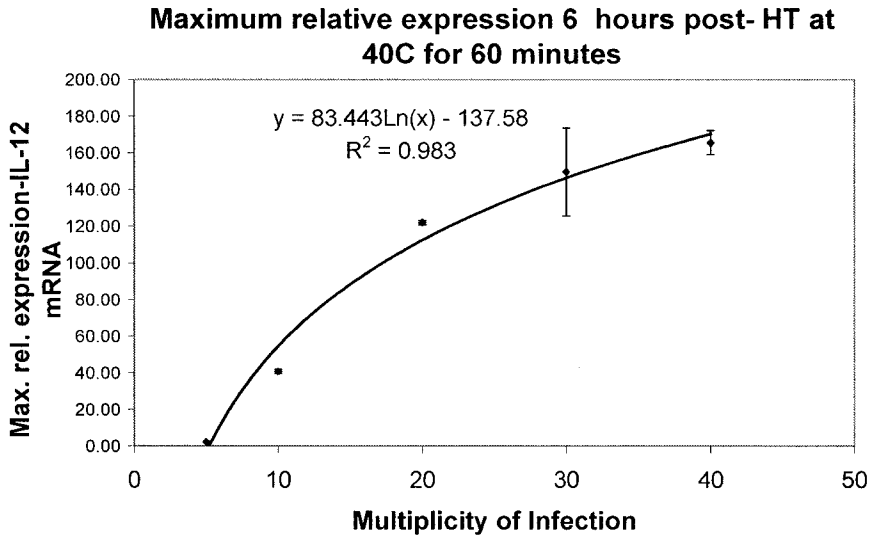

Figure 5b

Figure 5- EFFECT OF MULTIPLICITY OF INFECTION (MOI)
CrFK cells were infected at various MOIs and heated at 40°C for 60 minutes. A dose-response relationship is seen (Fig. 5a) with the curve for maximum relative expression tending to flatten out at higher MOIs (Fig. 5b).

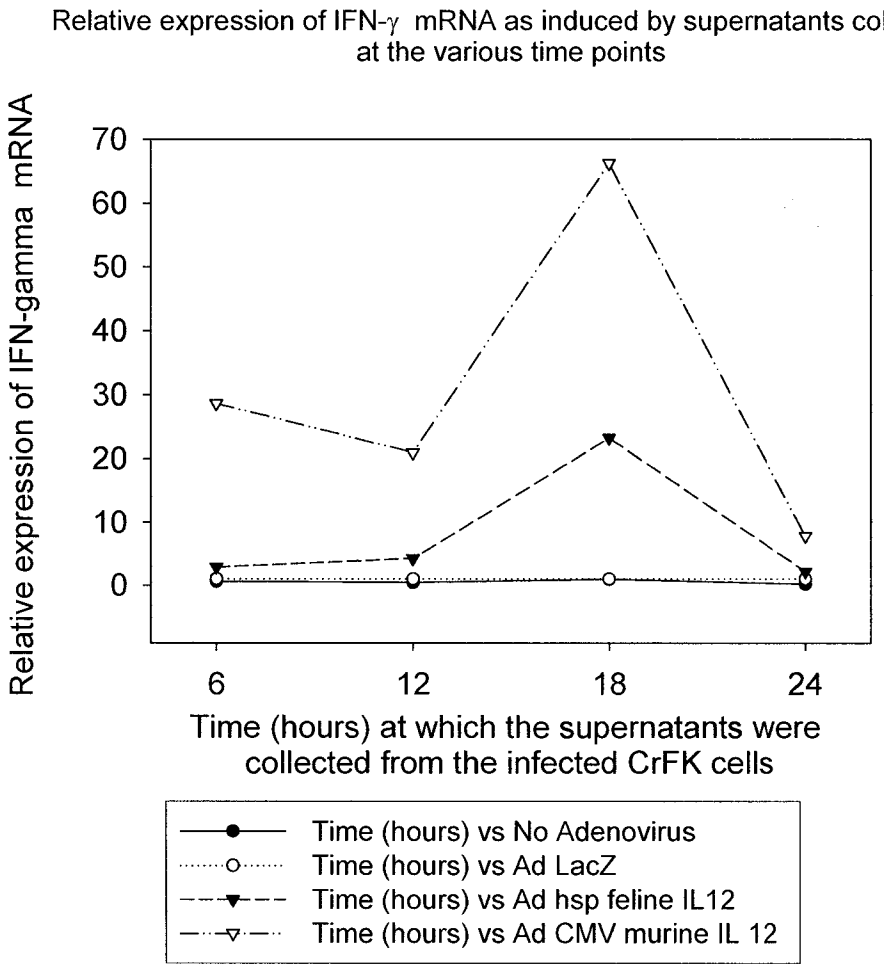

Figure 6- INDUCTION OF IFN-γ

Functionality of IL-12 was assessed by adding 100 µl of supernatants obtained from Ad *hsp* fIL-12 infected CrFK cells to Con A stimulated naïve feline PBMCs. These CrFK cells had been heated at 41°C for 60 minutes and supernatants were collected at 6, 12, 18 and 24 hours post- HT. The PBMCs were lysed 12 hours later (to allow action of IL-12 upon its target cells and the production of IFN-γ mRNA). The maximum induction was seen in the PBMCs in which supernatant from the 18 hour post- HT CrFK cells had been added suggesting that this sample contained the maximum amount of IL-12 protein.

	Relative expression of IFN-γ mRNA (average ± SD)	
Volume of supernatant added	**100 µl**	**200 µl**
'6 hours post- HT'supernatant	6.4 ± 2.3	6.7 ± 2.4
'12 hours post- HT'supernatant	12.1 ± 6.3	30.88 ± 15.6

Table 2- Supernatants from Ad *hsp* fIL-12 infected cells heated at 41°C for 60 minutes containing the IL-12 protein were collected at 6 and 12 hours post- HT. These supernatants were added to naïve feline PBMCs in volumes of 100 µl or 200 µl to assess any dose response effect for IL-12 protein in inducing production of IFN-γ. At the earlier time point (6 hours), when there would have been little IL-12 protein production, no difference was seen for the two doses but by the 12 hour time point an approximately twofold increase in relative expression of IFN-γ mRNA was seen for the higher dose of added IL-12 protein.

hours post-HT. This suggests that the maximum IL-12 protein would have been present at that time- point. It has also been seen that the maximal mRNA levels are seen 6 hours post- HT. Hence, it takes approximately 12 hours for IL-12 protein synthesis after mRNA transcription.

Another experiment was done to see if there is a dose- response effect in IFN-γ production from the PBMCs in response to different doses of IL-12. Results shown in Table 2 suggest a dose- response relationship in the induction of IFN-γ. The supernatant collected at the 6 hour post- HT time point would not have much IL-12 protein, therefore, no difference is seen for the relative expression but there would be more IL-12 protein present in the supernatants at the 12 hour time point and a difference in relative expression of IFN-γ mRNA is noted.

Hence, the IL-12 being produced in cells infected with the construct is functional and is able to induce production of its downstream product in a dose- dependent manner.

DISCUSSION

Interleukin 12, a pro- inflammatory cytokine, has been found to have significant anti-cancer activity *in vitro* and *in vivo*[1-10,37,49,58]. However, there have been limited clinical successes largely owing to the toxicity profile of IL-12 and mortalities in Phase II trials when administered systemically[42,43]. As an alternative to using systemic administration of this potent cytokine, we have elected to test an intra-tumoral replication defective adenoviral gene therapy approach to achieve relatively high intratumoral transgene expression, while minimizing systemic exposure to the cytokine. The feline Interleukin-

12 gene was placed under the control of a highly inducible heat shock promoter (400-bp hsp70B promoter) as an additional means of controlling cytokine expression. To answer important methodological questions that relate to optimizing the use of this approach clinically we conducted a series of *in vitro* experiments. Important considerations were: 1) the MOI required to obtain significant levels of transgene expression, 2) timing of hyperthermia treatment after introduction of the adenovirus, 3) the effects of temperature on level of gene expression, 4) whether factors other than hyperthermia can alter levels of gene expression, and 5) whether the gene product produced is functional.

Real time reverse transcriptase PCR was chosen as the method used to evaluate cytokine mRNA levels in part because the antibodies needed to determine protein levels of these feline cytokines are not readily available. Real time PCR offers several advantages, the most important being the ability to express results in quantitative terms rather than qualitative estimates and it is very sensitive to differences in cDNA copy numbers between samples. The $2^{-\Delta\Delta Ct}$ method[56] used to calculate relative expression of cytokine mRNA levels allows mathematical normalization of the amount of cDNA used per reaction and hence the reported fold expression is independent of the number of cells from which the mRNA is isolated.

GAPDH was used as the housekeeping gene. It is an important glycolytic pathway enzyme. It is used as an internal standard as its synthesis occurs in all nucleated cell types since it is necessary for survival. Despite recent criticisms about the use of GAPDH as the internal control[59-61], other systematic studies have shown that it still remains one of the most stable control genes in various cell types[55,62]. Importantly, its expression is not known to be affected by temperature[63].

Twenty- four hours were allowed for optimal adenoviral infection of the cells based on reports in literature[48,58], and then the cells were heated. The maximal IL-12 mRNA expression was seen at 6 hours post- HT followed by a rapid decline which is consistent with that reported in the literature[64].

A gradual 3.5 fold increase in the maximal expression of IL-12 mRNA was seen with temperature for 39°C, 40°C and 41°C. These fold increases seem to reflect the Arrhenius relationship for effectiveness of cell killing using hyperthermia. A 4- fold decrease in effectiveness is seen with each degree centigrade fall in temperature below the breakpoint. However, the level of gene expression seen at 42°C was much greater than that at 41°C. At 43°C and 44°C there was significant cell killing from direct cytotoxic effects of hyperthermia on the CrFK cells. Also, in a clinical situation, it is difficult achieving temperatures greater than 42°C. Hence, a complete profile of IL-12 expression at these temperatures was not studied. It is essential for the cellular machinery to remain viable after heating to allow production of immunomodulatory cytokines.

Initially the cells were divided into three groups, those infected with the Ad *hsp* fel IL12 construct, those infected with Ad LacZ (control) and cells not infected with any virus. It was established that the IL-12 mRNA expression levels were similar in the non- infected and Ad LacZ infected cells. In later experiments, only two groups were studied, Ad *hsp* fel IL12 infected and Ad LacZ infected to control for any difference in expression due to adenoviral infection *per se*.

A logarithmic increase was seen with increasing MOI for the maximal expression at 6 hours and the curve tended to plateau at higher MOI. The decrease with time was more gradual at higher MOIs (20, 30 and 40) than at lower MOIs (5 and 10). These findings

serve to emphasize the importance of titrating the dose to be injected into tumors in *in vivo* studies with the tumor volume to try and achieve an optimum MOI. A similar dose response was not seen in the study by Borrelli *et al* [48]. They had studied enhanced GFP expression using a CMV promoter and they attributed the nonproportionality to the nonlinear CMV promoter activity.

The PBMC stimulation experiments showed that there is an approximately 12 hour time-interval between maximal mRNA expression and maximal protein expression. This was also consistent with earlier reports[48,58].

Our study demonstrates that the heat shock promoter is a highly inducible promoter which can be triggered by hyperthermia. This promoter then causes the production of feline IL-12 in a temperature and multiplicity of infection (MOI) dependent manner. The IL-12 protein is effective in inducing the production of IFN-γ from feline peripheral blood mononuclear cells. This expression system, thus, offers as attractive approach to local cancer immunotherapy while minimizing the potential systemic toxicity of interleukin 12. Future plans with this vector include a phase I trial in feline soft tissue sarcoma patients combining radiation therapy and hyperthermia-induced IL-12 expression.

REFERENCES

1 Brunda MJ *et al.* Role of interferon-gamma in mediating the antitumor efficacy of interleukin-12. *J Immunother Emphasis Tumor Immunol* 1995; **17:** 71-77.

2 Puisieux I *et al.* Canarypox virus-mediated interleukin 12 gene transfer into murine mammary adenocarcinoma induces tumor suppression and long-term antitumoral immunity. *Hum Gene Ther* 1998; **9:** 2481-2492.

3 Seetharam S *et al.* Enhanced eradication of local and distant tumors by genetically produced interleukin-12 and radiation. *Int J Oncol* 1999; **15:** 769-773.

4 Golab J, Zagozdzon R. Antitumor effects of interleukin-12 in pre-clinical and early clinical studies (Review). *Int J Mol Med* 1999; **3:** 537-544.

5 Shi F *et al.* Intratumoral injection of interleukin-12 plasmid DNA, either naked or in complex with cationic lipid, results in similar tumor regression in a murine model. *Mol Cancer Ther* 2002; **1:** 949-957.

6 Liu Y *et al.* In situ adenoviral interleukin 12 gene transfer confers potent and long-lasting cytotoxic immunity in glioma. *Cancer Gene Ther* 2002; **9:** 9-15.

7 Yao L *et al.* Contribution of natural killer cells to inhibition of angiogenesis by interleukin-12. *Blood* 1999; **93:** 1612-1621.

8 Voest EE *et al.* Inhibition of angiogenesis in vivo by interleukin 12. *J Natl Cancer Inst* 1995; **87:** 581-586.

9 Duda DG *et al.* Direct in vitro evidence and in vivo analysis of the antiangiogenesis effects of interleukin 12. *Cancer Res* 2000; **60:** 1111-1116.

10 Coughlin CM *et al.* Interleukin-12 and interleukin-18 synergistically induce murine tumor regression which involves inhibition of angiogenesis. *J Clin Invest* 1998; **101:** 1441-1452.

11 Kobayashi M *et al.* Identification and purification of natural killer cell stimulatory factor (NKSF), a cytokine with multiple biologic effects on human lymphocytes. *J Exp Med* 1989; **170:** 827-845.

12 Gately MK, Wolitzky AG, Quinn PM, Chizzonite R. Regulation of human cytolytic lymphocyte responses by interleukin-12. *Cell Immunol* 1992; **143:** 127-142.

13 Metzger DW *et al.* Interleukin-12 acts as an adjuvant for humoral immunity through interferon-gamma-dependent and -independent mechanisms. *Eur J Immunol* 1997; **27:** 1958-1965.

14 Pham-Nguyen KB *et al.* Role of NK and T cells in IL-12-induced anti-tumor response against hepatic colon carcinoma. *Int J Cancer* 1999; **81:** 813-819.

15 Kodama T *et al.* Perforin-dependent NK cell cytotoxicity is sufficient for anti-metastatic effect of IL-12. *Eur J Immunol* 1999; **29:** 1390-1396.

16 Watanabe M *et al.* Intradermal delivery of IL-12 naked DNA induces systemic NK cell activation and Th1 response in vivo that is independent of endogenous IL-12 production. *J Immunol* 1999; **163:** 1943-1950.

17 Rakhmilevich AL *et al.* Interleukin-12 gene therapy of a weakly immunogenic mouse mammary carcinoma results in reduction of spontaneous lung metastases via a T-cell-independent mechanism. *Cancer Gene Ther* 2000; **7:** 826-838.

18 Cui J *et al.* Requirement for Valpha14 NKT cells in IL-12-mediated rejection of tumors. *Science* 1997; **278:** 1623-1626.

19 Zilocchi C *et al.* Interferon gamma-independent rejection of interleukin 12-transduced carcinoma cells requires CD4+ T cells and Granulocyte/Macrophage colony-stimulating factor. *J Exp Med* 1998; **188:** 133-143.

20 North RJ, Kirstein DP. T-cell-mediated concomitant immunity to syngeneic tumors. I. Activated macrophages as the expressors of nonspecific immunity to unrelated tumors and bacterial parasites. *J Exp Med* 1977; **145:** 275-292.

21 Berendt MJ, North RJ, Kirstein DP. The immunological basis of endotoxin-induced tumor regression. Requirement for a pre-existing state of concomitant anti-tumor immunity. *J Exp Med* 1978; **148:** 1560-1569.

22 Le HN, Lee NC, Tsung K, Norton JA. Pre-existing tumor-sensitized T cells are essential for eradication of established tumors by IL-12 and cyclophosphamide plus IL-12. *J Immunol* 2001; **167:** 6765-6772.

23 Saffran DC *et al.* Immunotherapy of established tumors in mice by intratumoral injection of interleukin-2 plasmid DNA: induction of CD8+ T-cell immunity. *Cancer Gene Ther* 1998; **5:** 321-330.

24 Segal JG *et al.* The role of IFN-gamma in rejection of established tumors by IL-12 : source of production and target. *Cancer Res* 2002; **62:** 4696-4703.

25 Nastala CL *et al.* Recombinant IL-12 administration induces tumor regression in association with IFN-gamma production. *J Immunol* 1994; **153:** 1697-1706.

26 Zou JP *et al.* Systemic administration of rIL-12 induces complete tumor regression and protective immunity: response is correlated with a striking reversal

of suppressed IFN-gamma production by anti-tumor T cells. *Int Immunol* 1995; **7:** 1135-1145.

27 Yu WG *et al.* Molecular mechanisms underlying IFN-gamma-mediated tumor growth inhibition induced during tumor immunotherapy with rIL-12. *Int Immunol* 1996; **8:** 855-865.

28 Tsung K *et al.* Immune response against large tumors eradicated by treatment with cyclophosphamide and IL-12. *J Immunol* 1998; **160:** 1369-1377.

29 Manetti R *et al.* Interleukin 12 induces stable priming for interferon gamma (IFN-gamma) production during differentiation of human T helper (Th) cells and transient IFN-gamma production in established Th2 cell clones. *J Exp Med* 1994; **179:** 1273-1283.

30 Brunda MJ *et al.* Antitumor and antimetastatic activity of interleukin 12 against murine tumors. *J Exp Med* 1993; **178:** 1223-1230.

31 Tannenbaum CS *et al.* Cytokine and chemokine expression in tumors of mice receiving systemic therapy with IL-12. *J Immunol* 1996; **156:** 693-699.

32 Cavallo F *et al.* Antitumor efficacy of adenocarcinoma cells engineered to produce interleukin 12 (IL-12) or other cytokines compared with exogenous IL-12. *J Natl Cancer Inst* 1997; **89:** 1049-1058.

33 Tahara H *et al.* Fibroblasts genetically engineered to secrete interleukin 12 can suppress tumor growth and induce antitumor immunity to a murine melanoma in vivo. *Cancer Res* 1994; **54:** 182-189.

34 Zitvogel L *et al.* Cancer immunotherapy of established tumors with IL-12. Effective delivery by genetically engineered fibroblasts. *J Immunol* 1995; **155:** 1393-1403.

35 Wu NZ, Klitzman B, Dodge R, Dewhirst MW. Diminished leukocyte-endothelium interaction in tumor microvessels. *Cancer Res* 1992; **52:** 4265-4268.

36 Lohr F *et al.* Systemic vector leakage and transgene expression by intratumorally injected recombinant adenovirus vectors. *Clin Cancer Res* 2001; **7:** 3625-3628.

37 Lohr F *et al.* Enhancement of radiotherapy by hyperthermia-regulated gene therapy. *Int J Radiat Oncol Biol Phys* 2000; **48:** 1513-1518.

38 Lode HN *et al.* Gene therapy with a single chain interleukin 12 fusion protein induces T cell-dependent protective immunity in a syngeneic model of murine neuroblastoma. *Proc Natl Acad Sci U S A* 1998; **95:** 2475-2480.

39 Rakhmilevich AL *et al.* Gene gun-mediated skin transfection with interleukin 12 gene results in regression of established primary and metastatic murine tumors. *Proc Natl Acad Sci U S A* 1996; **93:** 6291-6296.

40 Car BD, Eng VM, Lipman JM, Anderson TD. The toxicology of interleukin-12: a review. *Toxicol Pathol* 1999; **27:** 58-63.

41 Oppenheim JJ, Feldmann M, Durum SK. *Cytokine reference : a compendium of cytokines and other mediators of host defense*. Academic Press: San Diego, 2001.

42 Cohen J. IL-12 deaths: explanation and a puzzle. *Science* 1995; **270:** 908.

43 Atkins MB *et al.* Phase I evaluation of intravenous recombinant human interleukin 12 in patients with advanced malignancies. *Clin Cancer Res* 1997; **3:** 409-417.

44 Whitley D, Goldberg SP, Jordan WD. Heat shock proteins: a review of the molecular chaperones. *J Vasc Surg* 1999; **29:** 748-751.

45 Parcellier A *et al.* Heat shock proteins, cellular chaperones that modulate mitochondrial cell death pathways. *Biochem Biophys Res Commun* 2003; **304:** 505-512.

46 Nollen EA, Morimoto RI. Chaperoning signaling pathways: molecular chaperones as stress-sensing 'heat shock' proteins. *J Cell Sci* 2002; **115:** 2809-2816.

47 Morimoto RI, Tissiáeres A, Georgopoulos C. *The Biology of heat shock proteins and molecular chaperones*. Cold Spring Harbor Laboratory Press: Plainview , N.Y., 1994.

48 Borrelli MJ *et al.* Heat-activated transgene expression from adenovirus vectors infected into human prostate cancer cells. *Cancer Res* 2001; **61:** 1113-1121.

49 Li CY, Dewhirst MW. Hyperthermia-regulated immunogene therapy. *Int J Hyperthermia* 2002; **18:** 586-596.

50 Wang Q, Finer MH. Second-generation adenovirus vectors. *Nat Med* 1996; **2:** 714-716.

51 Yang Y *et al.* Cellular immunity to viral antigens limits E1-deleted adenoviruses for gene therapy. *Proc Natl Acad Sci U S A* 1994; **91:** 4407-4411.

52 Zhang Y, Schneider RJ. Adenovirus inhibition of cell translation facilitates release of virus particles and enhances degradation of the cytokeratin network. *J Virol* 1994; **68:** 2544-2555.

53 He TC *et al.* A simplified system for generating recombinant adenoviruses. *Proc Natl Acad Sci U S A* 1998; **95:** 2509-2514.

54 Graham FL, Smiley J, Russell WC, Nairn R. Characteristics of a human cell line transformed by DNA from human adenovirus type 5. *J Gen Virol* 1977; **36:** 59-74.

55 Leutenegger CM *et al.* Quantitative real-time PCR for the measurement of feline cytokine mRNA. *Vet Immunol Immunopathol* 1999; **71:** 291-305.

56 Livak KJ, Schmittgen TD. Analysis of relative gene expression data using real-time quantitative PCR and the 2(-Delta Delta C(T)) Method. *Methods* 2001; **25:** 402-408.

57 Pfaffl MW. A new mathematical model for relative quantification in real-time RT-PCR. *Nucleic Acids Res* 2001; **29:** e45.

58 Huang Q *et al.* Heat-induced gene expression as a novel targeted cancer gene therapy strategy. *Cancer Res* 2000; **60:** 3435-3439.

59 Yamada H, Chen D, Monstein HJ, Hakanson R. Effects of fasting on the expression of gastrin, cholecystokinin, and somatostatin genes and of various housekeeping genes in the pancreas and upper digestive tract of rats. *Biochem Biophys Res Commun* 1997; **231:** 835-838.

60 Foss DL, Baarsch MJ, Murtaugh MP. Regulation of hypoxanthine phosphoribosyltransferase, glyceraldehyde-3-phosphate dehydrogenase and beta-actin mRNA expression in porcine immune cells and tissues. *Anim Biotechnol* 1998; **9:** 67-78.

61 Bustin SA. Absolute quantification of mRNA using real-time reverse transcription polymerase chain reaction assays. *J Mol Endocrinol* 2000; **25:** 169-193.

62 Vandesompele J *et al.* Accurate normalization of real-time quantitative RT-PCR data by geometric averaging of multiple internal control genes. *Genome Biol* 2002; **3:** RESEARCH0034.

63 Coss RA *et al.* Intracellular acidification abrogates the heat shock response and compromises survival of human melanoma cells. *Mol Cancer Ther* 2003; **2:** 383-388.

64 Li GC *et al.* Adenovirus-mediated heat-activated antisense Ku70 expression radiosensitizes tumor cells in vitro and in vivo. *Cancer Res* 2003; **63:** 3268-3274.

Chapter 3

INDUCTION OF THE *HUMAN HEAT SHOCK PROMOTER* BY NUTRITIONAL STRESS

ABSTRACT

The heat shock response is an evolutionarily conserved protective mechanism in cells. Heat shock proteins serve as molecular chaperones to prevent protein denaturation when the cells are exposed to any kind of stress. They were first observed in response to the cells being heated but many other types of physiological or pathological stresses may also induce the heat shock response. We have used the heat shock promoter as an inducible promoter in an adenoviral construct used to deliver the interleukin-12 (IL-12) gene to cancer cells. In initial experiments production of IL-12 mRNA was noted even in cells that had not been heated. This phenomenon has been explored in detail in the present chapter and implications for the tumor microenvironment and host cancer cachexia discussed.

INTRODUCTION

The heat shock response is an evolutionarily conserved protective mechanism first described in *Drosophila melanogaster* salivary glands in response to heat[1]. In fact the production of heat shock proteins is seen in response to various types of cellular stresses including environmental stresses (amino acid analogues, transition heavy metals, inhibitors of energy metabolism), pathophysiological states (fever, oxidant injury, ischemia, aging) and even during normal physiological states like cell division and growth and differentiation[2, 3]. The human heat shock promoter hsp 70b is a highly inducible promoter and has been employed to control the expression of genes of interest in experimental and clinical settings in several systems[4-11]. Using this promoter in cancer gene immunotherapy allows the combination of hyperthermia, a well- established modality for cancer therapy, and targeted inducible gene- expression. The hsp70 promoter is tightly regulated but highly inducible following heat shock. Temperatures needed to induce this response are in a clinically relevant temperature range (eg between 39^0C and 42^0C) and repeated heat treatments can maintain elevated levels of gene expression for extended periods of time[8].

Interleukin- 12 is a pro- inflammatory cytokine which has been extensively studied in pre- clinical and clinical settings for various types of cancer[6, 12-18]. However, when the recombinant interleukin-12 protein is administered systemically it can result in severe life- threatening toxicities[19-22]. We, therefore, designed a construct in which the feline interleukin-12 gene has been placed under control of the *human heat shock promoter* and a replication deficient adenovirus type 5 is used as the vehicle for gene delivery. This construct has been designed for use in a Phase I clinical trial in feline soft tissue

sarcomas. Prior to its use *in vivo* we tested this construct extensively *in vitro* to determine interleukin-12 expression in relation to temperature, multiplicity of infection and biological functionality in terms of inducing downstream production of interferon-gamma (IFN-γ) from its target cells (Chapter 2).

During the course of our experiments we were surprised by a phenomenon in which interleukin-12 mRNA levels were highly elevated in certain cases even when the cells infected with the construct had not been heated. We investigated this further and found that the heat shock promoter is induced if the infected cells are subjected to nutritional stresses. This might be a significant advantage in the nutritionally stressed tumor microenvironment. However, a corollary to this is that if this adenoviral vector leaks into the general circulation and infects distant organs like the liver, a deleterious effect may occur in patients with cancer cachexia with disrupted metabolic processes.

MATERIALS AND METHODS

Cell culture system- Crandell Feline Kidney (CrFK) cells were cultured in DMEM (Cellgro) supplemented with 10% fetal bovine serum and 1% penicillin- streptomycin (CrFK media) in six- well tissue culture plates. For glucose and glutamine supplementation experiments, DMEM without glucose and glutamine was purchased from Biosource International (Camarillo, CA).

Design of vector- The AdEasy system (Stratagene, La Jolla, CA) was used to construct the adhspflL12. The two subunits (p35 and p40) of the feline IL12 were amplified from cDNA of CrFK cell line and sequence-verified. They were then connected into one gene

expression unit by use of a flexible linker sequence (Gly4Ser). A 400-bp hsp70B promoter was then used to control the expression of the modified feline IL12 gene. The whole hsp-fIL12 gene expression cassette was then transferred into an adenovirus shuttle plasmid. The shuttle plasmid was cotransfected into 293 cells to derive Ad *hsp* fIL12. Amplification and isolation of the virus was achieved following standard protocols[23, 24].

Adenoviral Infection- Cells were plated in six- well plates in 2 ml of CrFK media at various densities. Twenty- four hours later, cells in one of the representative wells were trypsinized and counted using a hemocytometer. Total number of cells was thus obtained and the volume of adenoviral construct stock solution needed for an MOI of 20 was determined. This volume was resuspended in 300μl of sterile PBS and added to each well after drawing off the media for a period of 30 minutes at room temperature after which fresh CrFK media was added back to all wells. The plates were then placed back in the incubator at 37°C and 5% CO_2. Inhibition of cell growth was achieved using aphidicolin (Sigma-Aldrich, St. Louis, MO) at a concentration of 2 μg/ml. Cell viability post hyperthermia was assessed by the trypan blue dye exclusion test.

Irradiation- Irradiation of infected cells was done using a ^{137}Cs γ- irradiator at 3.9 Gy/ minute.

Reactive oxygen species and pH changes- To assess the role played by reactive oxygen species (ROS) and changes in pH in the induction of the heat shock promoter, CrFK cells

were plated in 35mm Petri dishes. The cells were examined at low and high densities and in presence of various deficient media for presence of ROS and changes in pH.

For the detection of ROS, H2DCFDA (Molecular Imaging Products, Ann Arbor, MI) was added at a concentration of 10μM in the cell culture media. The cells were incubated for 45 minutes at 37°C and 5%CO_2 and the Petri dishes were imaged directly under FITC fluorescence. Cells irradiated to a dose of 10 Gy using ^{137}Cs γ- rays were used as positive controls.

SNARF-1 (Molecular Imaging Products, Ann Arbor, MI) was used for pH change measurement. The procedure used was as described[25]. Briefly, cells plated in T-25 flasks were trypsinized (0.03% trypsin) and SNARF-1 dye loaded at a concentration of 5μg/ml. A standard calibration was constructed over the range of pH 7.0 to 8.0 using high potassium calibration (HPC) buffers with the cells permeabilized using nigericin. Intracellular pH was of the cells plated at various densities was determined flow cytometrically from the standard curve.

RNA isolation and cDNA synthesis- Cells were lysed and RNA isolated using TRIzol Reagent (GibcoBRL, Carlsbad, CA) as per manufacturers protocol. RNA purity was assessed spectrophotometrically. Total isolated RNA was treated with DNase I (Invitrogen, Carlsbad, CA) to remove any genomic DNA. cDNA synthesis was then carried out using Superscript II RNase H^- Reverse Transcriptase (Invitrogen). Each reaction mixture contained 10 μl of RNA solution to which was added 4μl First strand buffer (5X), 1 μl dNTP (10mM), 1 μl DTT (0.1M), 0.25 μl RNase out (40U/ μl), 0.25 μl SuperScript II (200 U/ μl), 2 μl of random hexamers (300ng/ μl) and 1.5 μl DNase,

RNase free water giving a total of 20 µl per reaction mixture. This was incubated at 42°C for 50 minutes following which 30 µl of DNase, RNase free water was added to the mix and the enzymes inactivated by placing the reaction tubes on a 95°C heat- block for 5 minutes. The cDNA was then stored at –20°C till the time of RT- PCR.

Real Time PCR- We employed real- time reverse transcriptase PCR to detect and quantitatively express the production of feline interleukin-12 and GAPDH mRNA. Sequences for the primers and probes were obtained from the literature[26] and purchased from MWG Biotech (High Point, NC).

Feline GAPDH	
Forward- GAPDH.57f	GCC GTG GAA TTT GCC GT
Reverse- GAPDH.138r	GCC ATC AAT GAC CCC TTC AT
Probe- GAPDH.77p	CTC AAC TAC ATG GTC TAC ATG TTC CAG TAT GAT TCC A
IL 12 p40	
Forward- IL12.253f	TGG CTT CAG TTG CAG GTT CTT
Reverse- IL12.333r	TGG ACG CTA TTC ACA AGC TCA
Probe- IL12.283p	CGG TTT GAT GAT GTC CCT GAT GAA GAA GCT

The reporter dye attached covalently at the 5' end was FAM (6- carboxyfluorescin) and the quencher bound to the 3' end was TAMRA (6- carboxytetramethylrhodamine).

Real time PCR was performed using the Applied Biosystems ABI Prism 7000 (Foster City, CA). The amplification protocol was: 2 min at 50°C, 10 min at 95°C, 40 cycles of 15s at 95°C and 60 s at 60°C.

Cycle threshold values were obtained from the ABI software were exported and the $2^{-\Delta\Delta Ct}$ method[27] was used to determine the relative expression of the genes of interest. Briefly, a standard housekeeping gene (eg. GAPDH, β- actin, β_2 microglobulin) is chosen as an internal control gene. This serves to normalize the amount of cDNA loaded for each reaction. An untreated control was selected as the 'calibrator' and the relative expression data is obtained as the fold change in gene expression normalized to the chosen endogenous reference gene and relative to the untreated control.

RESULTS

IL-12 mRNA production is related to the initial cell plating density- Crandell feline kidney cells were plated in six- well tissue culture plates at various initial densities and infected with the Ad *hsp* feline IL-12 gene construct at a MOI of 20. They were allowed to grow exponentially in 2 ml of CrFK media in a humidified incubator at a constant temperature of 37°C and 5% CO_2 concentration. Thirty hours after the virus had been added to the cells, they were lysed, RNA isolated and cDNA synthesized. Real time PCR

Initial cell count per well ($X10^5$)	Confluence	Relative expression
1.44 $X10^5$	30-35%	15.5 ±2.5
3.75 $X10^5$	40-45%	14.8 ± 1.2
5.00 $X10^5$	50-55%	132.6 ± 29.2
1.00 $X10^6$	75-80%	486.3 ± 92.5
1.52 $X10^6$	90-95%	963.8 ± 292.1

Table 1- CrFK cells were infected with Ad *hsp* fIL12 construct. After infection the cells were kept in the incubator for 30 hours at 37°C, 5% CO_2. Column 1 is the cell count per well at the time of infection. Column 2 shows the approximate confluency of cells per well in the six- well tissue culture plate. Column 3 values are expressed as mean ± SD (of triplicates) of fold changes in expression in infected cells over uninfected cells.

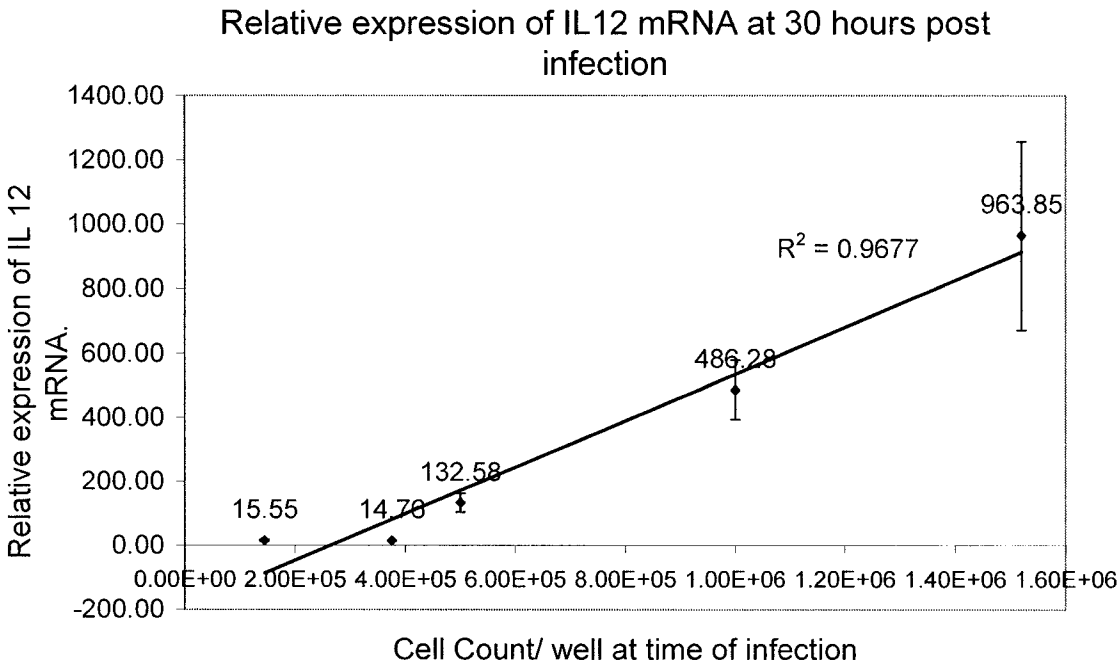

Figure 1 IL-12 mRNA PRODUCTION IS RELATED TO THE INITIAL CELL PLATING DENSITY

CrFK cells were infected with Ad *hsp* fIL12 construct. After infection the cells were kept in the incubator for 30 hours at 37°C, 5% CO_2. The IL12 mRNA expression, used as a marker for *hsp* induction, is linearly related to the cell count per well (and hence plating density). The values are expressed as mean ± SD (of triplicates) of fold changes in expression in infected cells over uninfected cells.

was performed to relatively quantify the amount of IL-12 mRNA. The results (Table 1 and Figure 1) are expressed as a fold increase over the non-treated cells, i.e. cells not infected with the Ad *hsp* feline IL-12 gene construct. The relative increase was linearly related to the cell count at the time of plating and hence the plating density. This was an unexpected finding as these cells had not been heated and therefore no IL-12 production had been expected. Further experiments were then conducted to confirm these observations and try to delineate the factors involved.

Prevention of exponential cell growth inhibits the IL-12 production- Aphidicolin is a specific DNA α- polymerase inhibitor which possesses anti- mitotic and anti- viral properties. It was determined that the addition of aphidicolin in a concentration of 2 μg/ ml effectively inhibited cell growth in the CrFK cells without effecting cell viability (data not shown). To rule out any potential anti- viral properties of aphidicolin we studied the effect of addition of aphidicolin on heat-induced Ad*hsp*fIL-12 production in CrFK cells. The time dependent profile was reduced approximately 1.5 fold, but not completely blocked (Figure 2 a). This confirmed that the addition of aphidicolin did not significantly reduce IL-12 production through anti- adenoviral mechanisms.

Aphidicolin was then added to Ad*hsp*fIL12 infected CrFK cells. The relative expression of IL-12 mRNA increased over the days of the experiment in the control group as seen in Figure 2 b. However, in cells that had not been allowed to divide and grow exponentially, there was no major increase. We postulated that this could be due to the nutritional stress that was being induced in the exponentially growing cells as no fresh nutrient media had been replaced over the three days of the experiment.

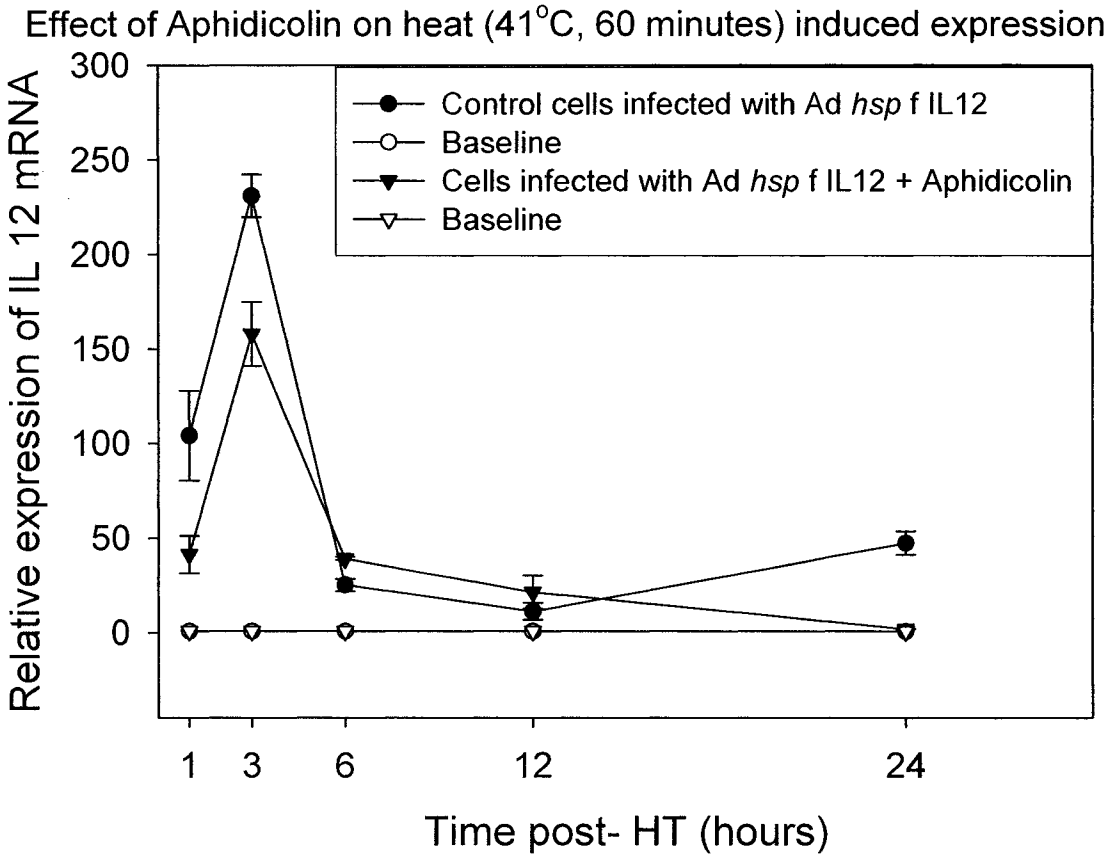

Figure 2a

Figure 2 PREVENTION OF EXPONENTIAL CELL GROWTH INHIBITS IL-12 PRODUCTION

a) To ascertain that the concentration of aphidicolin (2μg/ml) used in our growth inhibition experiments was not anti- adenoviral infected were heated at 41°C for 60 minutes in the presence and absence of aphidicolin. A 1.5 fold decrease was seen in maximal expression for cells with aphidicolin added. However, the overall profiles and trend of expression were similar in the two cases. Each point is mean ± SD of triplicates.

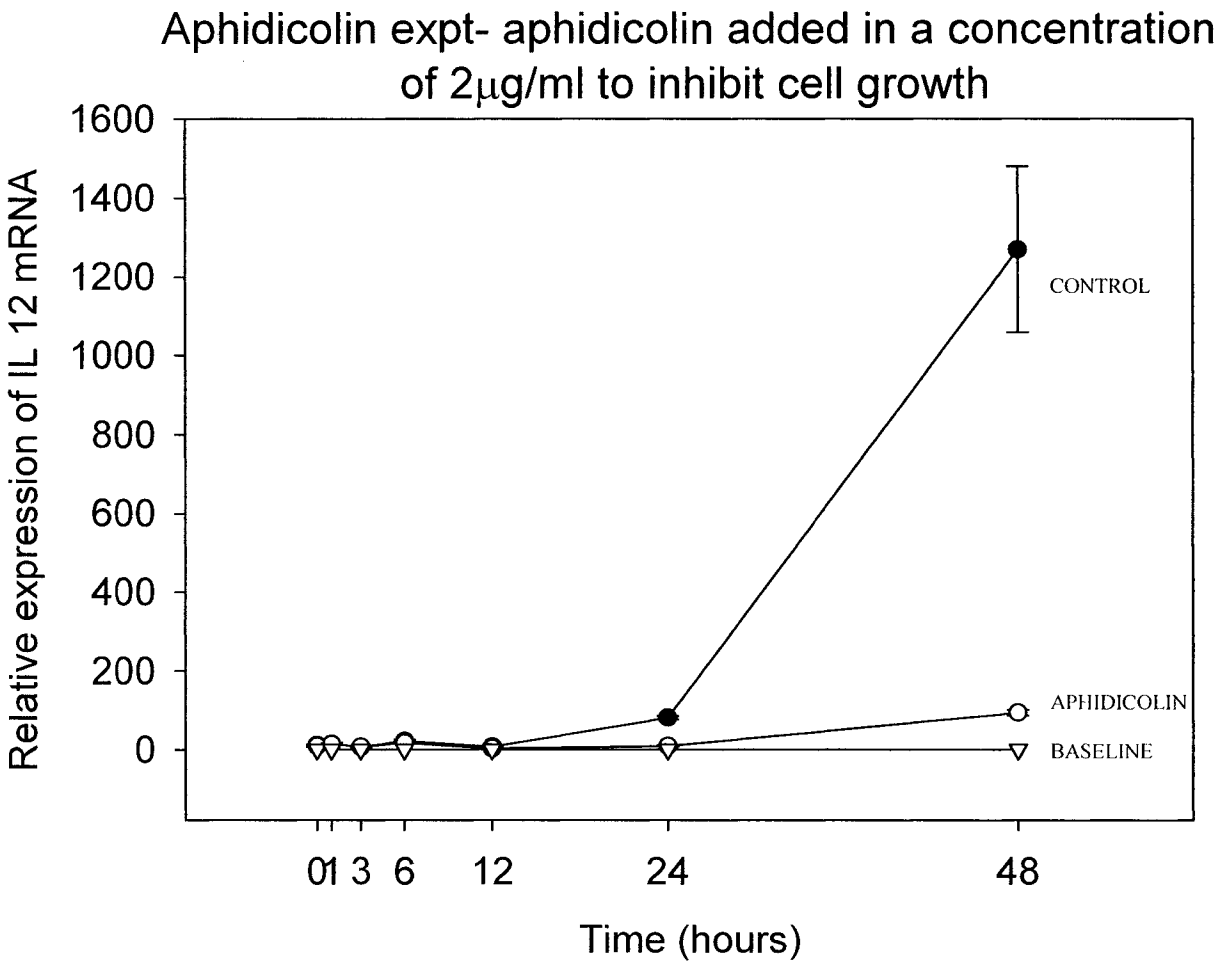

Figure 2b

b) In the control group (closed circles) where the infected CrFK cells were allowed to grow in number exponentially without replacement of media, the relative expression of IL-12 mRNA progressively increased. In cells where the cell growth was inhibited with the addition of aphidicolin (2μg/ml), this increase was effectively inhibited (open circles). Each point is mean ± SD of triplicates.

Regular addition of fresh nutrient media prevents IL-12 production- Two groups of Ad*hsp*fIL-12 infected cells were studied over a period of three days. In both groups, 24 hours were allowed for infection, media containing any free- floating virus was removed, attached cells washed with PBS and fresh media added. Subsequently, in one group (called the 'Media Change' group) 2 ml of fresh nutrient media was replaced every 12 hours. In the other group ('Control'), the media was not replaced and the cells were allowed to grow exponentially in the media where the cellular nutrients would be gradually depleted. At the end of the experiment the number of cells in both groups was determined to be the same (data not shown). In the 'Control' group, large fold increases in feline IL12 mRNA production were seen at the 24-hour and 48-hour time points. This increase was not seen in the 'Media change' group of cells where fresh cellular nutrients were in constant supply (Figure 3).

Deficiencies of major cellular nutrients glucose and glutamine induces hsp- Glucose and glutamine are the major cellular nutrients in the DMEM media. DMEM without these constituents was obtained and glucose and glutamine were added in various concentrations to determine whether the specific absence of these nutrient factors resulted in the induction of *hsp*, and which of the two factors is more important. CrFK cells were infected with Ad *hsp* fIL-12 over a period of 24 hours. The CrFK media was then replaced with media containing glucose supplemented in concentrations of 0 g/L, 1g/L and 4.5 g/L with or without the addition of glutamine at a concentration of 584 mg/L. After 8 hours in this media, real time PCR was performed to determine the levels of IL-12 mRNA (Figure 4a). The high levels of IL-12 mRNA in the cells which were deprived

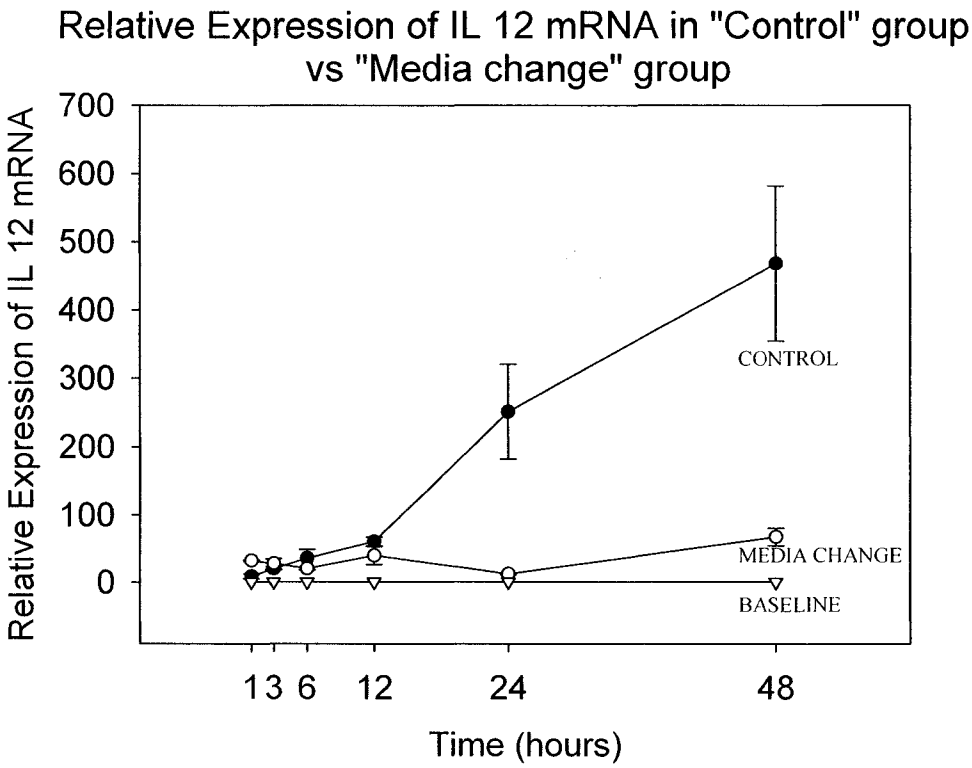

Figure 3 REGULAR ADDITION OF FRESH NUTRIENT MEDIA PREVENTS IL-12 PRODUCTION

CrFK cells were infected and divided into two groups. In the 'Control' group CrFK media added on Day 1 was not replaced over the 48 hours of the experiment. In the 'Media- change' group of cells, fresh nutrient media was replaced every 12 hours. Addition of fresh media prevented fold increase in IL-12 mRNA expression. Each point is mean ± SD of triplicates.

of their nutrients as compared to those cells where the nutrients were present in the recommended concentrations suggested that the *heat shock promoter* is indeed induced by nutritional deficiencies. The inhibition of IL-12 mRNA production in the presence of even one of the two factors suggests that the presence of one is effectively able to compensate for the absence of the other. In the next experiment glutamine was supplemented at increasing concentrations (0 mg/L, 146 mg/L, 292 mg/L, 438 mg/L and 584 mg/L) in the absence of glucose and compared to 'complete' media (Glutamine- 584 mg/L, Glucose 4.5 g/L). Again, the cells were kept in these deficient media for a period of 8 hours after 24 hours of adenoviral infection in complete CrFK media. The results in this case showed a decreasing trend in IL-12 mRNA induction with increasing nutrient supplementation (Figure 4b).

These experiments suggest that specific cellular nutrient deficiency is able to effectively induce the heat shock promoter as evidenced by the expression of feline IL-12 that has been placed under its control.

Intracellular pH becomes more alkaline with increasing cell density- To study changes in pH as a contributory factor for *hsp* induction, CrFK cells were plated in the regular CrFK media containing buffered DMEM. The media pH remained within the ideal range of 7.8 ± 0.5 at high cell concentrations and 100% confluence. Even after ten days of being in the same media, the change in pH was 7.3 to 7.4, the lower limit of normal range.

Intracellular pH was measured using flow cytometry with SNARF-1 as the pH indicator. With increase in cell density a shift in intracellular pH to alkaline was noted. At 30% to

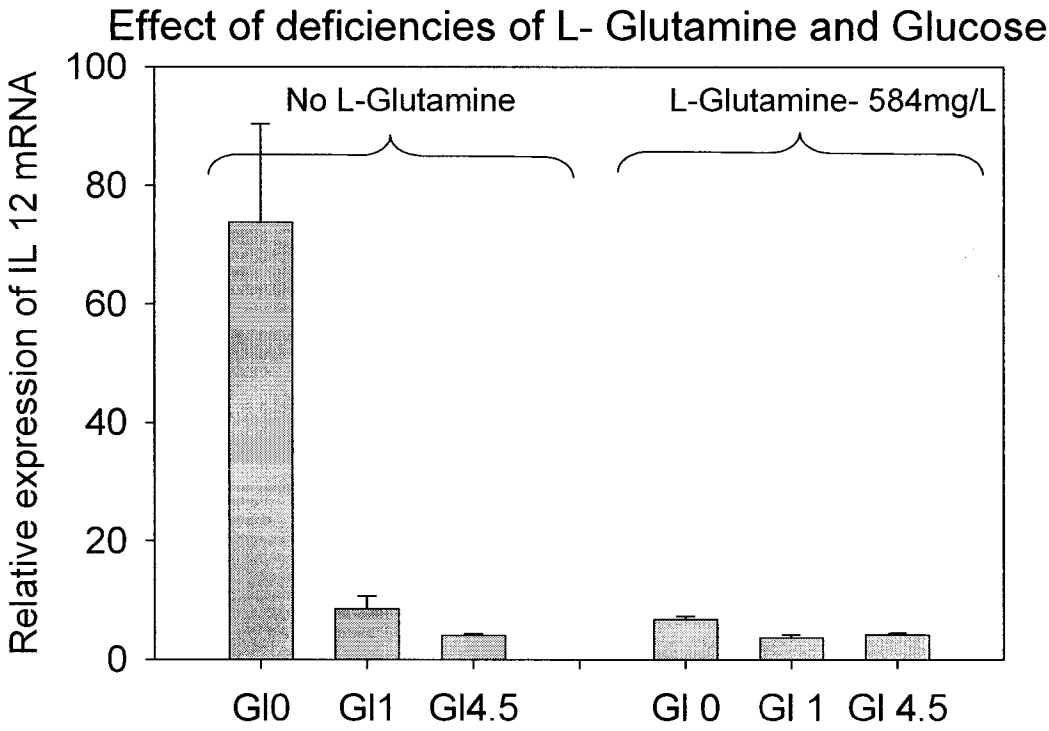

Figure 4a

Figure 4 DEFICIENCIES OF MAJOR CELLULAR NUTRIENTS GLUCOSE AND GLUTAMINE INDUCES HSP

Figure 4a) CrFK cells were infected with the Ad *hsp* fIL12 construct and kept in complete CrFK media for 24 hours, after which this media was replaced with various deficient media for a period of 8 hours. Cells were then lysed, RNA isolated, cDNA synthesized and real- time PCR carried out for relative IL12 mRNA expression. Cells with media deficient in both glucose and glutamine showed the maximal expression. Addition of any of these two nutrient substrates inhibited *hsp* induction. Each bar is mean ± SD of triplicates.

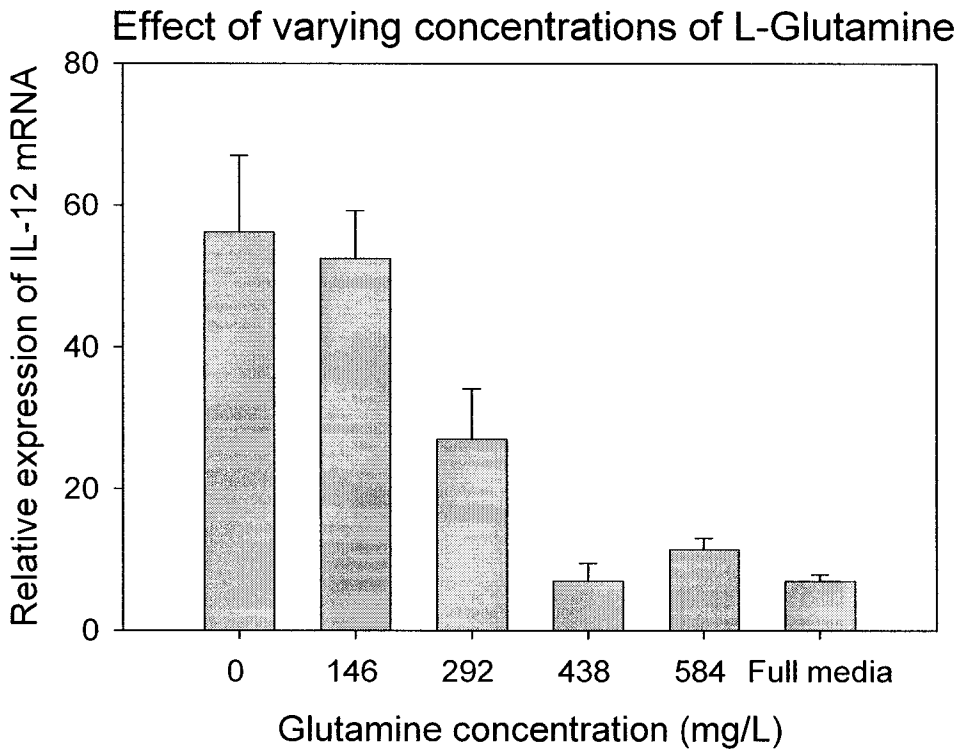

Figure 4b

Figure 4 DEFICIENCIES OF MAJOR CELLULAR NUTRIENTS GLUCOSE AND GLUTAMINE INDUCES HSP

Figure 4b) CrFK cells were infected with the Ad *hsp* fIL12 construct and kept in complete CrFK media for 24 hours, after which this media was replaced with media containing L- glutamine at various concentrations with (Full media) and without glucose (all others) and with or without 10% FBS (as a source of free fatty acids) for a period of 8 hours. There is an inverse relation between L- glutamine concentration and *hsp* induction in the presence of 10% FBS. No difference is seen in the absence of FBS, suggesting a role for ketogenic FFA metabolism in *hsp* induction. Each bar is mean ± SD of triplicates.

40%, 70% to 80% and 100% confluence the intracellular pH values were 7.70±0.02, 7.82±0.05 and 7.85±0.04 respectively.

Production of reactive oxygen species does not induce hsp- H2DCFDA, a reporter dye for ROS production, was used to assess the production of ROS in cells plated at low and high densities. Figures 5a shows the positive control for ROS, cell irradiated to a dose of 10Gy. Cells at low or high density did not show any increased ROS production.

To evaluate the role of reactive oxygen species in the induction of the *heat shock promoter,* CrFK cells were infected with the Ad*hsp*flL-12 construct at an MOI of 20 and after a period of 24 hours of infection the media in the infected cells was replaced by two different types of DMEM media, one with the addition of 10% FBS and the other without FBS. It has been reported in literature that there are reactive oxygen species in DMEM even without the presence of any cells and this can be effectively quenched by the addition of 10% FBS[28, 29]. The two sets of cells were then irradiated to doses of 0Gy, 2Gy, 10Gy and 20Gy using a ^{137}Cs γ- irradiator at a dose rate of 3.9 Gy/min to induce the production of reactive oxygen species. Six hours post treatment was the time point chosen for the lysis of cells and collection of RNA as this time point shows the maximum induction of IL-12 mRNA production post- hyperthermia. These high doses would result in a low clonogenic surviving fraction if plated and observed after a few days. However, we are interested in short- term cellular morphological viability to enable the production of IL-12 by the gene construct using the cellular machinery. The attachment of the CrFK cells to the tissue culture plate was confirmed at the time of cell lysis suggesting that major cell death had not yet occurred. Any manipulation, which would induce the *hsp*,

would result in detectable levels of mRNA at this 6 hours time- point without any significant cell death. However, no difference in the induction of the IL-12 mRNA levels over uninfected cells was seen post- irradiation in both the sets of media. The mRNA levels were actually slightly higher in the unirradiated cells (Figure 5b). The fold increases in the unirradiated cells were similar to those seen when the cells were plated at the same low- density in earlier experiments. Therefore, the production of reactive oxygen species even at doses as high as 20Gy did not induce any IL-12 mRNA over the baseline. These experiments suggest that presence of ROS may not be a contributing factor for *hsp* induction in our selected system.

DISCUSSION

The heat shock promoter has been used as an efficiently inducible promoter in various pre- clinical and clinical settings[4-11]. We have placed the feline IL-12 gene under control of the *hsp* with the intent of combining this with radiation therapy and hyperthermia in a clinical trial in cats with soft tissue sarcomas. The aim is to achieve spatial and temporal control of the expression of potential hematologic and hepatic toxicity of IL-12 protein by intratumoral injections and local tumor hyperthermia.

The use of real-time PCR to quantify relative IL-12 mRNA expression allowed us to detect changes in *hsp* induction in response to cell plating density, inhibition of cell growth, radiation and manipulations in cellular nutrients.

Our *in vitro* experiments revealed that, in our selected system- Crandell feline kidney (CrFK) cells infected with the Ad *hsp* feline IL-12 gene construct, there was significant

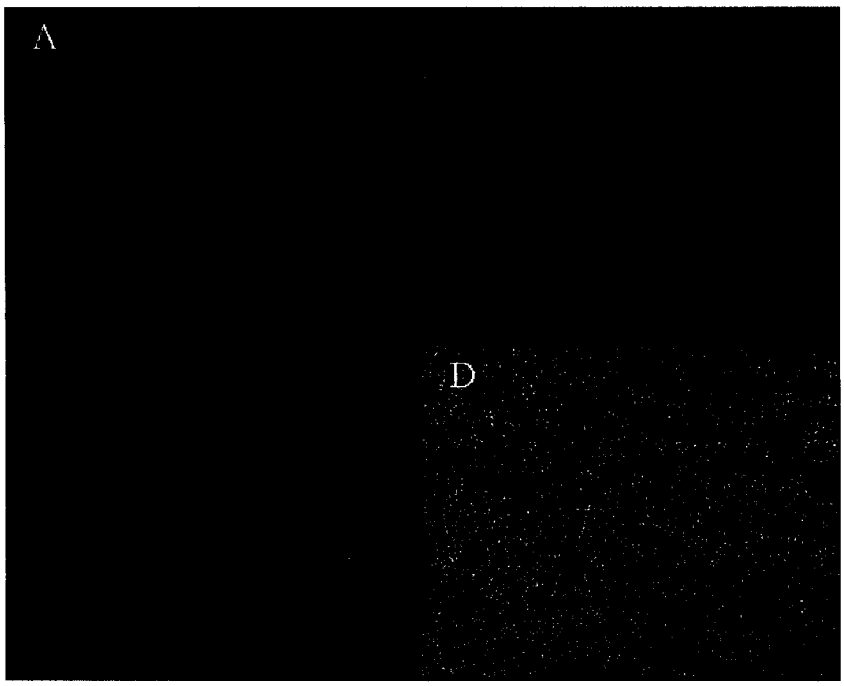

Figure 5a

Figure 5 EFFECT OF ROS
Cells were plated at low and high densities and the presence of ROS was detected using H2DCFDA compared to a positive control (irradiated cells).
Figure 5a) A. CrFK cells irradiated to a dose of 10Gy γ- rays, positive control. B. Cells at low density showing no ROS presence. C. Area of high density not showing any distinct ROS presence. D. Same field as in c, showing the 100% confluence of cells.

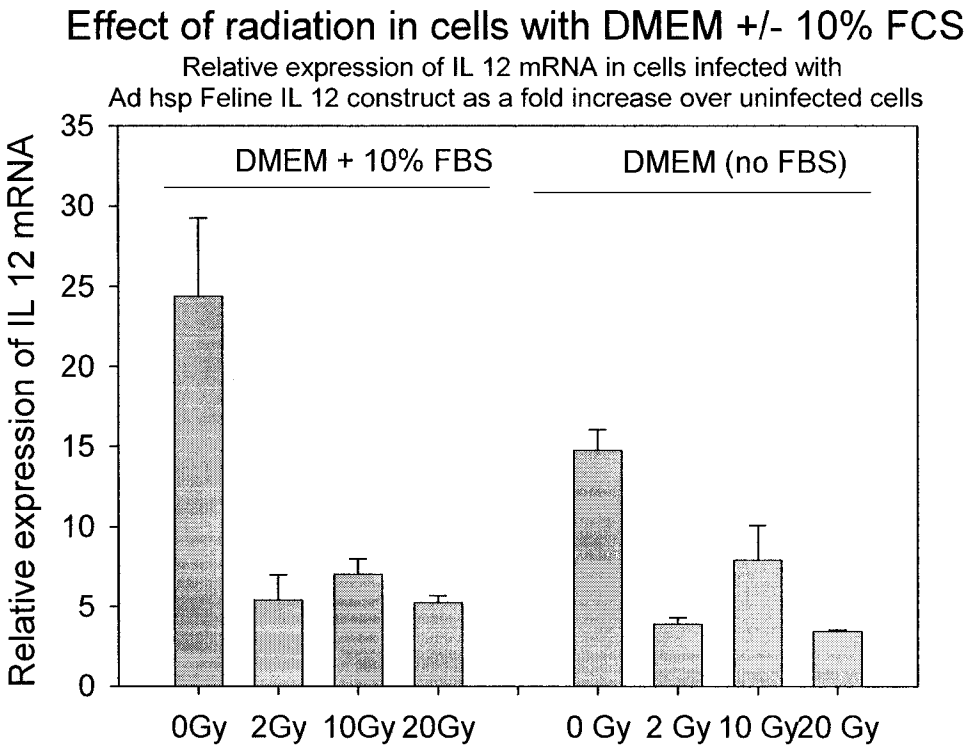

Figure 5b

Figure 5 EFFECT OF ROS

Figure 5b) Ad *hsp* fIL12 infected CrFK cells were allowed to grow in the CrFK media for 24 hours. One hour prior to irradiation, this media was replaced with media with or without 10% FBS (addition of FBS effectively reduces any ROS otherwise present in the DMEM). Reactive oxygen species produced in the cells by radiation did not induce the *hsp* whose activity was assessed by measuring fold increases in IL-12 mRNA. Each bar is mean ± SD of triplicates.

production of IL-12 mRNA in non- heated cells. The initial experiments showed that the relative expression of IL-12 mRNA as a surrogate indicator of *hsp* induction is linearly and proportionally related to the density of cell plating. This suggested that, in addition to hyperthermia, nutritional stress might also play a role in inducing the heat shock promoter. Glucose and glutamine are the main energy providing substrates in cultured mammalian cells. Initial experiments were done using DMEM media deficient in glucose and glutamine to study the effect of varying concentrations of these energy- producing substrates. We found that elimination of both these substrates results in IL-12 mRNA production and the presence of any one of these two negates this effect. This induction can be prevented if the cells are not allowed to grow exponentially and rapidly utilize the specific nutrients in the cell culture media. Aphidicolin is an anti- mitotic and anti- viral DNA α- polymerase inhibitor. We used aphidicolin at a concentration of 2 μg/ml, a concentration that has been shown to be non- toxic to adenoviruses[30-32]. We also confirmed the ability of Ad*hsp*fIL12 infected cells to produce IL-12 mRNA when heated at 41°C for 60 minutes in the presence of aphidicolin.

It has been shown that an alkaline shift of external pH, but not internal pH, induces heat shock proteins in a manner similar to induction by heat[33]. We examined changes in extracellular and intracellular pH in our cells. There was no change in media pH over the days of the experiment and this ruled out extracellular pH as being a contributing factor for *hsp* induction. A shift in intracellular pH to alkaline was noted as the cell density increased. This observation has previously been reported in literature[34].

Ionizing radiation produces reactive oxygen species (ROS) in biological systems. Examples of these ROS molecules are hydrogen peroxide, hydroxyl radical and

superoxide anion. Reactive oxygen species are known to induce the heat shock response[2, 35-37]. Hydrogen peroxide has been shown to induce heat shock protein 70 in cells via the JAK/STAT pathway[37]. We examined the ability of ROS to induce the *hsp* in our system by exposing the infected cells to high doses of radiation (2Gy, 10Gy and 20Gy). The addition of 10% FBS has been reported to effectively inhibit the presence of ROS in DMEM[28, 29]. We assessed *hsp* induction in both the presence and absence of 10% FBS but no IL-12 mRNA was detected in the irradiated cells. There was no ROS presence in the highly confluent cells in culture and also no increased IL-12 mRNA production in cells irradiated to doses of 2, 10 and 20 Gy indicating that in our system ROS might not be a contributing factor for *hsp* induction. These doses of radiation would have resulted in reproductive cell death that would be evident if these cells were plated, allowed to grow and form colonies. However, we harvested these cells 6 hours post radiation. At this time the cells would still be morphologically viable.

Benjamin *et al*[38] studied the effects of glucose deprivation and metabolic inhibitor rotenone on the DNA binding activity of heat shock factor (HSF) in myogenic cells. They found that depletion of cellular ATP stores (less than 30% of control levels) was sufficient stimulus to induce DNA- HSF binding. Changes in pH without ATP depletion failed to activate HSF. It is possible that a similar *hsp* induction is being observed in our system. Deficiency of ATP producing substrates (glucose and glutamine) leads to ATP depletion in the cells with consequent *hsp* induction. In the presence of any one of these substrates, ATP stores do not reach subcritical levels and *hsp* is not induced.

The induction of the *hsp* by nutritional stress and consequent expression of the gene of interest would be advantageous in the nutritionally stressed tumor microenvironment.

After intratumoral injection of an *hsp* controlled construct, the primary method of induction is intended to be local hyperthermia. However, it is known that heat distribution in the tumor is heterogeneous. In such a case, we can still rely on poor tumor nourishment to potentially compensate for uneven heat distribution. It has also been demonstrated by Borrelli *et al* [8] that repeated induction of the *hsp* is possible. Thus, after the primary induction by heat a secondary induction might be seen in response to another inducing factor. This has been demonstrated *in vitro* in our experiments using this construct in conjunction with hyperthermia (Chapter 2).

There is evidence that even after intratumoral injections adenoviral construct leakage and subsequent infection of liver, kidney and lung can occur[7, 10]. This could lead to negative consequences in cases of cancer cachexia especially when a potent cytokine like interleukin-12 is being employed. Cancer cachexia is a term used to describe a condition consisting of severe weight loss, anorexia and fat and muscle wasting. Although no definite association has been shown with stage or duration of the cancer, it generally tends to be more severe in advanced stages. Treatment in the form of chemotherapy and radiation therapy also adversely contributes to cachexia

Numerous metabolic abnormalities are associated with cancer cachexia. Abnormal glucose metabolism is manifested as increased whole body glucose turnover due to decreased use by skeletal muscles and increased hepatic glucose production through the Cori's cycle[39, 40]. There is also glucose intolerance. Blood glucose concentrations are high but the cells are insulin resistant and this elevated glucose is not utilized by the cells for energy needs[40-43]. The tumor cells, on the other hand, start acting like glucose 'traps'. Glucose uptake and lactate release is increased in tumor cells, possibly due type II

hexokinase (HKII) seen in these cells which is unresponsive to regular hormonal and external stimuli[44].

Glutamine is classified as a conditionally essential amino acid. The skeletal muscles are the main storage sites for glutamine, which serves as the primary metabolic fuel for small enterocytes, lymphocytes, macrophages and fibroblasts. Glutamine serves as a non-carbohydrate source of energy via its participation in the Krebs cycle. It is the primary "gluconeogenic" amino acid. Production of glucose from glutamine takes place mainly in the liver. Kidneys can also contribute as much as 25% to whole-body glucose production. Glutamine is also the principal amino acid utilized by tumor cells. Tumors act as a sort of 'nitrogen trap' by exhibiting enzymatic capabilities for selective degradation of essential amino acids[45] and such a 'trap' has been demonstrated for glutamine as well[46]. A sodium- dependent glutamine transporter system has been seen in tumor cells[47]. Blood glutamine levels decrease to less than 50% of normal because of the rapid and massive uptake by tumor cells.

These glucose and nitrogen traps may lead to an overall depletion of the two major energy producing substrates in the body, glucose and glutamine, for the normal cells of the body. If these cells are infected by the adenoviral construct, they may start producing IL-12, thus defeating the main aim of using this approach to limit toxicity.

In conclusion, we have shown that the heat shock promoter may be induced by nutritional deficiency in the infected cells. This may be a consequence of depletion of ATP stores below normal levels. Hence constructs utilizing the heat shock promoter as an inducible promoter should be used with caution especially when the downstream gene is encoding a potent pro- inflammatory cytokine such as IL-12. Interleukin-12, has also been shown

to be one of the cytokine factors mediating cancer cachexia via its downstream product interferon-γ[48-50].

REFERENCES

1. Ritossa F. Discovery of the heat shock response. *Cell Stress Chaperones* 1996;1:97-98.

2. Morimoto RI, Tissiáeres A, Georgopoulos C. The Biology of heat shock proteins and molecular chaperones. Plainview, N.Y.: Cold Spring Harbor Laboratory Press; 1994.

3. Leppa S, Sistonen L. Heat shock response--pathophysiological implications. *Ann Med* 1997;29:73-78.

4. Blackburn RV, Galoforo SS, Corry PM, *et al.* Adenoviral-mediated transfer of a heat-inducible double suicide gene into prostate carcinoma cells. *Cancer Res* 1998;58:1358-1362.

5. Braiden V, Ohtsuru A, Kawashita Y, *et al.* Eradication of breast cancer xenografts by hyperthermic suicide gene therapy under the control of the heat shock protein promoter. *Hum Gene Ther* 2000;11:2453-2463.

6. Huang Q, Hu JK, Lohr F, *et al.* Heat-induced gene expression as a novel targeted cancer gene therapy strategy. *Cancer Res* 2000;60:3435-3439.

7. Lohr F, Hu K, Huang Q, *et al.* Enhancement of radiotherapy by hyperthermia-regulated gene therapy. *Int J Radiat Oncol Biol Phys* 2000;48:1513-1518.

8. Borrelli MJ, Schoenherr DM, Wong A, *et al.* Heat-activated transgene expression from adenovirus vectors infected into human prostate cancer cells. *Cancer Res* 2001;61:1113-1121.

9. Lee YJ, Galoforo SS, Battle P, *et al.* Replicating adenoviral vector-mediated transfer of a heat-inducible double suicide gene for gene therapy. *Cancer Gene Ther* 2001;8:397-404.

10. Lohr F, Huang Q, Hu K, *et al.* Systemic vector leakage and transgene expression by intratumorally injected recombinant adenovirus vectors. *Clin Cancer Res* 2001;7:3625-3628.

11. Li GC, He F, Shao X, *et al.* Adenovirus-mediated heat-activated antisense Ku70 expression radiosensitizes tumor cells in vitro and in vivo. *Cancer Res* 2003;63:3268-3274.

12. Puisieux I, Odin L, Poujol D, *et al.* Canarypox virus-mediated interleukin 12 gene transfer into murine mammary adenocarcinoma induces tumor suppression and long-term antitumoral immunity. *Hum Gene Ther* 1998;9:2481-2492.

13. Seetharam S, Staba MJ, Schumm LP, *et al.* Enhanced eradication of local and distant tumors by genetically produced interleukin-12 and radiation. *Int J Oncol* 1999;15:769-773.

14. Golab J, Zagozdzon R. Antitumor effects of interleukin-12 in pre-clinical and early clinical studies (Review). *Int J Mol Med* 1999;3:537-544.

15. Shi F, Rakhmilevich AL, Heise CP, *et al.* Intratumoral injection of interleukin-12 plasmid DNA, either naked or in complex with cationic lipid, results in similar tumor regression in a murine model. *Mol Cancer Ther* 2002;1:949-957.

16. Liu Y, Ehtesham M, Samoto K, *et al.* In situ adenoviral interleukin 12 gene transfer confers potent and long-lasting cytotoxic immunity in glioma. *Cancer Gene Ther* 2002;9:9-15.

17. Rakhmilevich AL, Janssen K, Hao Z, *et al.* Interleukin-12 gene therapy of a weakly immunogenic mouse mammary carcinoma results in reduction of spontaneous lung metastases via a T-cell-independent mechanism. *Cancer Gene Ther* 2000;7:826-838.

18. Li CY, Dewhirst MW. Hyperthermia-regulated immunogene therapy. *Int J Hyperthermia* 2002;18:586-596.

19. Oppenheim JJ, Feldmann M, Durum SK. Cytokine reference: a compendium of cytokines and other mediators of host defense. San Diego: Academic Press; 2001.

20. Cohen J. IL-12 deaths: explanation and a puzzle. *Science* 1995;270:908.

21. Car BD, Eng VM, Lipman JM, *et al.* The toxicology of interleukin-12: a review. *Toxicol Pathol* 1999;27:58-63.

22. Atkins MB, Robertson MJ, Gordon M, *et al.* Phase I evaluation of intravenous recombinant human interleukin 12 in patients with advanced malignancies. *Clin Cancer Res* 1997;3:409-417.

23. He TC, Zhou S, da Costa LT, *et al.* A simplified system for generating recombinant adenoviruses. *Proc Natl Acad Sci U S A* 1998;95:2509-2514.

24. Graham FL, Smiley J, Russell WC, *et al.* Characteristics of a human cell line transformed by DNA from human adenovirus type 5. *J Gen Virol* 1977;36:59-74.

25. Wieder ED, Hang H, Fox MH. Measurement of intracellular pH using flow cytometry with carboxy-SNARF-1. *Cytometry* 1993;14:916-921.

26. Leutenegger CM, Mislin CN, Sigrist B, *et al.* Quantitative real-time PCR for the measurement of feline cytokine mRNA. *Vet Immunol Immunopathol* 1999;71:291-305.

27. Livak KJ, Schmittgen TD. Analysis of relative gene expression data using real-time quantitative PCR and the 2(-Delta Delta C(T)) Method. *Methods* 2001;25:402-408.

28. Grzelak A, Rychlik B, Bartosz G. Reactive oxygen species are formed in cell culture media. *Acta Biochim Pol* 2000;47:1197-1198.

29. Grzelak A, Rychlik B, Bartosz G. Light-dependent generation of reactive oxygen species in cell culture media. *Free Radic Biol Med* 2001;30:1418-1425.

30. Kwant MM, van der Vliet PC. Differential effect of aphidicolin on adenovirus DNA synthesis and cellular DNA synthesis. *Nucleic Acids Res* 1980;8:3993-4007.

31. Ariga H. Effect of aphidicolin on the elongation step of adenovirus DNA replication in vitro. *Biochem Biophys Res Commun* 1983;113:87-95.

32. Oguro M, Yamashita T, Ariga H, *et al.* Adenovirus DNA synthesized in the presence of aphidicolin. *Nucleic Acids Res* 1984;12:1077-1086.

33. Taglicht D, Padan E, Oppenheim AB, *et al.* An alkaline shift induces the heat shock response in Escherichia coli. *J Bacteriol* 1987;169:885-887.

34. Galkina SI, Sud'ina GF, Dergacheva GB, *et al.* Regulation of intracellular pH by cell-cell adhesive interactions. *FEBS Lett* 1995;374:17-20.

35. Moraitis C, Curran BP. Reactive oxygen species may influence the heat shock response and stress tolerance in the yeast Saccharomyces cerevisiae. *Yeast* 2004;21:313-323.

36. Vacca RA, de Pinto MC, Valenti D, *et al.* Production of reactive oxygen species, alteration of cytosolic ascorbate peroxidase, and impairment of mitochondrial metabolism are early events in heat shock-induced programmed cell death in tobacco Bright-Yellow 2 cells. *Plant Physiol* 2004;134:1100-1112.

37. Madamanchi NR, Li S, Patterson C, *et al.* Reactive oxygen species regulate heat-shock protein 70 via the JAK/STAT pathway. *Arterioscler Thromb Vasc Biol* 2001;21:321-326.

38. Benjamin IJ, Horie S, Greenberg ML, *et al.* Induction of stress proteins in cultured myogenic cells. Molecular signals for the activation of heat shock transcription factor during ischemia. *J Clin Invest* 1992;89:1685-1689.

39. Kokal WA, McCulloch A, Wright PD, *et al.* Glucose turnover and recycling in colorectal carcinoma. *Ann Surg* 1983;198:601-604.

40. Shaw JH, Wolfe RR. Glucose and urea kinetics in patients with early and advanced gastrointestinal cancer: the response to glucose infusion, parenteral feeding, and surgical resection. *Surgery* 1987;101:181-191.

41. Humberstone DA, Shaw JH. Metabolism in hematologic malignancy. *Cancer* 1988;62:1619-1624.

42. Shaw JH, Humberstone DM, Wolfe RR. Energy and protein metabolism in sarcoma patients. *Ann Surg* 1988;207:283-289.

43. Holroyde CP, Reichard GA. Carbohydrate metabolism in cancer cachexia. *Cancer Treat Rep* 1981;65 Suppl 5:55-59.

44. Goel A, Mathupala SP, Pedersen PL. Glucose metabolism in cancer. Evidence that demethylation events play a role in activating type II hexokinase gene expression. *J Biol Chem* 2003;278:15333-15340.

45. Pitot HC, Potter VR, Morris HP. Metabolic adaptations in rat hepatomas. I. The effect of dietary protein on some inducible enzymes in liver and hepatoma 5123. *Cancer Res* 1961;21:1001-1008.

46. de Blaauw I, Heeneman S, Deutz NE, *et al.* Increased whole-body protein and glutamine turnover in advanced cancer is not matched by an increased muscle protein and glutamine turnover. *J Surg Res* 1997;68:44-55.

47. Wasa M, Bode BP, Abcouwer SF, *et al.* Glutamine as a regulator of DNA and protein biosynthesis in human solid tumor cell lines. *Ann Surg* 1996;224:189-197.

48. Matthys P, Dijkmans R, Proost P, *et al.* Severe cachexia in mice inoculated with interferon-gamma-producing tumor cells. *Int J Cancer* 1991;49:77-82.

49. Matthys P, Heremans H, Opdenakker G, *et al.* Anti-interferon-gamma antibody treatment, growth of Lewis lung tumours in mice and tumour-associated cachexia. *Eur J Cancer* 1991;27:182-187.

50. Patton JS, Shepard HM, Wilking H, *et al.* Interferons and tumor necrosis factors have similar catabolic effects on 3T3 L1 cells. *Proc Natl Acad Sci U S A* 1986;83:8313-8317.

Chapter 4

A PHASE I HYPERTHERMIA- INDUCED INTERLEUKIN- 12 GENE-THERAPY TRIAL IN SPONTANEOUSLY ARISING FELINE SOFT TISSUE SARCOMAS

ABSTRACT

Purpose and Objectives

Cytokine genes are the most widely and extensively studied immunostimulatory agents in cancer gene therapy. In several studies, interleukin-12 (IL-12) was the most effective cytokine in inducing the eradication of experimental tumors, preventing development of metastases and eliciting long-term antitumor immunity. Depending on the tumor model, IL-12 can exert anti- tumor activities via T- cells, natural killer (NK) cells, or NKT cells. Induction of cytokines, such as IFN-γ and IFN-inducible protein-l0 (IP10), has also been implicated as a mechanism of antitumor activity of IL-12.

Local and systemic administration of IL-12 protein has been studied in murine models and in Phase I/II human trials. However, IL-12 protein therapy has been limited by dose-dependent toxicity. Local and efficient expression of IL-12 and other cytokine genes in tumors represents an alternative immunotherapeutic approach that may avoid systemic toxicity of recombinant cytokines. To achieve this goal of localizing gene expression, a heat-inducible adenoviral gene therapy vector with feline IL-12 being placed under the control of a heat inducible promoter was developed. The rationale for using this heat shock promoter (hsp70B) is that hyperthermia is most likely to be used as an adjuvant therapy with radiation and chemotherapy in the treatment of cancers. Heating the tumor leads to activation of the *hsp* promoter and subsequent local IL12 production.

Materials and Methods

Thirteen cats with spontaneously arising soft tissue sarcomas presenting for treatment to the Colorado State University- Voss Veterinary Teaching Hospital and the Veterinary Teaching Hospital, NCSU were recruited for a Phase I dose escalation gene therapy trial.

The cats underwent radiation therapy to a total dose of 48 Gy in 16 fractions. Four- five days later the gene construct was injected intratumorally. 24 hours post- injection the tumor was heated to a target temperature of 41°C for 60 minutes using a microwave applicator. Cats were treated at increasing dose levels of viral construct. Tumor expression of cytokines interleukin-12 (IL-12) and interferon- γ (IFN- γ) was quantitatively determined using Real time PCR. The cats were monitored for hematologic and hepatic toxicity.

Results

High intratumoral levels of interleukin-12 were achieved with very low or absent interferon-γ. This could possibly be attributed to (1) In the large tumors there were low levels of IL- 12 due to low mutiplicity of infection (2) Even with high levels of IL 12 there were not enough of IL 12 target cells in the tumor (T- cells, NK cells) post- RT to produce IFN-γ (3) Inhomogeneous heat distribution in the tumor, some parts were heated to 45°C- 46°C, resulting in direct hyperthermia induced cytotoxocity and these cells were not able to produce IL-12. Hematologic and hepatic toxicity were dose dependent.

Conclusions

It is possible to limit the toxicity of interleukin- 12 using the hyperthermia induced gene-therapy approach. Cats with spontaneously arising soft tissue sarcomas serve as an excellent model for the study of this approach that can be similarly applied to human cancer treatment.

INTRODUCTION

Effective eradication of established tumors and generation of a lasting systemic immune response with a simple gene delivery system are important goals for cancer gene immunotherapy.

Cytokine genes are the most widely and extensively studied immunostimulatory agents in cancer gene therapy [1, 2]. In several studies, interleukin-12 (IL-12) was the most effective cytokine in inducing the eradication of experimental tumors, preventing development of metastases, and eliciting long-term antitumor immunity [3, 4]. Depending on the tumor model, IL-12 can exert anti- tumor activities via T cells [5-9], NK cells [10-14], or NKT cells[15]. Induction of cytokines, such as IFN-γ [5, 16-19] and IFN-inducible protein-10[20], has also been implicated as a mechanism of antitumor activity of IL-12.

In addition to its immunostimulatory properties, IL-12 possesses anti- angiogenic effects, thus inhibiting tumor formation and metastases [10, 21]. Angiogenesis, the process leading to the formation of new vessels from a preexisting vascular network, is essential for the growth, invasion, and metastasis of solid tumors.

Local and systemic administration of IL-12 protein has been studied in various murine models [5, 6, 13, 22] and in Phase I/II human trials [23, 24]. However, IL-12 protein therapy has been limited by dose-dependent toxicity [25]. Local and efficient expression of IL-12 and other cytokine genes in tumors represents an alternative immunotherapeutic approach that may avoid systemic toxicity of recombinant cytokines [7, 26, 27].

Intratumoral injections of adenoviral vectors or IL-12 plasmid DNA, naked or in complex with cationic lipid [28] have been tried to deliver therapeutic IL-12 with the rationale that IL-12 will be produced only in the virally infected tumors, thereby reducing systemic side

effects. A few reports have indicated the efficacy of this approach [29-31]. However, elevated systemic transgene levels are still observed in many cases as adenovirus can reach the circulation [32-34] and infect other organs; and the promoters in most previous reports are constitutively active, such as cytomegalovirus (CMV) based promoters. This combination makes it likely that intratumoral injection of this constitutively active adenovirus approach will still result in toxicity [35, 36].

To achieve this goal of localizing gene expression, a heat-inducible adenoviral gene therapy vector with murine IL-12 being placed under the control of a heat inducible promoter was developed at Duke University. The rationale for using this heat shock promoter (hsp) is that hyperthermia is most likely to be used as an adjuvant therapy with radiation and chemotherapy. Heating the tumor leads to activation of the *hsp* promoter and subsequent local IL12 production.

The feasibility of combining fractionated radiotherapy, hyperthermia and heat inducible gene therapy in a nonimmunogenic B16.F10 melanoma line that is syngenic with C57BL/6 mice was studied [37]. It was concluded that hyperthermia-regulated gene therapy in combination with radiation is feasible and therapeutically effective in murine tumors with no apparent systemic toxicity [37, 38].

Further, using the same scheme an adenoviral construct was developed with the feline IL12 gene replacing the murine IL-12 gene. This gene construct was studied in a phase I dose escalation trial in spontaneously arising feline soft tissue sarcomas. The main aim of this trial was to establish the maximum tolerated safe dose of the viral construct. The hypothesis being tested was that hyperthermia would induce high local intratumoral

levels of interleukin-12 with minimal circulating IL-12 and consequently reduce toxicity associated with the molecule.

MATERIALS AND METHODS

Patients- Client owned cats with spontaneously arising soft tissue sarcomas presenting for treatment to the Colorado State University (CSU) and North Carolina State University (NCSU) Veterinary Teaching Hospitals were recruited into the trial. Written, informed consent was obtained from the owners for inclusion in the trial.

The eligibility criteria were (1) Feline sarcomas with measurable disease (2) Prior surgery and chemotherapy acceptable (3) No prior radiation therapy (4) Metastasis acceptable (5) Health status able to complete 3 month study.

The staging studies included (1) Complete blood count (2) Serum chemistry (3) Urinalysis (4) Tumor biopsy (5) Metastasis check (6) Abdominal radiographs (7) CT scan for radiation therapy treatment planning.

A total of 13 cats were treated from July 2003 to March 2005. Eight received treatment at CSU and five at NCSU.

Design of vector- The AdEasy system (Stratagene) was used to construct the adhspfIL12. The two subunits (p35 and p40) of the feline IL-12 were amplified from cDNA of CRFK cell line and sequence-verified. They were then connected into one gene expression unit by use of a flexible linker sequence (Gly4Ser). A 400-bp hsp70B promoter was then used to control the expression of the modified feline IL-12 gene. The whole hsp-fIL12 gene expression cassette was then transferred into an adenovirus shuttle plasmid. The shuttle

plasmid was cotransfected into 293 cells to derive adhspflL12. Amplification and isolation of the virus was achieved following standard protocols[39, 40].

Radiation therapy- The cats were immobilized by administering general anesthesia and received radiation therapy using a 6MV linear accelerator (Siemens) at CSU and a telecobalt machine at NCSU. The total dose delivered was 48Gy in 16 fractions over 22 days. Treatment was started on Tuesday or Wednesday and hence finished on Tuesday or Wednesday of the third week, treating 5 days a week.

Gene injections- The intratumoral gene injections were delivered on the first Monday after completion of radiation therapy. There was, thus, a gap of 3-5 days between the end of radiation therapy and administration of the gene injection. The tumor dimensions were determined based on caliper and CT scan measurements. Tumor volume was calculated as (length X breadth X depth X $\pi/6$) cm^3. The viral construct (Ad*hsp*flL-12) was diluted in normal saline to a volume equal to 30% of the tumor volume. Needles were placed in the tumor in a 1cm X 1cm grid pattern. A CT scan was performed to ascertain that the needles were parallel, equidistant and reached the deep surface of the tumor. Necessary adjustments were made till the above conditions were satisfactorily met.

The total volume of injection was divided by the number of injection sites and equal volumes injected at each site (Figure 1). While injecting, the needle was gradually drawn out of the tumor vertically so as to inject along the needle track. Theoretically, each track would form a cylinder with a $1cm^2$ cross-sectional area using this injection technique.

Hyperthermia- Twenty- four hours were allowed for physical diffusion of the injected construct and adenoviral infection of the tumor cells. On Tuesday, two plastic catheters were placed in the tumor under CT scan guidance. Thermocouples for intratumoral temperature measurement would later be placed in these catheters during hyperthermia treatment. Local tumor hyperthermia was delivered using a 433 MHz microwave applicator. Deionized water was used as a coupling medium. Skin temperature was kept below 39^0C using a circulating water bolus (Figure 2). During hyperthermia the tumor temperature was manually measured at 3-5mm intervals using the thermocouple probes. The thermometers were calibrated before each treatment. The planned dose was 41^0C for 60 minutes. Recorded temperatures were entered into a database to calculate the hyperthermia dose parameters.

Biopsies- Core tissue biopsies were obtained using a 22-mm throw automated biopsy device (Manan Pro-Mag 2.2, Manan Medical Products, Northbrook, IL) with a 14- gauge needle. They were collected from the tumor during the week of gene therapy. In larger tumors biopsies were done on all days from Monday to Thursday. In the smaller tumors all four biopsies were not possible therefore tumor biopsies were collected only for Monday (baseline) and Wednesday (24 hours post- HT). All biopsies were performed under anesthesia and snap frozen in liquid nitrogen. They were stored at -80^0C till further processing.

Blood investigations- Blood samples were drawn through the jugular vein for CBC and chemistry panel. Hematologic and hepatic toxicities were assessed from blood investigation reports and graded based on values outlined in Table 1.

Cell lysis and RNA Isolation- The tumor tissue samples were lysed and RNA isolated using TRIzol Reagent (GibcoBRL) as per manufacturer's protocol. RNA purity was assessed spectrophotometrically.

cDNA synthesis- Total isolated RNA was treated with DNase I (Invitrogen) to remove any genomic DNA. cDNA synthesis was then carried out using Superscript II RNase H^- Reverse Transcriptase (Invitrogen, Carlsbad, CA). Each reaction mixture contained 10 µl of RNA solution to which was added 4µl First strand buffer (5X), 1 µl dNTP (10mM), 1 µl DTT (0.1M), 0.25 µl Rnase out (40U/ µl), 0.25 µl SuperScript II (200 U/ µl), 2 µl of random hexamers (300ng/ µl) and 1.5 µl DNase, RNase free water giving a total of 20 µl per reaction mixture. This was incubated at 42°C for 50 minutes following which 30 µl of DNase, RNase free water was added to the mix and the enzymes inactivated by placing the reaction tubes on a 95°C heat- block for 5 minutes. The cDNA was then stored at – 20°C till the time of RT- PCR.

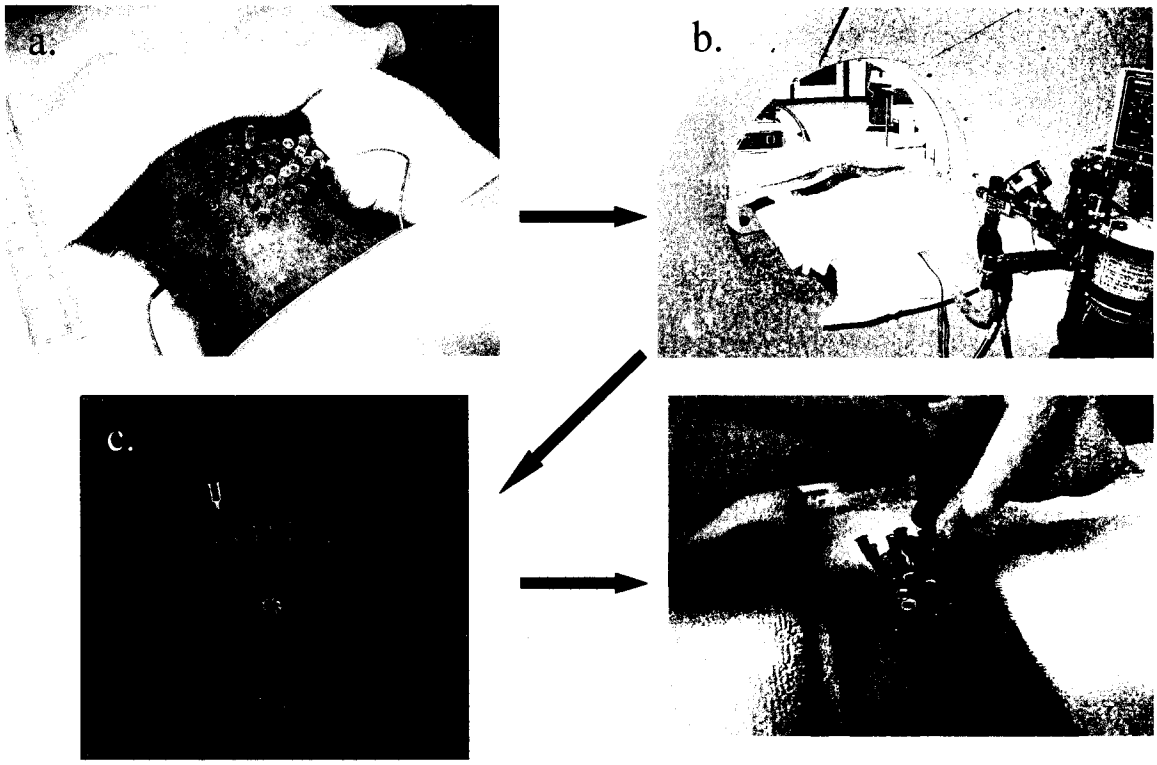

Figure 1- GENE INJECTION ON MONDAY
Figure 1a- Placement of needles in the tumor in a 1cmX1cm grid pattern.
Figure 1b- CT scan.
Figure 1c- Confirmation of placement of the needles.
Figure 1d- Injection of the diluted construct through each needle.

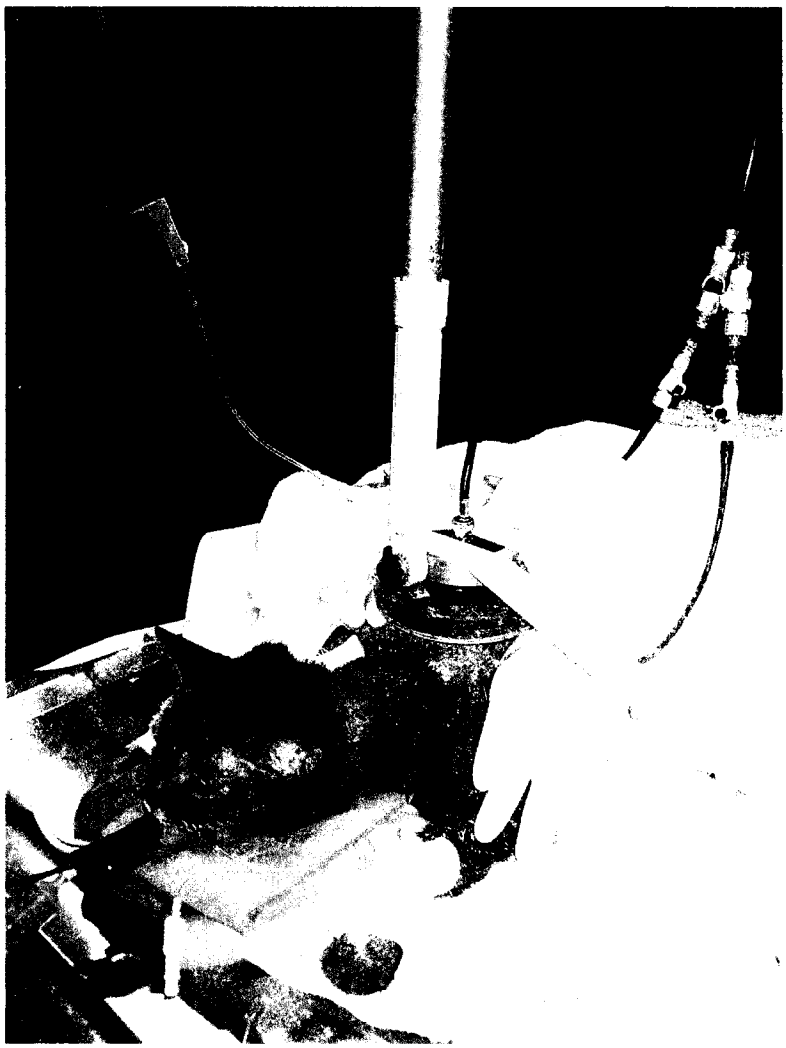

Figure 2- Hyperthermia delivered using a microwave applicator with the cat under anesthesia.

TOXICITY GRADING TABLE

SYSTEM	NORMAL	MILD TOXICITY	MODERATE TOXICITY	SEVERE TOXICITY
Hematologic				
- WBC ($X10^3/\mu l$)	5-17	3-5	2-3	<2
- Granulocytes ($X10^3/\mu l$)	4-10	2-4	1-2	<1
- Platelets ($X10^3/\mu l$)	150-500	80-150	40-80	<40
- PCV (%)	28-50	NA	15-28	<15
Hepatic				
- ALT (IU/L)	17-59	60-150	151-400	>400
- Alk. phos (IU/L)	2-40	41-120	121-400	>400
- Albumin (g/dL)	2.8-4.5	2.2-2.8	1.8-2.2	<1.8
- Bilirubin (mg/dL)	0-0.2	0.2-2.0	2.0-2.5	>2.5

Modified from National Cancer Institute (NCI) Common Toxicity Criteria (CTC) Version 2.0

Table 1- Toxicity grading table used in this study.

Real- time PCR- Real- time reverse transcriptase PCR was used to detect and quantitatively express the production of feline interleukin-12, interferon-γ and GAPDH mRNAs.

Sequences for the primers and probes were obtained from the literature[41] and purchased from MWG Biotech (High Point, NC).

Feline GAPDH

Forward- GAPDH.57f	GCC GTG GAA TTT GCC GT
Reverse- GAPDH.138r	GCC ATC AAT GAC CCC TTC AT
Probe- GAPDH.77p	CTC AAC TAC ATG GTC TAC ATG TTC CAG TAT GAT TCC A

IL 12 p40

Forward- IL12.253f	TGG CTT CAG TTG CAG GTT CTT
Reverse- IL12.333r	TGG ACG CTA TTC ACA AGC TCA
Probe- IL12.283p	CGG TTT GAT GAT GTC CCT GAT GAA GAA GCT

IFN- γ

Forward- IFN.141f	TGG TGG GTC GCT TTT CGT AG
Reverse- IFN. 225r	GAA GGA GAC AAT TTG GCT TTG AA
Probe- IFN. 152p	CAT TTT GAA GAA CTG GAA AGA GGA GAG TGA TAA AAC AAT

The reporter dye attached covalently at the 5' end was FAM (6- carboxyfluorescin) and the quencher bound to the 3' end was TAMRA (6- carboxytetramethylrhodamine).

Real time PCR was performed using the Applied Biosystems ABI Prism 7000 (Foster City, CA). The amplification protocol was: 2 min at 50°C, 10 min at 95°C, 45-50 cycles of 15s at 95°C and 60 s at 60°C. Cycle threshold values were obtained from the ABI software and the $2^{-\Delta\Delta Ct}$ method[42] was used to determine the relative expression of the genes of interest. Briefly, a standard housekeeping gene (eg. GAPDH, β- actin, β_2 microglobulin) is chosen as an internal control gene. This serves to normalize the amount of cDNA loaded for each reaction. An untreated control is selected as the 'calibrator'. The relative expression data is then obtained as the fold change in gene expression normalized to the chose endogenous reference gene and relative to the untreated control. By definition, the fold change in gene expression relative to the untreated control equals one.

Prior to using the $2^{-\Delta\Delta Ct}$ method for relative quantification, we validated its use for the primer and probe sequences and PCR conditions being employed in our experimental conditions. The methods and acceptable results are described in literature[42, 43]. Briefly, the target cDNA was serially diluted and real time PCR performed. Cycle threshold values for the serially diluted samples are plotted on a graph with the log dilution on the X- axis and cycle threshold values on the Y- axis. The slope of the line is used to obtain the efficiency of PCR amplification using the formula- Efficiency = $10^{(-1/slope)}$-1.

RESULTS

The results in this chapter have been divided into a detailed results section and a summarized results section. In the detailed results section all characteristics of each case included in the study are described including tumor dimensions, dose level, number of injection sites, hyperthermia data, cytokine production, toxicity and surgical histopathology. This serves to have all data assimilated and presented in one place for future reference.

The summarized results section is designed with the intent of using it for journal publication purposes. Table 2 shows the hyperthermia data for all cats. T50 and T90 signify the temperatures received by at least 50% or 90% of the tumor respectively.

Tmin and Tmax are the minimum and maximum temperatures recorded during the 60 minutes of treatment. As can be seen, the goal of delivering 41^0C for 60 minutes was reached in almost all the cases for about 50% of the tumor volume.

Table 3 has details of the dose levels, tumor volume, injection sites and cytokine production. There does not appear to be a correlation between tumor volume and IL-12 mRNA fold increase. Possible reasons for this are presented in the discussion section.

There was no IFN-γ detected in most cases at the 10^9 pfu and 10^{10} pfu dose levels. Four of five cases in the high dose ($4X10^{10}$ pfu) dose group showed detectable and calculable fold- increases in IFN-γ mRNA levels. However, this did not appear to correlate with the IL-12 induction in the same tumors. Possible reasons for this are also discussed.

Table 4 summarizes the worst grade of hematologic or hepatic toxicity noted during the week of gene therapy. Toxicities were seen to increase with dose.

In the detailed results section, it can be seen that most cats with detectable increases in IFN-γ levels had non- normal clinical courses. Apart from the hematologic and hepatic toxicity detectable by blood investigations, Cat no. 11 also had refusal to feed requiring placement of a feeding tube and pulmonary edema resulting in delayed surgery.

HYPERTHERMIA DATA

Cat no.	T50 (^{0}C)	T90 (^{0}C)	Tmin (^{0}C)	Tmax (^{0}C)
1	40.4	39.0	39.0	44.6
2	41.1	39.4	39.4	43.2
3	41.0	38.6	38.6	45.3
4	40.7	39.9	39.9	43.0
5	41.5	40.6	39.8	43.5
6	40.8	38.9	36.6	45.2
7	41.3	40.1	37.0	42.4
13	41.1	39.8	39.5	42.7
8	40.9	37.5	35.4	45.7
9	41.5	39.5	38.3	44.2
10	40.9	39.9	38.7	42.2
11	41.5	40.4	39.2	44.0
12	41.5	40.2	39.5	43.2

Table 2- Hyperthermia data for all cats. Cat no. 13 was treated at 10^{10} pfu dose level and hence has been placed between nos. 7 and 8.

Results

Cat no.	Dose level (pfu/tumor)	Tumor Volume (cm^3)	Injection sites	IL-12 mRNA (relative fold increase over baseline, 24 hours post- HT)	IFN-γ mRNA (relative fold increase over baseline, 24-48 hours post- HT)
1	10^9	130.0	38	2.7 ± 0.3	Trace (+/-)[@]
2	10^9	1.1	2	19 000[*] ± 5233	Trace (+/-)
3	10^9	26.0	15	97 ± 7	6.2 ± 0.9
4	10^{10}	2.5	2	3028 ± 114	Trace (+/-)
5	10^{10}	1.6	2	1685 ± 184	Trace (+/-)
6	10^{10}	12.4	16	358 ± 30	Trace (+/-)
7	10^{10}	2.3	2	3841 ± 643	Trace (+/-)
13	10^{10}	1.9	4	1858 ± 691	Trace (+/-)
8	$4X10^{10}$	5.0	10	1318 ± 312	42 ± 20
9	$4X10^{10}$	31.7	27	7043[#] ± 1145	1.7 ± 0.2
10	$4X10^{10}$	1.5	5	29 565 ± 9208	Trace (+/-)
11	$4X10^{10}$	37.0	20	14 658 ± 2055	152 ± 34
12	$4X10^{10}$	28.8	25	2793 ± 489	6.2 ± 2.5

[@]- IFN-γ production detectable in some PCR wells as increase in the real-time amplification curve, but not unequivocal

[*]- 48 hours post- HT, only one extra tumor biopsy possible due to small tumor size

[#]- Cat febrile after gene injection on Monday for approx. 12 hours

Table 3- Cytokine production data in all cats.

Toxicity summary

Cat no.	Dose level (pfu/tumor)	Hematologic*				Hepatic			
		W	G	Plt	PCV	ALT	ALP	Alb	Bili
1	10^9	**S**	Mo	N	Mo	N	N	Mi	N
2	10^9	Mi	Mi	N	Mo	Mi	N	N	N
3	10^9	N	N	N	N	N	N	N	N
4	10^{10}	Mi	Mi	Mi	Mo	Mi	N	N	Mi
5	10^{10}	Mo	Mo	Mi	Mo	Mi	Mi	N	Mi
6	10^{10}	Mo	Mo	Mi	Mo	Mi	Mi	N	Mi
7	10^{10}	Mi	Mi	N	N	Mi	Mi	N	Mi
13	10^{10}	Mi	Mi	Mi	N	Mi	N	N	N
8	$4X10^{10}$	Mi	Mi	**S**	**S**	Mo	N	Mi	**S**
9	$4X10^{10}$	Mi	Mi	Mi	Mo	N	N	Mi	Mi
10	$4X10^{10}$	Mo	Mi	Mi	N	N	N	N	N
11#	$4X10^{10}$	Mi	Mi	**S**	**S**	Mi	N	Mi	Mi
12	$4X10^{10}$	N	N	Mi	**S**	N	N	**S**	**S**

*- Drop in granulocyte counts seen in all cases approx. 48-72 hours post- HT
#- Also had pulmonary edema

W- WBC, G- granulocytes, Plt- platelets, PCV- packed cell volume, ALT- alanine aminotransferase, ALP- alkaline phosphatase, Alb- serum albumin, Bili- total bilirubin

N- normal, Mi- mild toxicity, Mo- moderate toxicity, S- severe toxicity

Table 4- Hematologic and hepatic toxicity table.

RESULTS (Detailed)

Cat No. 1

Name- SHADOW, Mettert

Treated at- Colorado State University

Radiation dose- 48 Gy/16 fractions

Week of gene therapy and hyperthermia- 7.7.03 to 7.11.03

Tumor dimensions- 8.5cm x 6.5cm x 4.5cm

Tumor volume- 130 cm^3

Dose of viral construct- 10^9 pfu

Number of intratumoral injection sites- 38

Hyperthermia Data-

T50 (^oC)- 40.4
T90 (^oC)- 39.0
Tmin (^oC)- 39.0
Tmax (^oC)- 44.6

Cytokine production

	Interleukin-12	Interferon- γ
Monday	Baseline (1)	Baseline (1)
Tuesday	1.0 ± 0.1	Nil
Wednesday	2.7 ± 0.3	+/-
Thursday	Nil	Nil

Toxicity table

	WBC	GRAN	LYM	PLT	PCV	ALT	ALP	ALB	T BILI	BUN	CRE
Mon (7/7/03)	3.6	3	0.4	299	19	36	8	2.3	0.2	18	1.1
Tue (7/8/03)	4.2	3.9	0.1	373	22	42	7	2.4	0.2	13	1.0
Wed (7/9/03)	3.6	3.3	0.2	303	22	42	8	2.4	0.2	11	1.0
Thu (7/10/03)	1.8	1.4	0.3	234	17	39	9	2.3	0.2	13	1.0
Fri (7/11/03)	3.2	2.8	0.4	288	24	43	11	2.6	0.2	12	1.0
Tue (7/15/03)	6.8	6.1	0.3	535	36	50	16	3	0.2	25	1.1
Mon (7/28/03)	6.4	5.2	0.8	326	38	36	12	3	0.1	22	1.2

Histopathology (7/29/03)

History: Previous radiation therapy and gene study.

DIAGNOSIS: Soft tissue sarcoma.

REMARKS: This neoplasm is consistent with vaccine-associated sarcoma.

Soft tissue mass (interscapular, per history) contains diffuse sheets of disorganized spindloid cells forming streaming bundles and occasional palisades interspersed with dense collagen bundles. Spindle cells are moderately/markedly pleomorphic with ovoid/spindloid euchromatic nuclei with prominent nucleoli and finely- stippled chromatin. Cytoplasm is faintly basophilic with indistinct cytoplasmic margins. There are 4-6 mitotic figures per high power field. There are abundant multinucleated cells with variable nuclear morphology which is similar to that of spindle cells. There is extensive fibroplasia and necrosis. There are multifocal, regionally moderate aggregates of lymphocytes and plasmacytes with few macrophages.

(The margins have not been commented upon as the surgeons did not aim at complete surgical resection due to extensive disease. A complete resection would have entailed highly morbid surgery and was thus decided against.)

Cat No. 2

Name- CALLIE, Brink

Treated at- North Carolina State University

Radiation dose- 48 Gy/16 fractions

Week of gene therapy and hyperthermia- 10.27.03 to 10.31.03

Tumor dimensions- 1.1cm x 1.7cm x 1.1cm

Tumor volume- $1.07cm^3$

Dose of viral construct- 10^9 pfu

Number of intratumoral injection sites- 2

Hyperthermia Data-

T50 (^oC)- 41.1
T90 (^oC)- 39.4
Tmin (^oC)- 39.4
Tmax (^oC)- 43.2

Cytokine production

	Interleukin-12	Interferon- γ
Monday	Baseline (1)	Baseline (1)
Tuesday	-	-
Wednesday	-	-
Thursday	19 000 ± 5 233	+/-

Toxicity table

	WBC	GRAN	LYM	PLT	PCV	ALT	ALP	ALB	T BILI	BUN	CRE
Mon (10/27/03)	3.6	3.31	0.11	n	34	86	21	3.2	0.1	26	1.4
Tue (10/28/03)	4.3	3.83	0.22	n	32	75	19	3.1	0.2	13	1.3
Wed (10/29/03)	3.9	3.16	0.23	n	25	57	14	2.9	0.2	17	1.3
Thu (10/30/03)	4.1	3.36	0.49	n	30	62	17	3.0	0.2	15	1.3
Fri (10/31/03)	4.3	3.23	0.52	n	41	43	20	3.3	0.2	18	1.6

Histopathology

Received for histopathology is the right forelimb. On the lateral aspect of the scapula, there is a subcutaneous, firm, L-shaped mass, measuring 1.5 x 1cm. This mass is 4cm from the anterior and caudal margins, and 3.5cm from the dorsal margin. The axillary lymph node is identified and measures approximately 0.5cm. Subcutaneous mass, slides 1 and 2: Two sections of mass are examined. The mass is composed of abundant hyalinized stromal material forming multiple coalescing nodules with scattered, individualized cells. These cells resemble macrophages or stromal cells. There are individual necrotic cells within the mass. There are multifocal peripheral infiltrates of lymphocytes and plasma cells around the mass. Subcutaneous mass, right scapular area: Soft tissue stromal cell mass with extensive hyalinization. The hyalinization of the soft tissue mass is consistent with previous radiation to the tissue and obscures morphology of the neoplastic cells. Because of the radiation-induced changes, only individual stromal cells are seen scattered in the hyalinized matrix and discrete viable cellular mass is not seen. There is no evidence of neoplastic cells in the skin and soft tissue margins or in the axillary lymph node.

Cat No. 3

Name- BELLA, Chappell

Treated at- North Carolina State University

Radiation dose- 48 Gy/16 fractions

Week of gene therapy and hyperthermia- 12.1.03 to 12.5.03

Tumor dimensions- 3.8cm x 3.9cm x 3.4cm

Tumor volume- $26cm^3$

Dose of viral construct- 10^9 pfu

Number of intratumoral injection sites- 15

Hyperthermia Data-

T50 (°C)- 41.0
T90 (°C)- 38.6
Tmin (°C)- 38.6
Tmax (°C)- 45.3

Cytokine production

	Interleukin-12	Interferon- γ
Monday	Baseline (1)	Baseline (1)
Tuesday	-	-
Wednesday	97 ± 7	6.2 ± 0.9
Thursday	1.2 ± 0.4	Nil

Toxicity table

	WBC	GRAN	LYM	PLT	PCV	ALT	ALP	ALB	T BILI	BUN	CRE
Mon (12/1/03)	8.2	7.29	0.41	n	39	60	16	3.3	0.2	32	1.5
Tue (12/2/03)	8.0	7.52	0.16	249	30	60	15	3.0	0.2		1.4
Wed (12/3/03)	8.6	7.57	0.52		30	50	15	2.9	0.2	26	1.7
Thu (12/4/03)	7.2	6.19	0.36		30	45	15	3.0	0.2	25	1.5
Fri (12/5/03)	8.6	7.05	0.86		37	60	19	3.3	0.1	30	1.5

Histopathology

Received for histopathology is the left forelimb. On the lateral surface of the scapula, there is a 4.5cm diameter, firm subcutaneous mass with a 2.5cm linear surgical scar on the haired skin. The edges of this mass are 3.5cm from the cranial tissue margin, 3.5cm from the dorsal tissue margin, and 3cm from the caudal tissue margin. Representative sections are taken through each tissue margin, as well as through the mass and underlying muscular layer. Subcutaneous mass, left scapula: Fibrosarcoma. Skin, cranial margin: Moderate, regionally extensive dermal fibrosis with histiocytic subdermal panniculitis and new vessel formation. The histologic appearance of this mass is consistent with, but not definitive for, an injection site fibrosarcoma. The majority of the mass is homogenous and eosinophilic (hyalinization, perhaps due to previous radiation therapy to the site). The viable cells are markedly anaplastic with frequent tumor giant cells and multinucleation. There are suspicious regions of reactive fibrous tissue that contain rare scattered anaplastic cells near the skeletal muscle layer deep to the tumor, however, the skeletal muscle is not affected, and this band of skeletal muscle lies dorsal to the scapula which is between the tumor and the deep surgical margin. Therefore, the surgical margins examined are free of tumor foci. The area of dermal fibrosis at the cranial skin margin may represent an old area of trauma.

Cat No. 4

Name- ARIEL, Trainor

Treated at- North Carolina State University

Radiation dose- 48 Gy/16 fractions

Week of gene therapy and hyperthermia- 2.9.04 to 2.13.04

Tumor dimensions- cm x cm x cm

Tumor volume- $2.43m^3$

Dose of viral construct- 10^{10} pfu

Number of intratumoral injection sites- 2

Hyperthermia Data-

T50 (^oC)- 40.7
T90 (^oC)- 39.9
Tmin (^oC)- 39.9
Tmax (^oC)- 43.0

Cytokine production

	Interleukin-12	Interferon- γ
Monday	Baseline (1)	Baseline (1)
Tuesday	43 ± 13	Nil
Wednesday	3028 ± 114	Nil
Thursday	31 ± 11	+/-

Toxicity table

	WBC	GRAN	LYM	PLT	PCV	ALT	ALP	ALB	T BILI	BUN	CRE
Mon (2/9/04)	3.3	2.77	0.33		28	51	13	2.7	0.1	15	0.9
Tue (2/10/04)	5.3	4.93	0.16	186	29	131	11	3.1	0.8	12	0.6
Wed (2/11/04)	6.1	5.18	0.49	141	26	89	12	3.1	0.3	13	0.7
Thu (2/12/04)	4.8	3.07	0.62		20	67	12	3.1	0.2	12	0.9
Fri (2/13/04)	6.9	5.24	0.89		32	59	20	3.4	0.2	18	1.1

Histopathology

The amputated entire right foreleg is submitted for histological evaluation. There is a moveable mass in the subcutis, measuring 1x 1.5x 0.7 cm, overlying the right dorsal spine of the scapula. The overlying skin is incised (2 cm long). The mass is 5 cm from dorsal skin margin, 3 cm from cranial margin and 4 cm from caudal margin, and does not appear to invade the underlying scapular bone or to the deep margin. There is an irregular shaped, hypocellular mass located in deep dermis to subcutaneous tissue and partially extending into the deep skeletal muscle. The mass has multifocal island of pale foci, which are composed of haphazardly arranged spindle cell proliferation within densely packed mature collagen tissue. Also, frequently individual spindle cells are observed in adjacent dense collagen tissue. The spindle cells have scant to moderate, amphophilic fibrillar cytoplasm with indistinct cell margin and oval to fusiform, vesicular nuclei with one to multiple, large central nucleoli. Rarely, karyomegalic cells observed. There is moderate anisocytosis and anisokaryosis. Two mitotic figures are observed in ten 400x fields. In the superficial dermis, there is focally extensive area of fibrous tissue with abundant vascular structure (granulation tissue) and multifocal histiocytic, neutrophilic and lymphocytic aggregates. Occasionally, histiocytes contain blue-gray material in their

cytoplasm. Dorsal skin margin (slide 2), cranial skin margin (slide 3), caudal skin margin (slide 4), deep muscular margin (slide 5): There is no evidence of tumor in the examined Subcutaneous mass, dorsal to right scapula: Fibrosarcoma with abundant dermal to subcutaneous fibrosis with granulation (scar) tissue. This tumor is largely composed of mature fibrous tissue with occasional intralesional basophilic stippled material (injected agent), a response to previous therapy and possibly remnants of previous vaccine reaction. However, multifocal persistent islands of neoplastic cells are observed. Tumor is extends into the deep skeletal muscle. There is no evidence of tumor at the surgical margins.

Cat No. 5

Name- OREO, Dirscherl

Treated at- Colorado State University

Radiation dose- 48 Gy/16 fractions

Week of gene therapy and hyperthermia- 7.5.04 to 7.9.04

Tumor dimensions- 1.5cm x 2cm x 1cm

Tumor volume- 1.57cm^3

Dose of viral construct- 10^{10} pfu

Number of intratumoral injection sites- 2

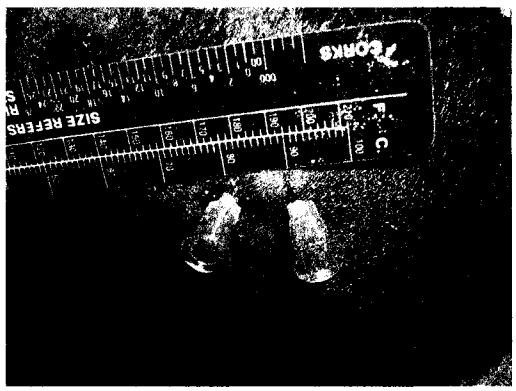

Hyperthermia Data-

T50 (°C)- 41.5
T90 (°C)- 40.6
Tmin (°C)- 39.8
Tmax (°C)- 43.5

Cytokine production

	Interleukin-12	Interferon- γ
Monday	Baseline (1)	Baseline (1)
Tuesday	-	-
Wednesday	1685 ± 184	+/-
Thursday	-	-

Toxicity table

	WBC	GRAN	LYM	PLT	PCV	ALT	ALP	ALB	T BILI	BUN	CRE
Mon (7/5/04)	3.2	2.2	0.7	314	28	85	50	3.7	0.1	21	2
Tue (7/6/04)	4.5	3.2	0.8	304	40	69	49	3.3	0.2	23	1.7
Wed (7/7/04)	2.7	1.8	0.6	164	23	72	41	3.2	0.3	14	1.3
Thu (7/8/04)	3.5	2.5	0.5	113	20	65	37	3.3	0.5	18	1.3
Fri (7/9/04)	3.7	2	0.4	271		97	57	3.7	0.2	21	1.8

Histopathology (7/26/04)

History: Clinical diagnosis of vaccine associated sarcoma on the left hip.

DIAGNOSIS: Haired skin = Mild chronic inflammation and seroma with vasculitis.

REMARKS: No tumor cells are noted.

1/Haired skin - The follicles in this section of skin are atrophied. There is inflammatory infiltration in the dermis and epidermis, as well as edema. Some vessels are mildly effaced by a suppurative inflammation.

2/Haired skin - There is a mild chronic inflammation and seroma formation between the skin and dermis. Hair follicles are atrophied.

3/Haired skin - There are segmental collections of macrophages that contain an amorphous, lightly basophilic material. There is mild inflammation.

4/Haired skin - There is chronic mixed inflammation and atrophy of hair follicles.

Left hip excision biopsy. Mild chronic inflammation and seroma with vasculitis. No mass or discrete tumor cells are noted.

Cat No. 6

Name- RAIN, Chenowith

Treated at- Colorado State University

Radiation dose- 48 Gy/16 fractions

Week of gene therapy and hyperthermia- 8.2.04 to 8.6.04

Tumor dimensions- 3.5cm x 4.5cm x 1.5cm

Tumor volume- $12.37cm^3$

Dose of viral construct- 10^{10} pfu

Number of intratumoral injection sites- 16

Hyperthermia Data-

T50 (°C)- 40.8
T90 (°C)- 38.9
Tmin (°C)- 36.6
Tmax (°C)- 45.2

Cytokine production

	Interleukin-12	Interferon- γ
Monday	Baseline (1)	Baseline (1)
Tuesday	176 ± 12	Nil
Wednesday	358 ± 30	+/-
Thursday	2.2 ± 1.7	Nil

Toxicity table

	WBC	GRAN	LYM	PLT	PCV	ALT	ALP	ALB	T BILI	BUN	CRE
Tue (7/27/04)	7.7	6.9	0.5	207	22	37	25	3	0.1	11	1
Mon (8/2/04)	5.6	4.7	0.4	350	25	46	27	3.3	0	18	0.3
Tue (8/3/04)	6.2	5.6	0.1	262	22	36	22	3	0.1	10	0.8
Wed (8/4/04)	3.4	2.8	0.3	167	18	29	22	2.8	0.1	12	0.8
Thu (8/5/04)	3.6	3	0.3	145	18	35	24	3.2	0.1	11	0.8
Fri (8/6/04)	4.1	2.8	0.7	100	20	38	25	3.3	0.1	12	1
Mon (8/16/04)	4.9	4.2	0.3	368	31						

Histopathology (8/16/04)

History: Lesion on the right dorsolateral cervical region.

DIAGNOSIS: Cervical mass = Scar tissue and necrosis.

REMARKS: There are no tumor cells noted in any of the three sections of mass evaluated. There is acceptable normal tissue, both laterally and deep to the scar tissue and necrosis, so margins are clear.

1/Cervical mass - There is a subcuticular mass of expansile collagen necrosis and muscle degeneration with fibrosis. There are moderate amounts of lymphocytes and few plasma cells surrounding and infiltrating normal tissue. There are many pools of red blood cells, fibrin, and degenerative neutrophils.

2/Cervical mass - Similar histologic description to that of Slide 1.

3/Similar histologic appearance and description to that seen in Slides 1 and 2.

Cat No. 7

Name- CLEOCATRA, Field

Treated at- North Carolina State University

Radiation dose- 48 Gy/16 fractions

Week of gene therapy and hyperthermia- 8.23.04 to 8.27.04

Tumor dimensions- 1.6cm x 2cm x 1.4cm

Tumor volume- $2.34cm^3$

Dose of viral construct- 10^{10} pfu

Number of intratumoral injection sites- 2

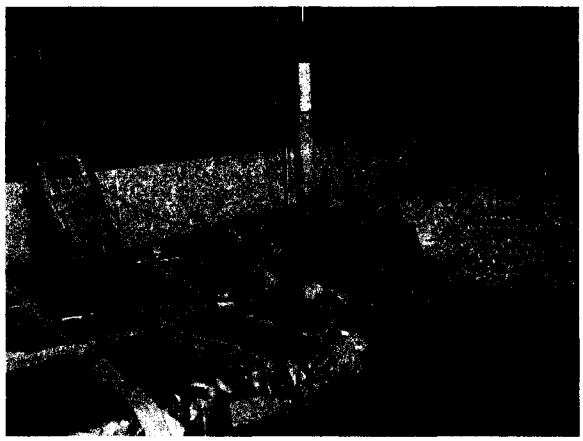

Hyperthermia Data-

T50 (°C)- 41.3
T90 (°C)- 40.1
Tmin (°C)- 37.0
Tmax (°C)- 42.4

Cytokine production

	Interleukin-12	Interferon- γ
Monday	Baseline (1)	Baseline (1)
Tuesday	-	-
Wednesday	3841 ± 643	Nil
Thursday	82 ± 16	+/-

Toxicity table

	WBC	GRAN	LYM	PLT	PCV	ALT	ALP	ALB	T BILI	BUN	CRE
Mon (8/23/04)	9.88	5.14	0.30	n	33	67	38	3.1	0.1	19	0.8
Tue (8/24/04)	6.55	5.11	0.26	n	29	71	32	3.0	0.2	13	0.7
Wed (8/25/04)	4.84	3.58	0.34	n	27	66	32	3.2	0.2	16	0.8
Thu (8/26/04)	8.12	5.60	0.49	n	27	60	37	3.3	0.3	18	0.9
Fri (8/27/04)	9.36	5.15	0.75	n	28	52	49	3.2	0.2	15	1

Histopathology

Received for histologic examination is a single container with a large, 9X7.4cm ovoid section of haired skin and subcutaneous tissue taken from the left thorax. There is an indistinct, 1.2-1.5cm nodular expansion within the central subcutaneous tissue.

Subcutaneous Nodule (slide 1): The superficial subcutaneous tissue contains an irregularly arranged, elongate to arboriform, moderately cellular population of fibroblasts arranged into bundles or fascicles interlaced with thin collagenous cords. Individual fibroblasts are mildly cellular inflammatory population composed of lymphocytes, plasma cells and macrophages. The separation between the deep border and this population of fibroblasts is approximately 1.3-1.4cm.

Dorsal border (slide 2): No neoplastic cells nor fibroblastic population is visualized.

Ventral border (slide 3): No neoplastic cells nor fibroblastic population is visualized.

Cranial border (slide 4): There is a focal, irregular, elongate bundle of similar appearing fibroblastic population with small volumes of collagen and adjacent lymphocytes and plasma cells extending to 1.5cm of the margin. Additionally, there is a small, irregular, focal aggregate of the pale basophilic, granular material is close approximation to this population (vaccine adjuvant vs dystrophic mineralization).

Caudal border (slides 5,6): No neoplastic cells nor fibroblastic population is visualized.

Diagnosis: Subcutaneous nodule- Fibroblastic nodular proliferation (presumed fibrosarcoma)

The elongate, flowing morphology of the fibroblasts within the subcutaneous nodule are strongly indicative of a previously excised or irradiated fibrosarcoma. However, the relative low cellularity and cellular distortion associated with previous therapy confounds definitive classification. The described basophilic granular material is morphologically consistent with vaccine adjuvant. However, if the region has received prior radiotherapy this may be mineralized cellular debris or stromal degeneration from free radical damage. If this population represents a previously treated fibrosarcoma, the margins appear free to within 1.3-1.5cm. However, due to the irregular, infiltrative nature of fibrosarcomas we strongly caution that margins are difficult to definitely establish and encourage thorough monitoring for neoplastic regrowth.

Cat No. 8

Name- FELIX, Burgess

Treated at- North Carolina State University

Radiation dose- 48 Gy/16 fractions

Week of gene therapy and hyperthermia- 10.4.04 to 10.8.04

Tumor dimensions- 2.3cm x 2.7cm x 1.6cm

Tumor volume- $5cm^3$

Dose of viral construct- $4X10^{10}$ pfu

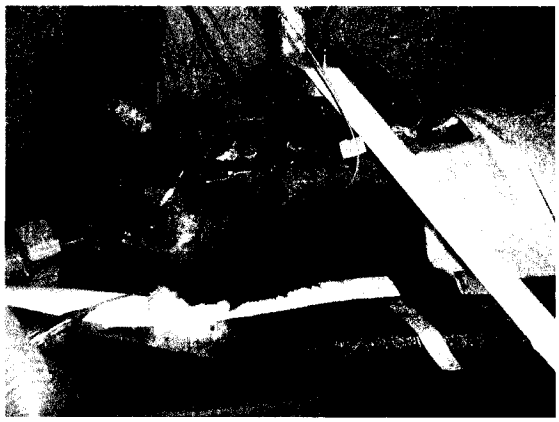

Number of intratumoral injection sites- 10

Hyperthermia Data-

T50 (°C)- 40.9
T90 (°C)- 37.5
Tmin (°C)- 35.4
Tmax (°C)- 45.7

Cytokine production

	Interleukin-12	Interferon- γ
Monday	Baseline (1)	Baseline (1)
Tuesday	658 ± 63	2.4 ± 1.9
Wednesday	1318 ± 312	42 ± 20
Thursday	21 ± 1	Nil

Toxicity table

	WBC	GRAN	LYM	PLT	PCV	ALT	ALP	ALB	T BILI	BUN	CRE
Mon (10/4/04)	6.05	4.66	1.03	N	26	31	20	2.9	0.1	50	2.3
Tue (10/5/04)	4.45	4.18	0.22	101	23	43	17	2.8	0.3	17	1.7
wed (10/6/04)	7.64	7.49	0.00	55	22	61	15	3.0	2.8	21	1.5
Thu (10/7/04)	5.07	3.85	0.86	39	13	58	14	2.8	1.6	25	1.5
Fri (10/8/04)	8.59	5.93	0.95	82	11	114	14	2.6	5.8	35	1.3

Clinical course

Twenty- four hours post- HT he had a fever of >39^{0}C which responded to dexamethasone NaPO4. Twenty- four hours later, temperature was again >39^{0}C, received piroxicam and temperature dropped. The cat was anemic the next day, received a whole blood transfusion about 8 hours later and lysed it (PCV never changed, bilirubin went up). Over the weekend the PCV held steady but did not improve but wasn't eating well. Started antibiotics with no great improvement over weekend. Started immunosuppressive steroid therapy on Monday which resulted in an increase in PCV and appearance of reticulocytes.

Histopathology

Interscapular mass: Fibrosarcoma. The mass present in the deep subcutaneous adipose tissue is confirmed to be a poorly cellular FSA with abundant, dense hyalinized collagenous tissue matrix. This FSA looks like it has been previously irradiated, causing the low cellularity and hyalinized appearance.

The mass is 1.5 cm from the left lateral margin, 2 cm from the right lateral margin, 2 cm from the cranial and 3 cm from the caudal. Deep margins and scapular margins show no signs of neoplasia.

Cat No. 9

Name- TINKER, Scott

Treated at- Colorado State University

Radiation dose- 48 Gy/16 fractions

Week of gene therapy and hyperthermia- 11.15.04 to 11.19.04

Tumor dimensions- 5.6cm x 3.6cm x 3cm

Tumor volume- $31.7cm^3$

Dose of viral construct- $4X10^{10}$ pfu

Number of intratumoral injection sites- 27

PROTOCOL DEVIATION- This cat was heated on Wednesday instead of Tuesday as she had high- grade fever on Monday after gene injection. One day was allowed for stabilization after control of fever and blood investigations were done to rule out hemolysis and toxicity before hyperthermia was delivered.

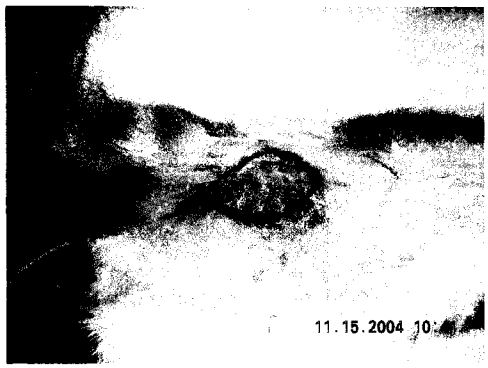

Hyperthermia Data-

T50 (°C)- 41.5
T90 (°C)- 39.5
Tmin (°C)- 38.3
Tmax (°C)- 44.2

Cytokine production

	Interleukin-12	Interferon- γ
Monday	Baseline (1)	Baseline (1)
Tuesday	25 ± 2	Nil
Wednesday	7043 ± 1145	1.7 ± 0.2
Thursday	23 ± 7	Nil
Friday	2 ± 1	Nil

Toxicity table

	WBC	**GRAN**	**LYM**	**PLT**	**PCV**	**ALT**	**ALP**	**ALB**	**T BILI**	**BUN**	**CRE**
Mon (11/15/04)	4	3.2	0.6	432	27	27	29	3	0.1	19	1.5
Tue (11/16/04)	11.3	10.8	0.2	291	21	45	16	3	0.3	15	0.9
Wed (11/17/04)	3.4	2.7	0.2	229	16	40	11	2.4	0.2	9	0.7
Thu (11/18/04)	5	4.5	0.4	195	22	48	23	2.8	0.3	9	1.2
Fri (11/19/04)	7.1	4.8	2.1	120	15	35	29	2.4	0.7	13	0.9
Sun (11/21/04)	7.5	5.9	0.5	113	19	37	30	2.7	0.4	12	0.9
Mon (12/6/04)	7	6.2	0.4	488	21	31	23	2.8	0.1	23	1.3

Histopathology (12/6/04)

History: Clinical diagnosis of fibrosarcoma.

DIAGNOSIS: 1/Inguinal mass = Osseous metaplasia.

2/Footpad biopsy = Mild mononuclear perivascular inflammation.

REMARKS: No tumor is identified within the sections examined. The osseous metaplasia is likely secondary to radiation tissue damage.

1/Fat pad inguinal biopsy - There are low numbers of lymphocytes, plasma cells, and macrophages around vessels and subcutaneous musculature in multiple small areas within the section.

2/Inguinal mass (haired skin margin) - Extending through the dermis and subcutis is a moderately well-defined multilobular mass composed of disorganized sheets and trabeculae of non-mineralized bone and cartilage within bands of fibrovascular

connective tissue. The bony areas consist of woven collagenous matrix around numerous random lacunae. The matrix towards the periphery of the mass is eosinophilic with frequent osteoblasts and osteoclasts, and contains osteocytes within the lacunae. Toward the center of the mass, the matrix is less well-defined, lightly eosinophilic, and the lacunae are frequently empty or contain pyknotic cells or karyorrhectic cellular debris. Throughout the bony regions, there are occasional cartilaginous areas containing numerous chondrocytes within an amphophilic to slightly basophilic matrix. Within the fibrovascular connective tissue and in the surrounding subcutaneous tissue, there are marked numbers of macrophages laden with dark brown globular pigment (hemosiderin). No neoplastic cells are present within the section.

3/Inguinal mass (lateral inked margin) - Within the section, there is a lymph node containing marked numbers of macrophages, similar to those in Slide 2, throughout the sinusoids diffusely. Otherwise, the section is within normal limits.

4-7/Inguinal mass (lateral inked margins) - No neoplastic cells are present and no histologic lesions are identified within the sections.

Osseous metaplasia secondary to radiation tissue damage. No tumor is identified within the sections examined.

NOTE: This cat had high fever overnight on Monday after the gene injection ranging from about 104^0F-105^0F. Fever lasted for more than 12 hours and temperature did not reduce with Prednisolone. On Tuesday, late morning, the temperature came down after administration of i.v. dexamethasone. The cat did not receive hyperthermia on Tuesday, as is the protocol. She was kept under observation and HT deferred till Wednesday.

HT was delivered on Wednesday after blood investigations were close to or within normal range and the cat looked clinically normal. Biopsy was collected *before* HT. Biopsies were done on all days of the week- Monday to Friday.

The maximum expression was seen in the Wednesday sample even before heating the tumor and on Thursday and Friday the values continued to decline suggesting that once the construct had been induced by the high- grade fever, there was no repeat induction by HT.

Cat No. 10

Name- KITTY, Froehlich

Treated at- Colorado State University

Radiation dose- 48 Gy/16 fractions

Week of gene therapy and hyperthermia- 1/24/05 to 1/28/05

Tumor dimensions- 1.3cm x 1.8cm x 1.2cm

Tumor volume- $1.5cm^3$

Dose of viral construct- $4X10^{10}$ pfu

Number of intratumoral injection sites- 5

Hyperthermia Data-

T50 (°C)- 40.9
T90 (°C)- 39.9
Tmin (°C)- 38.7
Tmax (°C)- 42.2

Cytokine production

	Interleukin-12	Interferon- γ
Monday	Baseline (1)	Baseline (1)
Tuesday	-	Nil
Wednesday	29 565 ± 9208	Nil
Thursday	-	Nil

Toxicity table

	WBC	GRAN	LYM	PLT	PCV	ALT	ALP	ALB	T BILI	BUN	CRE
Mon (1/24/05)	3.8	3.1	0.5	362	31	36	22	3	0.1	29	1.4
Tue (1/25/05)	5	4.8	0.1	222	31	49	14	2.9	0.1	20	0.9
Wed (1/26/05)	3.5	3.2	0.3	250	29	44	18	3.1	0.2	14	1.2
Thu (1/27/05)	2.6	2.2	0.2	226	29	44	22	3.1	0.1	27	1.6
Fri (1/28/05)	3	2.3	0.3	105	29	38	15	3.1	0.2	18	1.2
Thu (2/3/05)						47	16	2.9	0.2	18	1.3

Histopathology (2/3/05)

History: Diabetic. Mass in right caudal lung lobe.

DIAGNOSIS: Soft tissue sarcoma, grade 3.

REMARKS: Inked surgical margins are wide of the tumor by 2.5cm and deep of the tumor by 0.5cm.

1/Right hip mass, haired skin (lateral and deep margins) - Within the dermis and subcutis, there is a poorly-defined, expansile mass composed of multifocal to coalescing irregular patches of neoplastic mesenchymal cells within large sheets of collagenous fibrovascular connective tissue admixed with multifocal areas of necrosis, small pockets of marked suppurative inflammation, and moderate plasmacytic, lymphocytic and histiocytic inflammation diffusely. Neoplastic cells are organized into streams and intersecting bundles of elongate to spindloid cells with indiscrete cell margins and moderate amounts of eosinophilic fibrillar cytoplasm. Nuclei are oval to cigar-shaped and vesiculated with 1 to 3 prominent, variably sized nucleoli. Anisocytosis and anisokaryosis is moderate, mitotic figures are 1 per 2 high power field, and there are occasional large, bizarre multinucleated cells located throughout the section. Surgical margins are wide of the tumor by 2.5cm and deep of the tumor by 1cm.

2/Right hip mass, haired skin (lateral and deep margins) - This section is similar to Slide 1. Surgical margins are wide of the tumor by 3cm and deep of the tumor by 0.5cm.

3/Right hip mass, haired skin (lateral and deep margins) - The section is similar to Slide 1. Surgical margins are wide of the tumor by 2cm and deep of the tumor by 0.5cm.

4/Right hip mass, haired skin (lateral and deep margins) - The section is similar to Slide 1. Surgical margins are wide of the tumor by 3cm and deep of the tumor by 1cm.

5/Right hip mass, haired skin (lateral and deep margins) - The section is similar to Slide 1. Surgical margins are wide of the tumor by 2.5cm and deep of the tumor by 1.0cm.

Cat No. 11

Name- WINKY, Radke

Treated at- Colorado State University

Radiation dose- 48 Gy/16 fractions

Week of gene therapy and hyperthermia- 1/31/05 to 2/4/05

Tumor dimensions- 5cm x 4.7cm x 3cm

Tumor volume- $37cm^3$

Dose of viral construct- $4X10^{10}$ pfu

Number of intratumoral injection sites- 20

Hyperthermia Data-

T50 (^oC)- 41.5
T90 (^oC)- 40.4
Tmin (^oC)- 39.2
Tmax (^oC)- 44.0

Cytokine production

	Interleukin-12	Interferon- γ
Monday	Baseline (1)	Baseline (1)
Tuesday	1780 ± 783	Nil
Wednesday	14658 ± 2055	Nil
Thursday	62 ± 28	152 ± 34

Toxicity table

	WBC	GRAN	LYM	PLT	PCV	ALT	ALP	ALB	T BILI	BUN	CRE
Mon (1/31/05)	4.4	3.7	0.5	59	34	59	42	3.2	0.1	27	1.1
Tue (2/1/05)	7.7	7.5		81	32	146	30	3.5	0.1	13	0.7
Wed (2/2/05)	4.9	4.7		64	29	90	26	3.2	0.1	13	0.6
Thu (2/3/05)	3.5	3.3	0.1	59	27	58	22	3.2	0.2	16	1.2
Fri (2/4/05)	4.4	3.7	0.4	17	25	46	14	2.9	0.4	22	1.1
Sat (2/5/05)	6	4.2	1.1	47	12	35	10	2.5	0.3	21	0.7
Tue (2/8/05)	10.3	7	0.8	28	18	67	17	2.5	1.8	21	0.6
Fri (2/11/05)	7.6	4.9	0.6	88	15	57	23	2.8	0.4	20	0.7
Mon (2/14/05)	7.7	4.2	0.5	58	1						
Tue (2/15/05)						41	27	3	0.2	25	0.9

Histopathology (3/22/05)

History: Vaccine-associated sarcoma.

DIAGNOSIS: Shoulder mass = Vaccine-associated sarcoma and marked fibrosis.

REMARKS: Inked surgical margins are wide and free of tumor.

1/Deep mass biopsy (no surgical margins) - There is a poorly-demarcated expansile and infiltrative focal mass of neoplastic mesenchymal cells, 2x2mm in diameter, surrounded by a thick rim of dense hypocellular collagenous tissue within a section of loose fibrovascular connective tissue containing mild perivascular lymphoplasmacytic inflammation. Neoplastic cells are arranged in whorls and streams, and consist of elongate to fusiform cells with indistinct cell margins and moderate amounts of eosinophilic cytoplasm. Nuclei are ovoid to elongate with finely- stippled chromatin and 1 to 3 small nucleoli. Anisocytosis and anisokaryosis is moderate, and mitotic figures are 1 per 3 high power fields.

2/Skeletal muscle (inked surgical margins) - No tumor is present within the section and no histologic lesions are identified.

3/Skeletal muscle (inked surgical margins) - There is an area of dense hypocellular collagenous tissue, similar to Slide 1, 0.5cm deep to the inked surgical margin. No tumor is present within the section.

4/Skeletal muscle (inked surgical margin) - There is an area of dense hypocellular collagenous tissue, similar to Slide 1, 0.75cm deep to the inked surgical margin. No tumor is present within the section.

5/Skeletal muscle (inked surgical margin) - There is an area of dense hypocellular collagenous tissue, similar to Slide 1, 1cm deep to the deep inked surgical margin. No tumor is present within the section.

6-9/Scapula and skeletal muscle (inked surgical margins) - No tumor is present within the sections and no histologic lesions are identified.

NOTE: The cat was clinically normal for first 4 days of GT+HT but on Thursday night she developed fever of 103^0F -104^0F and had to be moved to CCU. She was refusing to feed and a feeding tube had to be placed. An X-ray chest revealed pulmonary edema, aspiration pneumonia and pleural effusion. The pleural effusion was drained and was found to be a transudate. The PCV dropped to 12 requiring a blood transfusion. As a consequence of these complications the surgery was delayed.

Cat No. 12

Name- MITTENS, McKnight

Treated at- Colorado State University

Radiation dose- 48 Gy/16 fractions

Week of gene therapy and hyperthermia- 2/7/05 to 2/11/05

Tumor dimensions- 5.5cm x 5cm x 2cm

Tumor volume- $28.8cm^3$

Dose of viral construct- $4X10^{10}$ pfu

Number of intratumoral injection sites- 25

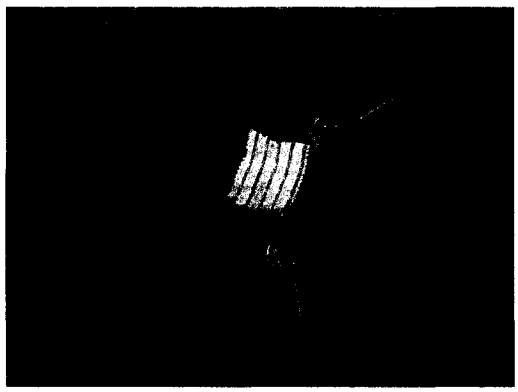

Hyperthermia Data-

T50 (^oC)- 41.5
T90 (^oC)- 40.2
Tmin (^oC)- 39.5
Tmax (^oC)- 43.2

Cytokine production

	Interleukin-12	Interferon- γ
Monday	Baseline (1)	Baseline (1)
Tuesday	470 ± 115	Nil
Wednesday	2793 ± 489	1.4 ± 1
Thursday	2602 ± 675	6.2 ± 2.5

Toxicity table

	WBC	GRAN	LYM	PLT	PCV	ALT	ALP	GGT	ALB	T BILI	BUN	CRE
Mon (2/7/05)	8	7	0.2	430	11	28	9	0	2.6	0.1	21	1.3
Tue (2/8/05) (transfusion)	8.9	7.7	0.2	346	21	25	11	0	2.5	0.1	17	1.1
Wed (2/9/05)	16.4	13.9	1	171	27	23	9	2	1.6	4.3	56	1.3
Thu (2/10/05)	13.2	11.7	3	122	14	26	7	1	1.9	2.1	17	0.6
Fri (2/11/05)	11.3	9.5	0.6	125	16	26	10	1	2.1	0.8	20	0.9
Wed (3/2/05)	10.8	7.7	0.9	294	22							

Histopathology (3/2/05)

History: Part of radiation therapy/gene therapy/hyperthermia study for VAS.

DIAGNOSIS: Left thigh mass = Soft tissue sarcoma with marked necrosis and granulation tissue, and bordering lymphoplasmacytic inflammation.

REMARKS: The majority of the mass is necrotic and granulated. Level of tumor still remains within the mass. Margins are very narrow and blend precariously with necrotic and granulated tissue examined. Excision appears complete, but is questionable.

1/Left thigh mass - Slide consists of a mass of predominate necrotic and granulation tissue with few areas of neoplastic spindle cells at the mass's periphery. Cells contain scant to moderate amount of pale eosinophilic cytoplasm and small round heterochromatic nuclei. Few mitotic figures are noted. There is marked lymphoplasmacytic inflammation in the bordering connective tissues. There is a very small, less than 1mm clearance of connective tissue overlying and underlying the removed mass.

2/Left thigh mass - Histologic description is similar to that in Slide 1.

3/Left thigh mass, lateral margins - Histologic description is similar to that of Slides 1 and 2. Lateral margin is approximately 1-1.5mm.

Cat No. 13

Name- GINGER, Fox

Treated at- Colorado State University

Radiation dose- 48 Gy/16 fractions

Week of gene therapy and hyperthermia- 2/28/05 to 3/4/05

Tumor dimensions- 1.8cm x 2cm x 1cm

Tumor volume- 1.88cm^3

Dose of viral construct- 10^{10} pfu (reverted back to previous dose level)

Number of intratumoral injection sites- 4

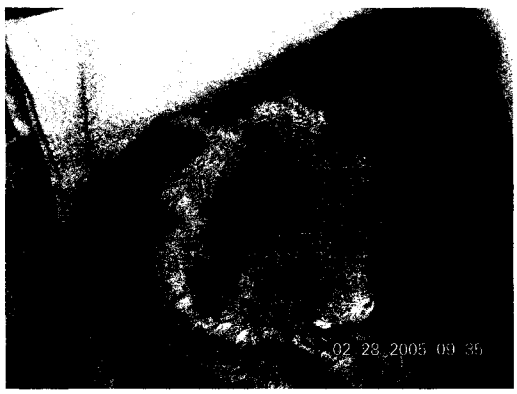

Hyperthermia Data-

T50 (°C)- 41.1
T90 (°C)- 39.8
Tmin (°C)- 39.5
Tmax (°C)- 42.7

Cytokine production

	Interleukin-12	Interferon- γ
Monday	Baseline (1)	Baseline (1)
Tuesday	-	-
Wednesday	1858 ± 691	+/-
Thursday	-	-

Toxicity table

	WBC	GRAN	LYM	PLT	PCV	ALT	ALP	GGT	ALB	T BILI	BUN	CRE
Mon (2/28/05)	2.9	2.2	0.1	408	28	53	29	0	3.5	0.1	38	1.5
Tue (3/1/05)	6.9	6.6	0.1	307	29	65	17	0	3.5	0.2	20	0.9
Wed (3/2/05)	7.1	6.7	0.1	311	29	60	15	0	3.7	0.2	20	1
Thu (3/3/05)	3.2	2.6	0.2	207	26	61	18	0	3.7	0.1	20	1.5
Fri (3/4/05)	5.2	3.7	0.7	188	31	54	22	0	3.8	0.1	33	1
Tue (3/8/05)	4.3	2.8	0.6	95	39	41	16	0	3.6	0.1	34	1.4

Histopathology (3/9/05)

History: STS, radiation treatment. Mass is of marble size.

DIAGNOSIS: Fibroplasia, fibrin deposition and granulation tissue (organizing seroma).

REMARKS: No neoplastic cells are seen in this sample.

Mass from the right hip area - This is a well-demarcated, unencapsulated mass that is composed of thin fibers of an eosinophilic amorphous matrix surrounding fibroblasts. Surrounding this mass is a rim of leukocytes and plasmacytes intermixed with fibroblasts and neovascularization with hemorrhage and edema. This mass is approximately 1cm from the deep margin of excision, and no neoplastic cells are seen.

DISCUSSION

Vaccine- or injection-site associated feline soft tissue sarcomas are a unique clinical entity. They were first recognized by Hendrick and Goldschmidt[44] as soft tissue sarcomas arising at the site of rabies vaccination in cats. The prevalence of sarcoma development after vaccination has been variously reported as between 1 in 10,000[45] to 1 in 1,000[46]. Cats with injection site sarcomas belong to a younger age group than cats with non-injection site sarcomas[47]. Hendrick *et al*[48] reported an average interval of 26 months between rabies vaccination and tumor development. In another study[45], the median interval was found to be 11 months between FeLV vaccination and tumor formation.

It is postulated that aluminum, used as an adjuvant in vaccines, leads to local reactions and chronic inflammation with subsequent development of the tumor[49]. The treatment for this disease involves multimodality therapy including radiation therapy and surgery[47].

These spontaneously arising soft tissue sarcomas provided us with the excellent opportunity of utilizing this model to conduct a phase I hyperthermia- induced interleukin-12 gene therapy trial. Another reason for choosing this group of patients was the fact that these tumors are easily accessible for direct intratumoral injections of the viral construct and amenable to being heated using the microwave applicator for hyperthermia.

Gene therapy and hyperthermia were added on to radiation therapy and surgery, which are the standard of care modalities for this cancer.

We used a replication deficient adenoviral vector and could not rely on adenoviral replication to progressively infect more and more of the tumor cells. Hence, we tried to achieve a homogeneous distribution in the tumor volume by multiple injections in a 1cm

X 1cm grid pattern covering the surface area of the tumor and injecting along the needle track.

Prior to starting the clinical trial, *in vitro* studies were done to characterize this construct. Crandell Feline Kidney (CrFK) cells were infected with Ad*hsp*fIL-12 and IL-12 mRNA production was analyzed with respect to heating temperature and multiplicity of infection (Chapter 2). The supernatants collected from these cells, containing the IL-12 protein, were added to naïve feline peripheral blood mononuclear cells (PBMCs) and subsequent IFN-γ mRNA production in these cells was assessed. This was done to ascertain that the IL-12 mRNA signal detected on real- time PCR was indeed leading to functional IL-12 protein.

We used real-time PCR because (1) no ELISA kits or antibodies were readily available for detection of feline cytokines (2) it is a sensitive technique which enabled the detection of mRNA even in the small tissue samples. Ideally, we had planned to biopsy the tumors on all days from Monday to Thursday to assess the dynamics of cytokine production. In the larger tumors we were able to achieve that aim and even collect two samples on the same day to have more tissue material available for analysis. However, in the smaller tumors, obtaining adequate tumor tissue was not possible. In those cases we biopsied only on Mondays (baseline sample) and Wednesdays (24 hours post- HT sample). The Monday sample in all cases was collected prior to gene injection and served as the baseline. mRNA levels in biopsy samples from the subsequent days were expressed as fold increases over the baseline.

The initial plan for dose escalation was to have dose groups of 10^9 pfu/tumor, 10^{10} pfu/tumor and 10^{11} pfu/tumor with three cats at each dose level. We used the modified

continual reassessment method (mCRM)[50], that allows changing increments by which the dose is escalated based on the observed toxicity. Three cats were treated at 10^9 pfu dose level with minimal or no toxicity. At the next dose level of 10^{10} pfu, initially 4 cats were treated. The next intended increase to 10^{11}pfu was not reached as a high enough concentration of the viral construct could not be produced. Therefore, the dose escalation was limited to $4X10^{10}$ pfu. Five cases were treated at this dose. Moderate to severe toxicities were seen in 4 of the 5 cases, as detailed in the results section. The only cat not showing toxicity was the one who had a prolonged high- grade fever on the day of gene injection (Monday). The hyperthermia had been delayed by a day in this case and there was no IFN-γ mRNA detectable in the tumor samples even with a 7000 fold increase over baseline in IL-12 mRNA. Because of the toxicities, some of the cats at this dose had extended stays in the Critical Care Unit (CCU) for recovery. It was thus decided to revert back to 10^{10} pfu for the last cat making the total number of cases at that dose five.

There was a high degree of variability on the fold- increase in IL-12 mRNA production. Factors responsible for this variability could be (1) Dose of virus injected (2) Volume of normal saline that the construct is diluted in and the number of injection sites- affects MOI (3) Tumor volume (4) Heating temperature achieved during hyperthermia (5) Percent necrosis of the tumor- relates to viable target cells (6) Site of tumor tissue sampled during biopsy (7) Elevation in body temperature- fever (8) CAR receptor status- affects transfection efficiency of the adenoviral vector.

There did appear to be some correlation between tumor volume and IL-12 expression at the different dose levels. The larger tumors showed lesser IL-12 mRNA fold0 increases compared to smaller tumors when injected with the same amount of virus.

Based on our *in vitro* experiments, an increase in IL-12 mRNA levels with increase in temperature would be expected. We did not note an increased expression with temperature *in vivo*, possibly because of other influencing factors.

We attempted to circumvent the problem of necrotic tumor biopsy samples by collecting two to three viable- looking biopsies on each day whenever the tumor size permitted. All samples collected on one day were pooled and analyzed.

There was no correlation seen between the IL-12 production in a tumor and the presence of IFN-γ mRNA. The production of IFN-γ is a function of the lymphocytes present in the tumor. In our trial all tumors had already undergone radiation therapy to a dose of 48Gy. This dose would have eliminated the lymphocyte pool in the tumors[51]. Also, we had injected the construct equally over the volume of the tumor. The center of the tumors, especially in the larger sized tumors, would be necrotic, with the lymphocytes mainly concentrated around the periphery. This is another factor that would lead to reduced IFN-γ levels. Possible strategies to increase interferon production could be (1) do the gene therapy and hyperthermia prior to radiation therapy (2) inject the construct differentially with more of it in the periphery or margins of the tumor and less in the center.

In our dose escalation study, IFN-γ was mainly absent at the lower doses. Its presence was unequivocally detected only at the $4X10^{10}$ pfu dose level. However, it was interesting to note that all cats that had IFN-γ levels detectable in their tumors were the ones that had a non-normal clinical course.

Local and systemic administration of IL-12 protein has been studied in various murine models [5, 6, 13, 22] and in Phase I/II human trials [23, 24]. However, IL-12 protein therapy has been limited by dose-dependent toxicity [25]. Human recombinant IL 12 is associated with

severe toxicity, even at doses as low as 1μg/kg/day[52]. Common toxicities included fever/chills, fatigue, nausea, vomiting, and headache. Routine laboratory changes included anemia, neutropenia, lymphopenia, hyperglycemia, thrombocytopenia, and hypoalbuminemia. Dose limiting toxicities included oral stomatitis and liver function test abnormalities, predominantly elevated transaminases. Interferon- γ has been implicated as the cytokine directly responsible for IL-12 toxicity[25, 53]. Pulmonary edema has also been reported in mice[53].

In our patients, particular attention was paid to reducing core body temperature if the cats started becoming febrile. They were closely monitored in the critical care unit with hourly rectal temperatures being recorded. If the temperature reached 39^0C (102.2^0F), the cage was cooled using a fan and intravenous fluids started. Any elevation in temperature beyond 39.5^0C (103.2^0F) was aggressively managed with antipyretics and/ or i.v. dexamethasone. These measures were necessary to prevent induction of the heat shock promoter in the disseminated adenoviral construct.

Blood investigations were done on all days of the week of gene- therapy to detect hematologic or hepatic toxicity. The toxicity grading was done based on a modified version of the National Cancer Institute (NCI) Common Toxicity Criteria (CTC) Version 2.0. Toxicities were nil to mild in the lowest dose group gradually becoming moderate to severe in the highest dose group.

At all dose levels a drop in granulocyte counts was seen 48-72 hours post hyperthermia (IL-12 gene induction) with a rapid recovery seen by the next day. In some cases the nadir was below the lower limit for normal and it was qualified as toxicity. In other cases the nadir remained within the normal range. Similarly there was a transient increase in

liver enzymes and/ or total bilirubin seen with rapid recovery. This rapid transient response could possibly be due to the direct immune- mediated destruction of the target cells and has previously been reported in primate models[54, 55].

At lower doses thrombocytopenia and granulocytopenia were common while at higher doses anemia was also seen. These anemias required blood transfusions and in those cases (Cat nos. 8, 11, 12) the total bilirubin values were elevated post- transfusion.

Cat no. 11 had also developed pulmonary edema. This complication along with refusal to feed and poor general condition necessitated about a two- week stay in the critical care unit. This cat recovered fully and was operated upon about six weeks post- gene- therapy.

Borrelli *et al*[56] had reported sustained high levels of green fluorescent protein, placed under control of the heat shock promoter, with repeated induction using heat at 41^0C for 2 hours. This study was done *in vitro.* One of our cats (No. 9) provided us with the opportunity to study if this was also possible in a clinical setting. This cat has fever that started a few hours after gene injection on Monday and persisted overnight despite anti-pyretic efforts. The core body temperature was 39.5^0C to 40.5^0C for more than 12 hours. The hyperthermia was not delivered on Tuesday. Only a biopsy was collected to assess cytokine production. After the cat had clinically stabilized, HT was delivered on Wednesday after a tumor biopsy. Biopsies collected during the week showed that the IL-12 mRNA levels continued to fall after the peak induced due to fever. A repeat *hsp* induction might possibly not have occurred as it had already been induced for a long duration (about 12 hours).

In conclusion, this trial served as a proof of principle that it is possible to deliver interleukin-12 safely using the hyperthermia- induced gene- therapy approach. The trial

was done in spontaneously arising soft tissue sarcomas in client- owned cats. This posed certain challenges as far as tumor tissue sample collection or procedural flexibility was concerned. However, this served as an excellent model for human soft tissue sarcomas or solid tumors, unlike studies done in transplanted tumors in mice.

We were able to establish the maximally tolerated safe dose (10^{10}pfu) with no mortalities. This dose is based on the recommendations outlined in a protocol proposed by Stewart *et al*[57]. The toxicities we saw could be related, to a certain extent, with the interferon-γ production in the tumors.

A major limitation in our study was the inability to measure tumor or serum levels of the cytokines.

In future we would like to-

1. Include cytokine (feline IL-12 and IFN-γ) assays as endpoints if such antibodies/ kits become readily available.
2. Titrate the viral dose to the tumor volume.
3. Differentially distribute the construct with more in the periphery.
4. Do the gene therapy prior to radiation therapy.
5. Have longer duration of follow- up to assess local recurrence, distant metastasis and overall survival.

REFERENCES

1. Colombo MP, Trinchieri G. Interleukin-12 in anti-tumor immunity and immunotherapy. *Cytokine Growth Factor Rev* 2002;13:155-168.

2. Leroy P, Slos P, Homann H, *et al.* Cancer immunotherapy by direct in vivo transfer of immunomodulatory genes. *Res Immunol* 1998;149:681-684.

3. Rakhmilevich AL, Janssen K, Turner J, *et al.* Cytokine gene therapy of cancer using gene gun technology: superior antitumor activity of interleukin-12. *Hum Gene Ther* 1997;8:1303-1311.

4. Cavallo F, Signorelli P, Giovarelli M, *et al.* Antitumor efficacy of adenocarcinoma cells engineered to produce interleukin 12 (IL-12) or other cytokines compared with exogenous IL-12. *J Natl Cancer Inst* 1997;89:1049-1058.

5. Nastala CL, Edington HD, McKinney TG, *et al.* Recombinant IL-12 administration induces tumor regression in association with IFN-gamma production. *J Immunol* 1994;153:1697-1706.

6. Rakhmilevich AL, Turner J, Ford MJ, *et al.* Gene gun-mediated skin transfection with interleukin 12 gene results in regression of established primary and metastatic murine tumors. *Proc Natl Acad Sci U S A* 1996;93:6291-6296.

7. Saffran DC, Horton HM, Yankauckas MA, *et al.* Immunotherapy of established tumors in mice by intratumoral injection of interleukin-2 plasmid DNA: induction of CD8+ T-cell immunity. *Cancer Gene Ther* 1998;5:321-330.

8. Fernandez NC, Levraud JP, Haddada H, *et al.* High frequency of specific CD8+ T cells in the tumor and blood is associated with efficient local IL-12 gene therapy of cancer. *J Immunol* 1999;162:609-617.

9. Lode HN, Dreier T, Xiang R, *et al.* Gene therapy with a single chain interleukin 12 fusion protein induces T cell-dependent protective immunity in a syngeneic model of murine neuroblastoma. *Proc Natl Acad Sci U S A* 1998;95:2475-2480.

10. Yao L, Sgadari C, Furuke K, *et al.* Contribution of natural killer cells to inhibition of angiogenesis by interleukin-12. *Blood* 1999;93:1612-1621.

11. Pham-Nguyen KB, Yang W, Saxena R, *et al.* Role of NK and T cells in IL-12-induced anti-tumor response against hepatic colon carcinoma. *Int J Cancer* 1999;81:813-819.

12. Kodama T, Takeda K, Shimozato O, *et al.* Perforin-dependent NK cell cytotoxicity is sufficient for anti-metastatic effect of IL-12. *Eur J Immunol* 1999;29:1390-1396.

13. Watanabe M, Fenton RG, Wigginton JM, *et al.* Intradermal delivery of IL-12 naked DNA induces systemic NK cell activation and Th1 response in vivo that is independent of endogenous IL-12 production. *J Immunol* 1999;163:1943-1950.

14. Rakhmilevich AL, Janssen K, Hao Z, *et al.* Interleukin-12 gene therapy of a weakly immunogenic mouse mammary carcinoma results in reduction of spontaneous lung metastases via a T-cell-independent mechanism. *Cancer Gene Ther* 2000;7:826-838.

15. Cui J, Shin T, Kawano T, *et al.* Requirement for Valpha14 NKT cells in IL-12-mediated rejection of tumors. *Science* 1997;278:1623-1626.

16. Brunda MJ, Luistro L, Hendrzak JA, *et al.* Role of interferon-gamma in mediating the antitumor efficacy of interleukin-12. *J Immunother Emphasis Tumor Immunol* 1995;17:71-77.

17. Manetti R, Gerosa F, Giudizi MG, *et al.* Interleukin 12 induces stable priming for interferon gamma (IFN-gamma) production during differentiation of human T helper (Th) cells and transient IFN-gamma production in established Th2 cell clones. *J Exp Med* 1994;179:1273-1283.

18. Gately MK, Warrier RR, Honasoge S, *et al.* Administration of recombinant IL-12 to normal mice enhances cytolytic lymphocyte activity and induces production of IFN-gamma in vivo. *Int Immunol* 1994;6:157-167.

19. Tannenbaum CS, Wicker N, Armstrong D, *et al.* Cytokine and chemokine expression in tumors of mice receiving systemic therapy with IL-12. *J Immunol* 1996;156:693-699.

20. Tannenbaum CS, Tubbs R, Armstrong D, *et al.* The CXC chemokines IP-10 and Mig are necessary for IL-12-mediated regression of the mouse RENCA tumor. *J Immunol* 1998;161:927-932.

21. Voest EE, Kenyon BM, O'Reilly MS, *et al.* Inhibition of angiogenesis in vivo by interleukin 12. *J Natl Cancer Inst* 1995;87:581-586.

22. Tahara H, Zitvogel L, Storkus WJ, *et al.* Murine models of cancer cytokine gene therapy using interleukin-12. *Ann N Y Acad Sci* 1996;795:275-283.

23. Golab J, Zagozdzon R. Antitumor effects of interleukin-12 in pre-clinical and early clinical studies (Review). *Int J Mol Med* 1999;3:537-544.

24. Rook AH, Wood GS, Yoo EK, *et al.* Interleukin-12 therapy of cutaneous T-cell lymphoma induces lesion regression and cytotoxic T-cell responses. *Blood* 1999;94:902-908.

25. Car BD, Eng VM, Lipman JM, *et al.* The toxicology of interleukin-12: a review. *Toxicol Pathol* 1999;27:58-63.

26. Colombo MP, Vagliani M, Spreafico F, *et al.* Amount of interleukin 12 available at the tumor site is critical for tumor regression. *Cancer Res* 1996;56:2531-2534.

27. Rakhmilevich AL, Timmins JG, Janssen K, *et al.* Gene gun-mediated IL-12 gene therapy induces antitumor effects in the absence of toxicity: a direct comparison with systemic IL-12 protein therapy. *J Immunother* 1999;22:135-144.

28. Shi F, Rakhmilevich AL, Heise CP, *et al.* Intratumoral injection of interleukin-12 plasmid DNA, either naked or in complex with cationic lipid, results in similar tumor regression in a murine model. *Mol Cancer Ther* 2002;1:949-957.

29. Puisieux I, Odin L, Poujol D, *et al.* Canarypox virus-mediated interleukin 12 gene transfer into murine mammary adenocarcinoma induces tumor suppression and long-term antitumoral immunity. *Hum Gene Ther* 1998;9:2481-2492.

30. Seetharam S, Staba MJ, Schumm LP, *et al.* Enhanced eradication of local and distant tumors by genetically produced interleukin-12 and radiation. *Int J Oncol* 1999;15:769-773.

31. Putzer BM, Hitt M, Muller WJ, *et al.* Interleukin 12 and B7-1 costimulatory molecule expressed by an adenovirus vector act synergistically to facilitate tumor regression. *Proc Natl Acad Sci U S A* 1997;94:10889-10894.

32. Lohr F, Huang Q, Hu K, *et al.* Systemic vector leakage and transgene expression by intratumorally injected recombinant adenovirus vectors. *Clin Cancer Res* 2001;7:3625-3628.

33. Bramson JL, Hitt M, Gauldie J, *et al.* Pre-existing immunity to adenovirus does not prevent tumor regression following intratumoral administration of a vector expressing IL-12 but inhibits virus dissemination. *Gene Ther* 1997;4:1069-1076.

34. Zhang R, Straus FH, DeGroot LJ. Effective genetic therapy of established medullary thyroid carcinomas with murine interleukin-2: dissemination and cytotoxicity studies in a rat tumor model. *Endocrinology* 1999;140:2152-2158.

35. Nasu Y, Bangma CH, Hull GW, *et al.* Adenovirus-mediated interleukin-12 gene therapy for prostate cancer: suppression of orthotopic tumor growth and pre-established lung metastases in an orthotopic model. *Gene Ther* 1999;6:338-349.

36. Emtage PC, Wan Y, Hitt M, *et al.* Adenoviral vectors expressing lymphotactin and interleukin 2 or lymphotactin and interleukin 12 synergize to facilitate tumor regression in murine breast cancer models. *Hum Gene Ther* 1999;10:697-709.

37. Lohr F, Hu K, Huang Q, *et al.* Enhancement of radiotherapy by hyperthermia-regulated gene therapy. *Int J Radiat Oncol Biol Phys* 2000;48:1513-1518.

38. Huang Q, Hu JK, Lohr F, *et al.* Heat-induced gene expression as a novel targeted cancer gene therapy strategy. *Cancer Res* 2000;60:3435-3439.

39. Zhang Y, Schneider RJ. Adenovirus inhibition of cell translation facilitates release of virus particles and enhances degradation of the cytokeratin network. *J Virol* 1994;68:2544-2555.

40. He TC, Zhou S, da Costa LT, *et al.* A simplified system for generating recombinant adenoviruses. *Proc Natl Acad Sci U S A* 1998;95:2509-2514.

41. Leutenegger CM, Mislin CN, Sigrist B, *et al.* Quantitative real-time PCR for the measurement of feline cytokine mRNA. *Vet Immunol Immunopathol* 1999;71:291-305.

42. Livak KJ, Schmittgen TD. Analysis of relative gene expression data using real-time quantitative PCR and the 2(-Delta Delta C(T)) Method. *Methods* 2001;25:402-408.

43. Pfaffl MW. A new mathematical model for relative quantification in real-time RT-PCR. *Nucleic Acids Res* 2001;29:e45.

44. Hendrick MJ, Goldschmidt MH. Do injection site reactions induce fibrosarcomas in cats? *J Am Vet Med Assoc* 1991;199:968.

45. Kass PH, Barnes WG, Jr., Spangler WL, *et al.* Epidemiologic evidence for a causal relation between vaccination and fibrosarcoma tumorigenesis in cats. *J Am Vet Med Assoc* 1993;203:396-405.

46. Macy DW, Hendrick MJ. The potential role of inflammation in the development of postvaccinal sarcomas in cats. *Vet Clin North Am Small Anim Pract* 1996;26:103-109.

47. Hauck M. Feline injection site sarcomas. *Vet Clin North Am Small Anim Pract* 2003;33:553-557, vii.

48. Hendrick MJ. Historical review and current knowledge of risk factors involved in feline vaccine-associated sarcomas. *J Am Vet Med Assoc* 1998;213:1422-1423.

49. Hendrick MJ, Goldschmidt MH, Shofer FS, *et al.* Postvaccinal sarcomas in the cat: epidemiology and electron probe microanalytical identification of aluminum. *Cancer Res* 1992;52:5391-5394.

50. O'Quigley J, Pepe M, Fisher L. Continual reassessment method: a practical design for phase 1 clinical trials in cancer. *Biometrics* 1990;46:33-48.

51. Cole S, Lewkowicz SJ, Townsend KM. Langerhans cell number and morphology in mouse footpad epidermis after X irradiation. *Radiat Res* 1984;100:594-606.

52. Atkins MB, Robertson MJ, Gordon M, *et al.* Phase I evaluation of intravenous recombinant human interleukin 12 in patients with advanced malignancies. *Clin Cancer Res* 1997;3:409-417.

53. Car B, Eng V, Schnyder B, *et al.* Role of interferon-gamma in interleukin 12-induced pathology in mice. *Am J Pathol* 1995;147:1693-1707.

54. Sarmiento UM, Riley JH, Knaack PA, *et al.* Biologic effects of recombinant human interleukin-12 in squirrel monkeys (Sciureus saimiri). *Lab Invest* 1994;71:862-873.

55. Watanabe N, Sypek JP, Mittler S, *et al.* Administration of recombinant human interleukin 12 to chronically SIVmac-infected rhesus monkeys. *AIDS Res Hum Retroviruses* 1998;14:393-399.

56. Borrelli MJ, Schoenherr DM, Wong A, *et al.* Heat-activated transgene expression from adenovirus vectors infected into human prostate cancer cells. *Cancer Res* 2001;61:1113-1121.

57. Stewart AK, Lassam NJ, Graham FL, *et al.* A phase I study of adenovirus mediated gene transfer of interleukin 2 cDNA into metastatic breast cancer or melanoma. *Hum Gene Ther* 1997;8:1403-1414.

Chapter 5

OBJECTIVE ASSESSMENT OF THE ANTI- ANGIOGENIC EFFECTS OF INTERLEUKIN- 12 DELIVERED BY A NOVEL HYPERTHERMIA INDUCED GENE CONSTRUCT

ABSTRACT

Interleukin-12 (IL-12) is a pro- inflammatory cytokine known to possess anti- cancer properties. It is also an anti- angiogenic molecule and this property has been studied extensively using various assays and systems. In this study we quantitatively measured the anti- angiogenic effect of IL-12 delivered using a adenoviral vector with a gene encoding for murine IL-12 placed under control of a heat shock promoter. The rationale behind this approach is to deliver IL-12 locally to the tumor with little or no systemic IL-12, thus limiting its toxicity. 4T1 tumors were grown in Balb/C mice and the Ad*hsp*mIL-12 construct was injected intratumorally. The tumors were heated after 24 hours using a water bath. At various time points post- heating the tumors were collected and quantitatively assessed for cytokine production and vascularity. A significant reduction was seen in the tumor vasculature of the treated group versus the control group mice. Generalized immunostimulation, a systemic effect of the IL-12 was seen. However, no systemic toxicity was noted when the livers were examined for hepatic necrosis. This study serves to establish that IL-12 can be safely delivered using a gene- based approach with the IL-12 gene placed under control of a heat shock promoter.

INTRODUCTION

The term *angiogenesis* refers to the process leading to the formation of new vessels. Under physiologic conditions angiogenesis is responsible for fetal development and wound healing and repair. Pathologic angiogenesis is seen in tumors. Here vessels from the host organ or tissue are recruited into the tumor tissue to enable the growth, invasion and metastasis of solid tumors. In the absence of angiogenesis, the tumors and their metastases may become necrotic and apoptotic or may remain inactive for long periods of time.

Interleukin- 12 (IL-12) is a potent pro- inflammatory cytokine possessing anti- cancer properties. An excellent review on interleukin-12 by Colombo and Trinchieri[1] outlines its anti- tumor, anti- metastatic, anti- angiogenic properties and the ability to elicit long term anti-tumor immunity. Voest *et al*[2] studied the role and possible mechanisms of action of IL-12 in antiangiogenesis. They studied the effect of IL-12 against basic fibroblast growth factor (bFGF) induced corneal neovascularization in immunocompetent C57BL/6 mice, SCID mice and natural killer cell defective beige mice. IL-12 (1μg/ day) was given intraperitoneally for two cycles of five days each with a two- day break in between. They found significant reduction in bFGF induced corneal neovascularization in the IL-12 treated mice. This effect was lost when the mice had also received an antibody against IFN-γ, suggesting that IFN-γ was an important mediator in the antiangiogenic effects of IL-12. They proposed that IFN-γ has two major effects (a) it induces production of interferon inducible protein-10 (IP-10), a member of the -C-X-C- chemokine family, which is directly antiangiogenic (b) IFN-γ inhibits metalloproteinase production. Metalloproteinases breakdown the extracellular matrix to allow new capillary

sprouts to grow through and thus inhibition of metalloproteinase activity might inhibit angiogenesis.

The possibility of using IFN-γ itself was also investigated. However, it was found to exhibit biphasic pharmacokinetics[3] and the same tumor growing at different sites had different relative sensitivities to IFN- γ[4]. IFN-γ induces the production of soluble anti-angiogenic factor interferon- inducible protein 10 (IP-10)[5]. This protein is expressed in activated mononuclear cells, keratinocytes, fibroblasts, endothelial cells and T cells. IP-10 was found to inhibit bFGF-induced neovascularization of Matrigel injected subcutaneously into athymic mice. In addition, IP-10, in a dose-dependent fashion, suppressed endothelial cell differentiation into tubular capillary structures in vitro[6]. The precise mechanism by which IFN- γ prevents new blood vessel formation remains unclear, but involves the production of IP-10 (CXCL10)[7] and monokine induced by interferon gamma (MIG/CXCL9)[8]. It has been suggested that the balance between the local concentrations of proangiogenic and antiangiogenic factors within a tumor dictates whether angiogenesis occurs. Since angiogenesis is required for tumors and metastases to grow beyond a few millimeters in diameter, angiogenesis inhibition is thought to be an important mechanism by which IL-12 controls tumor growth. Hence IL-12 is proposed to act through the activation of IFN- γ/ IP 10 axis. Other proposed mechanisms implicate direct natural killer (NK) cell mediated endothelial cytotoxicity[9] and downregulation of VEGFR-3 receptor[10].

Locally produced IL-12 controls the growth of solid tumors through at least three distinct mechanisms[11]. 1) Stimulation of T cell mediated killing of tumor cells 2) Suppression of tumor cell proliferation by IL-12 induced IFN-γ and 3) Inhibition of tumor angiogenesis.

Cavallo *et al*[12] summarized the main events leading to IL-12 induced tumor inhibition *in vivo*. An inverse relation has also been shown between vascular endothelial growth factor (VEGF) and IL-12[13, 14].

Local and systemic administration of IL-12 protein has been studied in various murine models [15-18] and in Phase I/II human trials [19, 20]. However, IL-12 protein therapy has been limited by dose-dependent toxicity [21]. Human recombinant IL-12 is associated with severe toxicity, even at doses as low as 1μg/kg/day[22]. Common toxicities included fever/chills, fatigue, nausea, vomiting, and headache. Routine laboratory changes included anemia, neutropenia, lymphopenia, hyperglycemia, thrombocytopenia and hypoalbuminemia. Dose limiting toxicities included oral stomatitis and liver function test abnormalities, predominantly elevated transaminases. IL-12 does not accumulate selectively in tumors. Most anticancer drugs and proteins have tumor: organ ratios less than 1 after intravenous injection and this poor accumulation may be responsible for the modest performance against solid tumors[23].

It has also been shown that recombinant IL-12 administration induces a transient period of profoundly impaired immune response that can compromise host protection against tumors[24, 25].

Local expression of IL-12 may avoid systemic toxicity of recombinant interleukin-12 administration[26-28].

Intratumoral injections of adenoviral vectors or IL-12 plasmid DNA, naked or in complex with cationic lipid [29] have been tried to deliver therapeutic IL-12 with the rationale that IL-12 will be produced only in the virally infected tumors, thereby reducing systemic side effects. A few reports have indicated the efficacy of this approach [30-32]. However,

elevated systemic transgene levels are still observed in many cases as adenovirus can reach the circulation [33-35] and infect other organs; and the promoters in most previous reports are constitutively active, such as cytomegalovirus (CMV) based promoters. This combination makes it likely that intratumoral injection of this constitutively active adenovirus approach will still result in toxicity [36, 37].

To achieve this goal of localizing gene expression, a heat-inducible adenoviral gene therapy vector with murine IL-12 placed under the control of a heat inducible promoter was developed at Duke University. The rationale for using this heat shock promoter (hsp) is that hyperthermia is most likely to be used as an adjuvant therapy with radiation and chemotherapy. Heating the tumor leads to activation of the *hsp* promoter and subsequent local IL-12 production.

The feasibility of combining fractionated radiotherapy, hyperthermia and heat inducible gene therapy in a nonimmunogenic B16.F10 melanoma line that is syngenic with C57BL/6 mice was studied [38]. It was concluded that hyperthermia-regulated gene therapy in combination with radiation is feasible and therapeutically effective in murine tumors with no apparent systemic toxicity [38, 39].

Hyperthermia involves localized delivery of heat to the tumor aimed at tumor cell killing. The tumors are heated to a temperature of 41°C- 44°C for 30- 60 minutes. It is now an established modality in the anti- cancer armamentarium and is frequently employed in combination with radiation therapy or chemotherapy.

Apart from its effects of directly killing cells by alterations in nuclear and cytoskeletal structures, metabolic pathways and intracellular signals, hyperthermia also demonstrates

anti- angiogenic effects[40, 41]. This may be due to endothelial cell killing, interference with cell replication, inhibition of cell migration, or a combination of these mechanisms[42].

Various *in vivo* assays have been described in literature to study angiogenesis and anti-angiogenesis. These include the rat corneal pocket assay, Matrigel plug assay, chorioallantoic membrane of the chick (CAM) assay, dorsal skin- fold chamber etc. Compared to these systems, which usually do not accurately mimic a tumor microenvironment, the use of mouse tumor models offers certain advantages[43]. The transplanted tumor models arise from a relatively homogeneous, fully transformed cells. After injection of the tumor cell line the tumors are seen within a few days and their response to therapeutic intervention can be followed easily.

The 4T1 mouse mammary adenocarcinoma cell line is derived from a single spontaneously arising mammary tumor from a BALB/BfC3H mouse[44]. It is a highly metastatic cell line, metastasizing hematogenously to lungs, heart, bone, brain and liver[45]. We studied both patent functional vasculature using lectin intravital perfusion (FITC-conjugated *Lycopersicon esculentum* lectin) and vascular antigen staining (CD31). The fluorescently conjugated plant lectin was injected into the tail vein of the mice and served to identify functional blood vessels after sacrificing the mice[46, 47].

A significant reduction in vasculature was noted in the treated group of mice as compared to the controls.

MATERIALS AND METHODS

Animals: BALB/c mice, 9-12 weeks of age weighing 20-25 grams were obtained from the Laboratory Animal Resources at Colorado State University.

Design of vector: The AdEasy system (Stratagene, La Jolla, CA) was used to construct the Ad*hsp*mIL12. The two subunits (p35 and p40) of the murine IL-12 were amplified and sequence-verified. They were then connected into one gene expression unit by use of a flexible linker sequence (Gly4Ser). A 400-bp hsp70B promoter was then used to control the expression of the modified murine IL-12 gene. The whole hsp-mIL12 gene expression cassette was then transferred into an adenovirus shuttle plasmid. The shuttle plasmid was cotransfected into 293 cells to derive Ad*hsp*mIL12. Amplification and isolation of the virus was achieved following standard protocols[48, 49].

Tumor cell injection: 4T1 cells were obtained from American Type Culture Collection (ATCC). $5X10^5$ cells were diluted in 50μl of PBS and injected into the left hind legs of the mice. Eight to ten days later the tumors reached a volume of $200mm^3$. Daily tumor measurements were done using calipers. Mice were euthanized at a tumor volume of ~1000 to $1200mm^3$. At this tumor size the left hind leg becomes paralyzed and non-functional and in some cases the skin starts ulcerating. This study was approved by the Colorado State University Animal Care and Use Committee.

Treatment groups: Tumor bearing mice were divided into the following treatment groups

(1) Control - intratumoral normal saline injection 50µl. (2) Injection of 10^8 pfu of Ad LacZ (empty vector) dissolved in 50µl of normal saline intratumorally + hyperthermia (3) Injection of 10^8 pfu of Ad*hsp*mIL-12 dissolved in 50µl of normal saline intratumorally (No HT) (4) Intratumoral normal saline injection 50µl + HT (5) Injection of 10^8 pfu of Ad*hsp*mIL-12 dissolved in 50µl of normal saline intratumorally + HT.

All intratumoral injections were given 24 hours prior to delivering hyperthermia.

Hyperthermia: The mice were anesthetized using 2% isoflurane and the tumors heated with the tumor bearing leg immersed in a water bath. The tumors were heated at 41°C for 60 minutes (Figure 1).

In Vivo *hypoxia and vascular markers*: Hypoxyprobe-1 (Chemicon International, Temecula, CA) was injected intraperitoneally at a dose of 75 mg/kg dissolved in 100µl of normal saline 90 minutes before euthanasia. *Lycopersicon* (tomato plant) lectin (Vector Laboratories, Burlingame, CA) conjugated with FITC was used as a marker for functional vasculature. It was injected via the tail vein in a dose of 100µg in 100µl of normal saline 3 minutes prior to euthanasia.

Tissue harvesting: Mice were euthanized by cervical dislocation under anesthesia. Within one minute of death, part of the tumor was collected in a cryotube and part embedded in Tissue-Tek optimum cutting temperature compound (OCT). Both parts were immediately frozen in liquid nitrogen. Lungs, liver and spleen were collected over the next 2-3 minutes and preserved in formalin.

FIGURES

Figure 1- Mouse hyperthermia setup

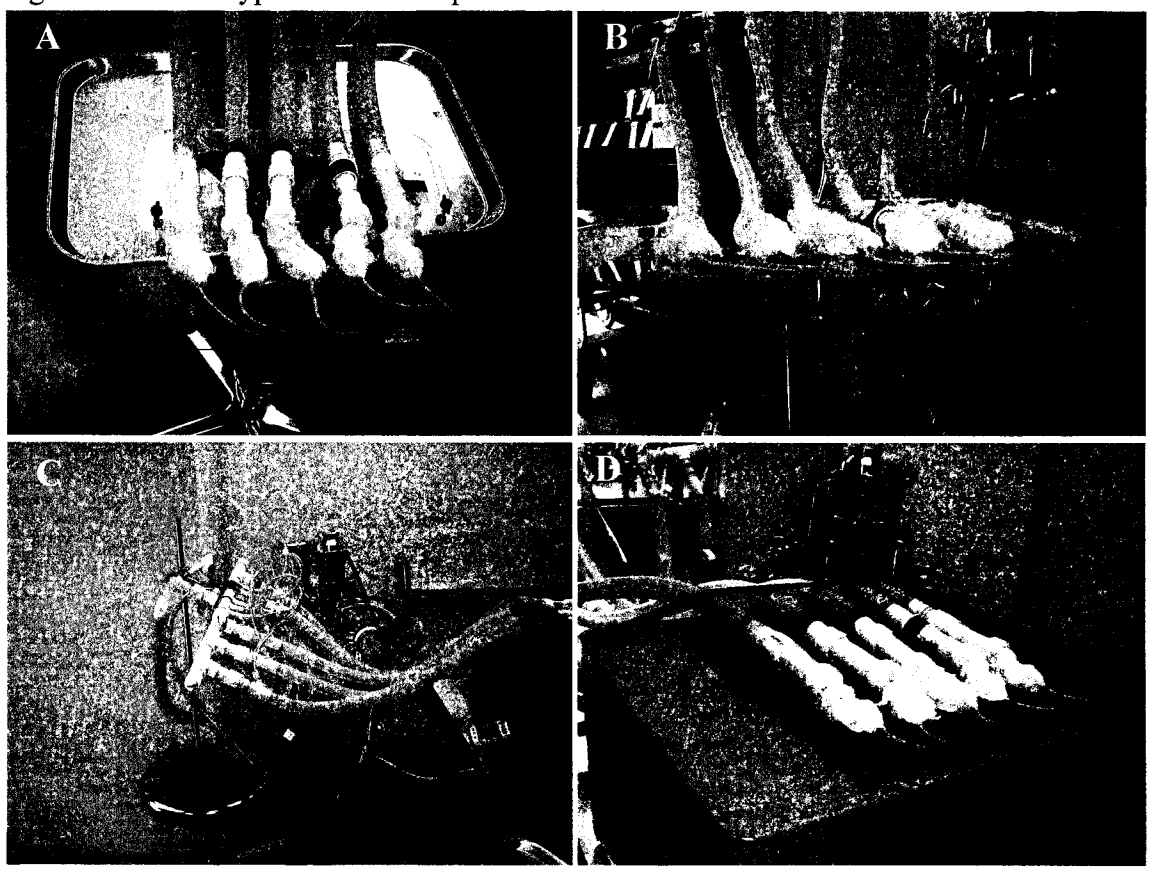

Figure 1 MOUSE HYPERTHERMIA SETUP

a. Five 1cm diameter holes were cut in a Perspex sheet designed to fit a VWR water bath.
b. The tumor bearing leg was drawn through the hole and weighted down with fish lead weights (8-9 grams).
c. A gas anesthesia machine was used to deliver Isoflurane. A single outlet was split into 5 to enable anesthetizing and heating 5 mice at a time.
d. After anesthetizing the mice the Perspex sheet was lowered into the water bath and it rested on a ridge inside the bath with the tumor bearing leg suspended in water at desired temperature.

RNA isolation and cDNA synthesis- Tumor samples were lysed and RNA isolated using TRIzol Reagent (GibcoBRL) as per manufacturer's protocol. RNA purity was assessed spectrophotometrically. Total isolated RNA was treated with DNase I (Invitrogen) to remove any genomic DNA. cDNA synthesis was then carried out using Superscript II RNase H$^-$ Reverse Transcriptase (Invitrogen, Carlsbad, CA). Each reaction mixture contained 10μl of RNA solution to which was added 4μl First strand buffer (5X), 1μl dNTP (10mM), 1μl DTT (0.1M), 0.25μl RNase out (40U/μl), 0.25μl SuperScript II (200 U/μl), 2μl of random hexamers (300ng/μl) and 1.5μl DNase, RNase free water giving a total of 20μl per reaction mixture. This was incubated at 42°C for 50 minutes following which 30μl of DNase, RNase free water was added to the mix and the enzymes inactivated by placing the reaction tubes on a 95°C heat- block for 5 minutes. The cDNA was then stored at –20°C till the time of RT- PCR.

Real Time PCR- We employed real- time reverse transcriptase PCR to detect and quantitatively express the production of murine genes of interest and GAPDH mRNA. Sequences for the primers and probes were obtained from the literature[50-53] and purchased from MWG Biotech (High Point, NC).

Murine Cytokine Gene Sequences (All 5'→ 3')

IL-12 p40

Forward- GGA AGC ACG GCA GCA GAA TA

Reverse- AAC TTG AGG GAG AAG TAG GAA TGG

Probe- CAT CAT CAA ACC AGA CCC GCC CAA

IFN- γ

Forward- TCA AGT GGC ATA GAT GTG GAA GAA

Reverse- TGG CTC TGC AGG ATT TTC ATG

Probe- TCA CCA TCC TTT TGC CAG TTC CTC CAG

IP-10

Forward- GCC GTC ATT TTC TGC CTC AT

Reverse- GCT TCC CTA TGG CCC TCA TT

Probe- TCT CGC AAG GAC GGT CCG CTG

PAI-1

Forward- CAG AGC AAC AAG TTC AAC TAC ACT GA

Reverse- CAG CGA TGA ACA TGC TGA GG

Probe- ATG ACG TCG TGG AAC TGC CCT ACC A

VEGF

Forward- TGT ACC TCC ACC ATG CCA AGT

Reverse- TGG AAG ATG TCC ACC AGG GT

Probe- CCA GCG AAG CTA CTG CCG TCC AAT T

GAPDH

Forward- TTC ACC ACC ATG GAG AAG GC

Reverse- GGC ATG GAC TGT GGT CAT GA

Probe- TGC ATC CTG CAC CAC CAA CTG CTT AG

The reporter dye attached covalently at the 5' end was FAM (6- carboxyfluorescin) and the quencher bound to the 3' end was TAMRA (6- carboxytetramethylrhodamine).

Real time PCR was performed using the Applied Biosystems ABI Prism 7000 (Foster City, CA). The amplification protocol was: 2 min at 50°C, 10 min at 95°C, 45 cycles of 15s at 95°C and 60 s at 60°C.

Cycle threshold values were obtained from the ABI software were exported and the $2^{-\Delta\Delta Ct}$ method[54] was used to determine the relative expression of the genes of interest. Briefly, a standard housekeeping gene (eg. GAPDH, β- actin, β_2 microglobulin) is chosen as an internal control gene. This serves to normalize the amount of cDNA loaded for each reaction. An untreated control was selected as the 'calibrator' and the relative expression data is obtained as the fold change in gene expression normalized to the chosen endogenous reference gene and relative to the untreated control.

Prior to using the $2^{-\Delta\Delta Ct}$ method for relative quantification, we validated its use for the primer and probe sequences and PCR conditions being employed in our experimental conditions. The methods and acceptable results are described in literature[54, 55]. Briefly, the target cDNA was serially diluted and Real time PCR performed. Cycle threshold values for the serially diluted samples are plotted on a graph with the log dilution on the X- axis and cycle threshold values on the Y- axis. The slope of the line is used to obtain the efficiency of PCR amplification using the formula- Efficiency = $10^{(-1/slope)}$-1.

Imaging for functional vasculature: Five micron thick frozen sections of the tumors were made and stored in the dark at -80°C. Tumor sections were imaged for FITC fluorescence using a Zeiss Axioplan 2 microscope (Carl Zeiss) with the KS 400 image analysis software. An area of the tumor away from the periphery was chosen for image capture. Images were captured at 100X. Five to six separate sections from 4-5 mice per group

were captured for further image analysis. The X- and Y- coordinates of each image were recorded to enable the same area to be imaged after CD31 and hypoxyprobe staining.

Immunohistochemistry-Immunohistochemical staining was performed using standard manual techniques on a vertical slide staining system (Credenza, Thermo Electron Corporation, Philadelphia, PA). Cryosections were fixed in -20° C acetone for 10 minutes and then allowed to dry at room temperature for 30 minutes before proceeding. All reagents and kits were purchased from Vector Laboratories, Burlingame, CA unless otherwise noted. In all cases a control section was processed in which the primary antibody was replaced with simple antibody diluent. For monoclonal antibodies another negative control was run with isotype similar non- specific antibody replacing the primary antibody at a similar concentration.

Hypoxyprobe/ CD 31 staining:

Fixed sections were stained following the horseradish peroxidase based M.O.M. immunodetection kit with a hypoxyprobe 1-Mab1 (Chemicon International, Temecula, CA) as the primary Ab at a 1:50 dilution in antibody diluent (DakoCytomation, Carpinteria, CA). DAB substrate was used to visualize the immunoreactive complexes. Sections were incubated overnight in a rat monoclonal anti-mouse CD31 primary antibody (Clone MEC 13.3, BD Pharmingen, San Diego, CA) at 1:100 dilution in antibody diluent. A secondary biotinylated rabbit anti rat IgG antibody at 1:100 dilution was applied and followed with a horseradish peroxidase streptavidin at 1:250 dilution in PBS. A VIP peroxidase substrate kit was used for visualization. Sections were

dehydrated through ascending serially concentrated alcohol baths and mounted in a xylene based permanent mounting media.

IL-12/ IP-10 staining:

Fixed sections were incubated overnight in primary antibody, rat monoclonal anti-mouse IL-12 (Clone C15.6, Biosource, Camarillo, CA) at 1:100 dilution in antibody diluent or Rabbit anti-mouse IP-10 (Peprotech, Rocky Hill, NJ) at 1:200 dilution in antibody diluent. A biotinylated secondary rabbit anti-rat IgG or goat anti-rabbit IgG at 1:100 dilution was applied and followed with a horseradish peroxidase streptavidin at 1:250 dilution. DAB substrate was used to visualize the immunoreactive complexes. Sections were dehydrated through ascending serially concentrated alcohol baths and mounted in a xylene-based permanent mounting media.

Image analysis: The saved images were quantitatively analyzed for the parameters of interest using Scion Image (NIH). The 'density slice' was fixed for a color of interest (FITC- green, CD31- blue, hypoxyprobe- orange/ red) and the area occupied by the stain was obtained from the software expressed as pixels. All images for a particular color were analyzed using the same 'density slice'.

Statistics: Pixel areas for FITC, CD31 and hypoxyprobe staining were compared between the treatment groups using the ANOVA test with pairwise comparison between groups.

RESULTS

Cytokine RT-PCR- Real time PCR was performed to quantitatively detect presence of IL-12, IFN-γ, IP-10, PAI-1 and VEGF mRNAs with GAPDH as the housekeeping gene. Initially, experiments were performed to detect efficiency of amplification for the genes of interest. After ascertaining that the PCR amplification efficiency was in the 90%-95% range using our primer and probe sequences, the real time PCR for various treatment groups was performed. Results are shown in Figure 2. Each bar represents the average ± SEM of cytokine expression in tumors from 5 mice with each sample run in triplicate. The expression levels in the treatment groups are normalized to control group (group 1). The groups mentioned in the graphs are as follows- Group 1 – Normal saline injection, Control. Tumor and tissue samples collected at the same time as treatment group (five days post- HT); Group 2 – Ad LacZ + HT. Tumor and tissue samples collected 5 days post- HT; Group 3 – Ad *hsp* mIL-12, no HT. Tumor and tissue samples collected at the same time as treatment group (5 days post- HT); Group 4 – Normal saline injection, HT only. Tumor and tissue samples collected 5 days post- HT; Group 5a – 6 hours post- HT; Group 5b – 24 hours post- HT; Group 5c – 5 days post- HT.

Maximum IL-12 mRNA levels were seen in the tumor samples collected 6 hours post-HT (Group 5a). By 24 hours post- HT (Group 5b) the level had reduced by about 2.5 logs (Figure 2a). There was mRNA present even on the 6^{th} day post – HT. IL-12 mRNA was also elevated in Group 3, where the Ad*hsp*fIL-12 had been injected intratumorally but no hyperthermia had been delivered.

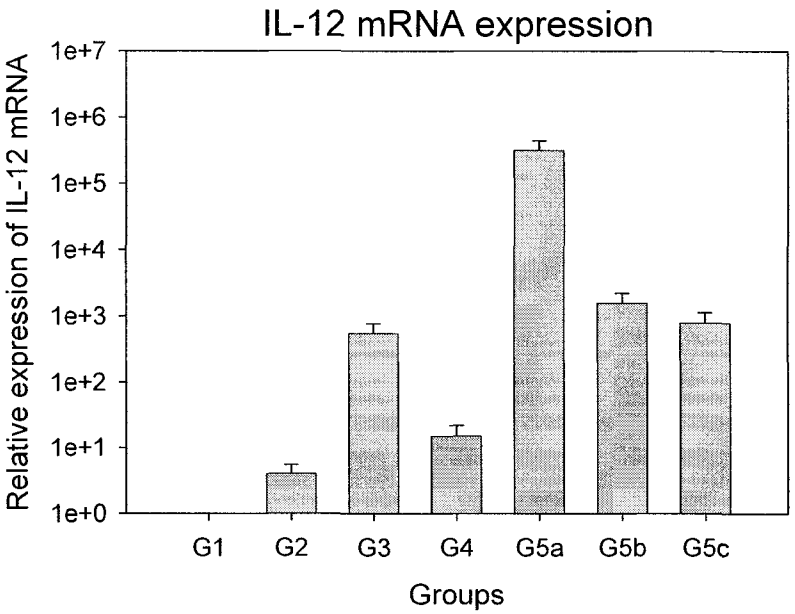

Figure 2a

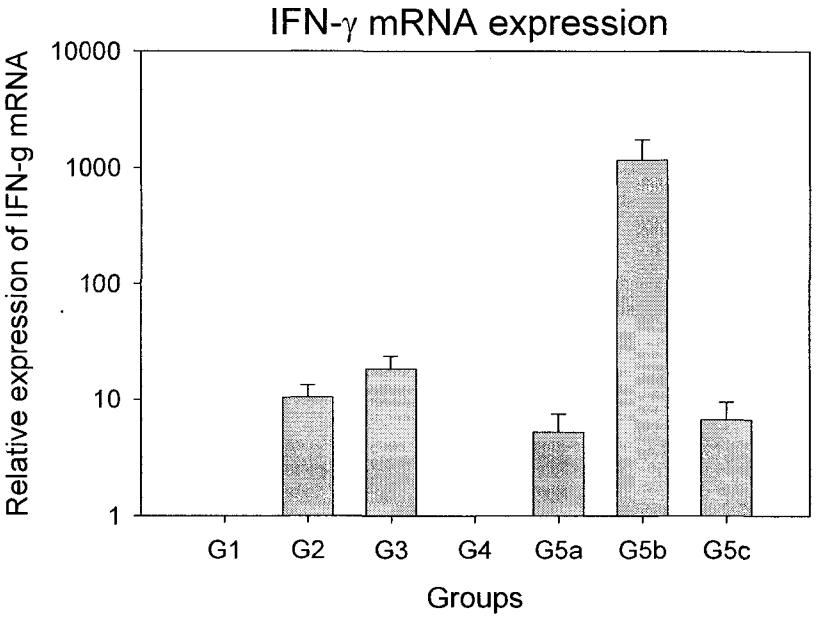

Figure 2b

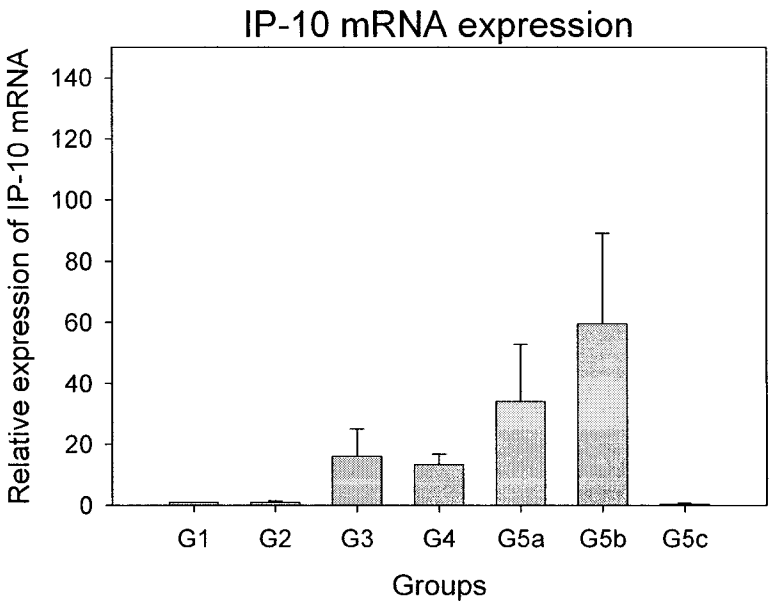

Figure 2c

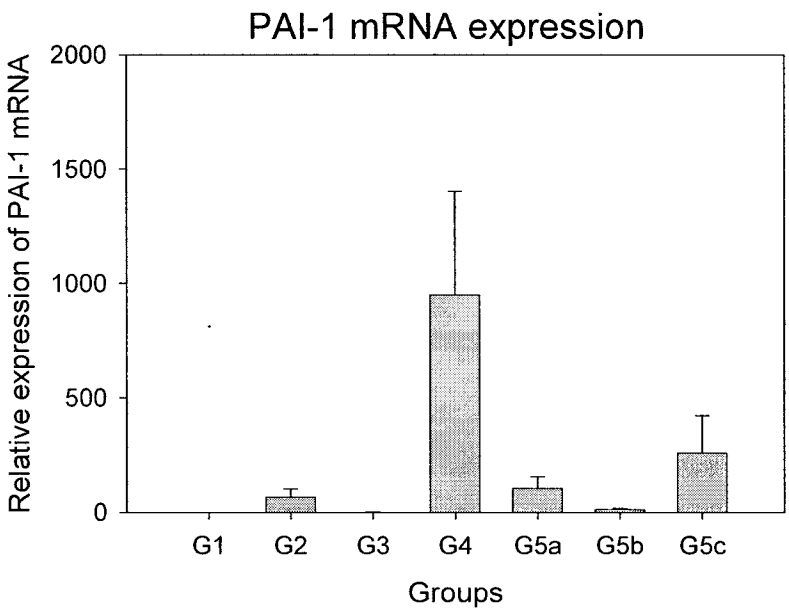

Figure 2d

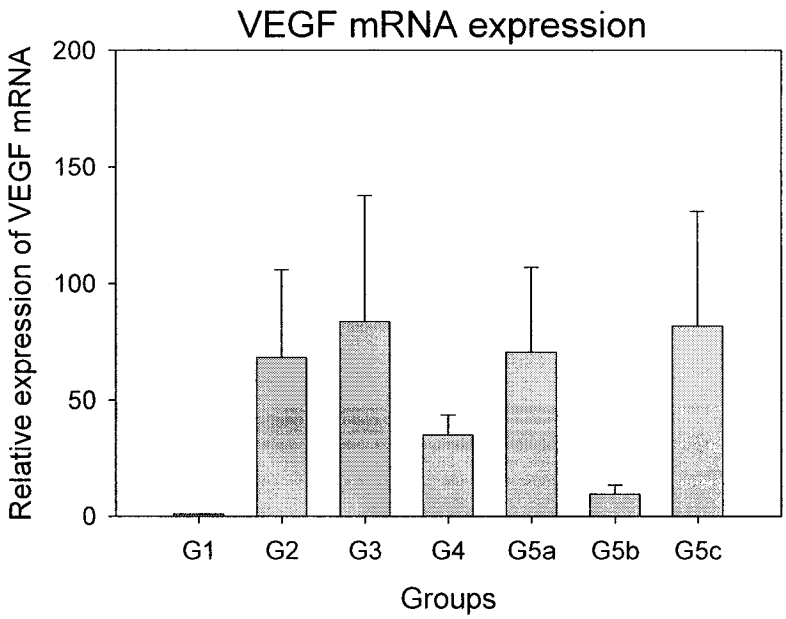

Figure 2e

Figure 2- RELATIVE EXPRESSION OF mRNAs IN THE TREATED GROUPS 2 TO 5C NORMALIZED TO GROUP 1. (Each bar represents samples from 5 mice each in triplicate ± SEM). Group 1 – Normal saline injection, Control. Tumor and tissue samples collected at the same time as treatment group (five days post- HT); Group 2 – Ad LacZ + HT. Tumor and tissue samples collected 5 days post- HT; Group 3 – Ad *hsp* mIL-12, no HT. Tumor and tissue samples collected at the same time as treatment group (5 days post-HT); Group 4 – Normal saline injection, HT only. Tumor and tissue samples collected 5 days post- HT; Group 5a – 6 hours post- HT; Group 5b – 24 hours post- HT; Group 5c – 5 days post- HT.

a. Interleukin-12 (IL-12)
b. Interferon- γ (IFN-γ)
c. Interferon inducible protein- 10 (IP-10)
d. Plasminogen activator inhibitor (PAI-1)
e. Vascular endothelial growth factor (VEGF)

This suggested *hsp* induction by factors other than hyperthermia. Peak IFN-γ levels were noted 24 hours post- HT (Figure 2b) corresponding to the time- point at which the IL-12 protein levels would be highest. IP-10 mRNA also followed the same trend. However, as opposed to IL-12 and IFN-γ mRNA levels, which were still high in Group 5c, the IP-10 levels had returned to baseline (Figure 2c). PAI-1 was highest in Group 4 (HT only) (Figure 2d). VEGF levels were elevated in all groups (Figure 2e). There were highly varying fold- increases in mRNA within the groups, as represented by the large error-bars. In groups 5a-c, the levels appeared to be inversely related to the IL-12 levels.

Tumor growth curves- After the tumors reached sizes of approximately 3-4 mm in diameter, daily tumor measurements were done using calipers. Tumor volume was calculated as- short axis^2 X long axis X $\pi/6$. Relative tumor volumes are shown in Figure 3. A statistical analysis using analysis of variance (ANOVA) with pairwise comparison revealed a statistically significant ($p<0.05$) difference between the control and Ad*hsp*flL-12+HT group and no difference between control and HT only or between HT only and Ad*hsp*flL-12+HT.

Image analysis for vascular area- Five to six tumor sections from 4-5 mice per group were examined at 100X for Tomato lectin-FITC fluorescence and CD31 staining (Figures 4 to 6). Image analysis was done and the results are shown in Figures 8 and 9 respectively.

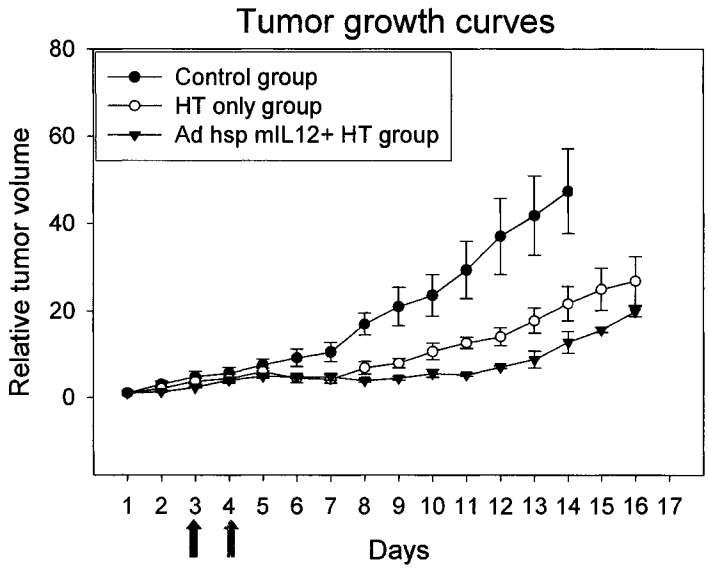

Figure 3- TUMOR GROWTH CURVES
The blue arrow on day 3 represents the day of injection and the red arrow the day of hyperthermia. Each point is the relative tumor volume normalized to day 1 and error bars are SEM.

Figure 8a and 9a show the total area in pixels and 8b and 9b show the same data expressed as a percentage of the total tumor area imaged. As can be seen from the graph, the area occupied by functional patent vasculature (FITC staining) is less than the area staining for vascular antigens (CD31 staining) by a factor of about 3. In the control group it is 1.05± 0.85% and 3.5± 1.75% for FITC and CD31 respectively. In the treatment group it is 0.26± 0.22% and 0.84± 0.62% for FITC and CD31.

A statistically significant ($p<0.05$) decrease in tumor vasculature was seen in group 5 as compared to all other groups for FITC as well as CD31 staining. In group 3, where the vector had been injected but the tumor was not heated, the difference was also significant as compared to controls.

Image analysis for hypoxia- Hypoxyprobe staining was done to assess areas of tumor hypoxia in the different groups. Figure 10 shows the results. In the control group and groups 2-4 the tumor hypoxic area was 9.5%-11.5% with standard deviations of 6%-7%, however in the Ad*hsp*flL-12+HT group, the hypoxic area was 19.8± 7.5%. This increase was statistically significant ($p<0.05$).

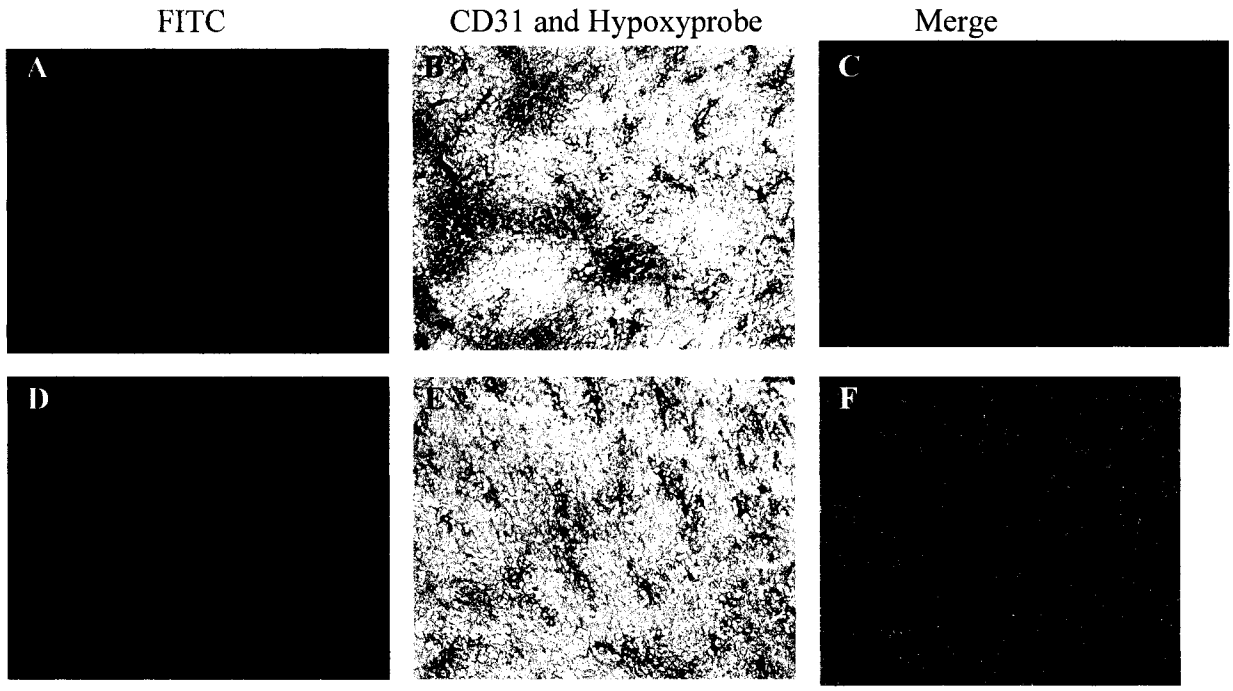

Figure 4- SAME AREA OF A TUMOR SECTION IMAGED FOR TOMATO LECTIN-FITC STAINING AND SUBSEQUENTLY FOR CD31 (VIOLET) AND HYPOXYPROBE (BROWN).
Figures 4a and d- Tomato lectin- FITC.
Figures 4b and e- Same coordinates on the slide imaged for CD31 and hypoxyprobe staining.
Figures 4c and f- Image 4a and 4d overlaid on 4b and 4e to show correspondence between functional vasculature and CD31 staining. Area stained by CD31 is larger than FITC indicative of greater presence of the antigen than is actually patent functional vessels.

CONTROL (100X)

GROUP 5 (100X)

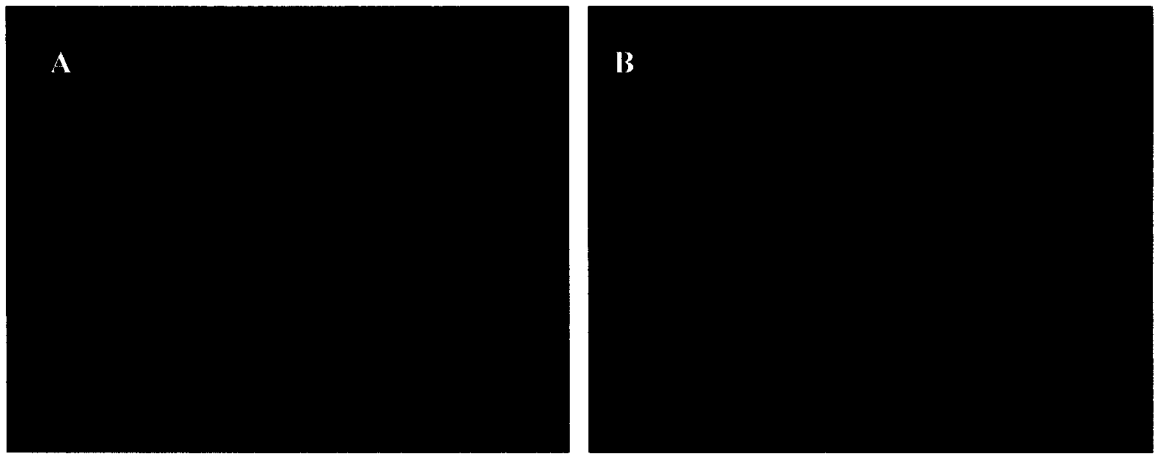

Figure 5- FITC IMAGES OF CONTROL AND TREATED GROUP
Figure 5a- Image from a control tumor section showing the patent vasculature in green.
Figure 5b- Image from an IL-12 treated tumor 6 days post- hyperthermia showing much reduced vasculature.

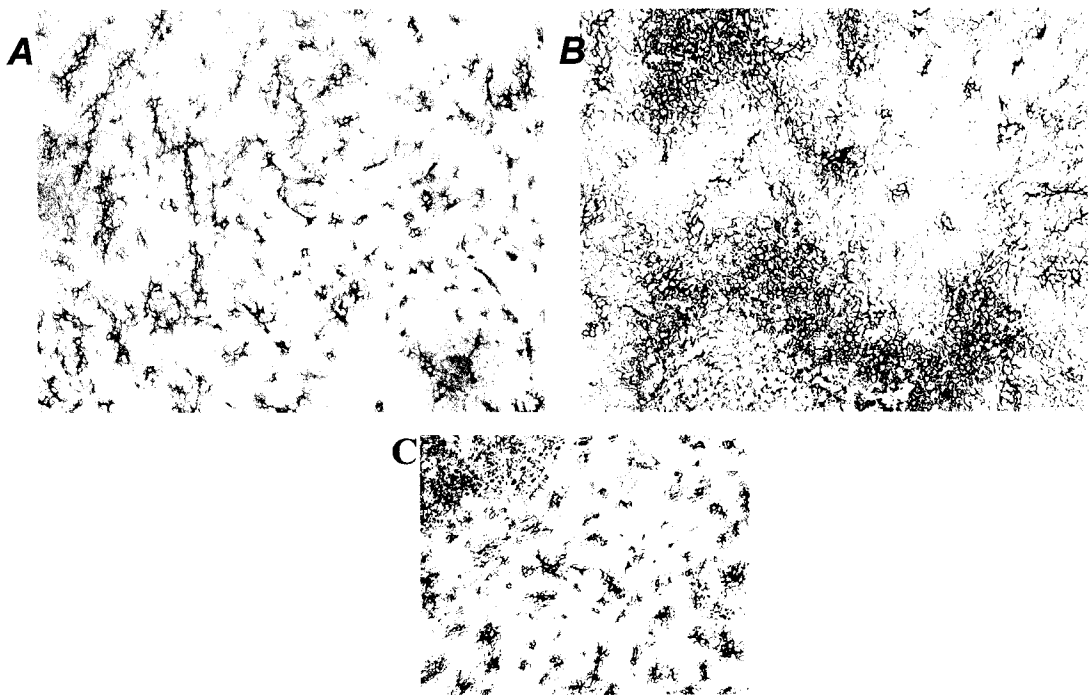

Figure 6- CD31 (VIOLET) AND HYPOXYPROBE (BROWN) STAINING (100X)
Figure 6a- Example of a section from a control group tumor showing large areas staining positive for CD31 antigen with small areas of hypoxia
Figure 6b- Example of a section from a treated group tumor showing reduced CD31 staining and larger areas of hypoxia.
Figure 6c- Contrast and brightness of the captured image was adjusted to increase the color differential between CD31 positive and Hypoxyprobe positive areas to enable quantification using the Scion image software.

A. B.

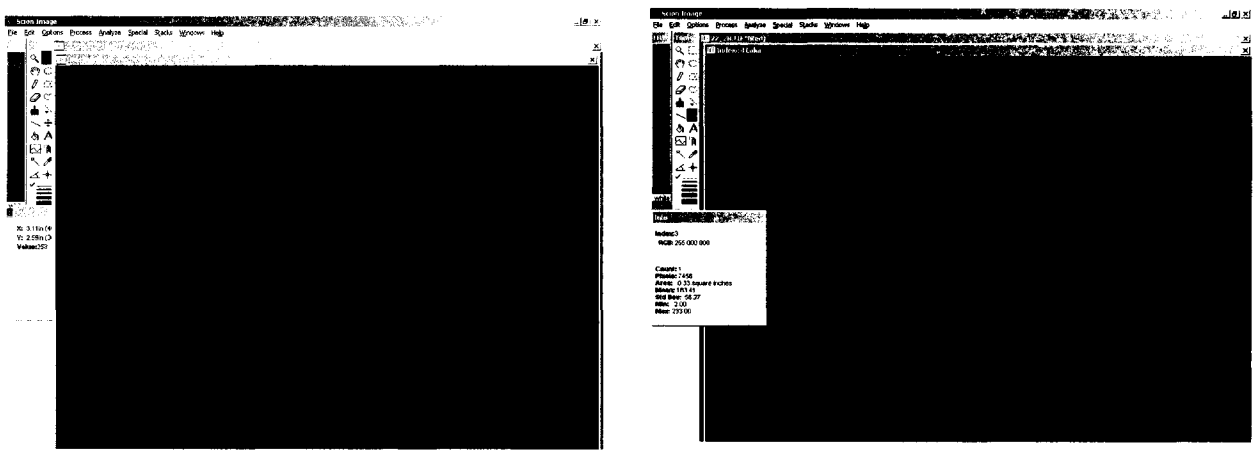

Figure 7- SCREEN IMAGES OF THE SCION IMAGE (NIH) SOFTWARE
Figure 7a. An image to be analyzed is opened in the software.
Figure 7b. A "density slice" can be selected to include all the areas of interest to be analyzed. Clicking on the "Analyze" will give the area in pixels occupied by the selected region.

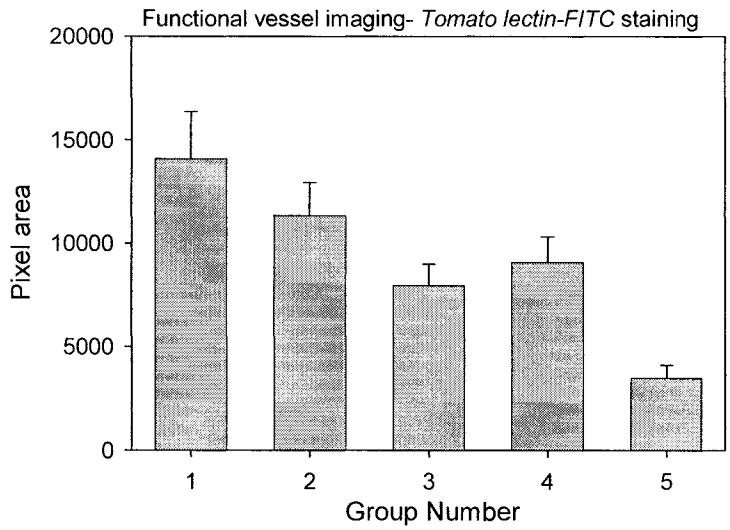

Figure 8a

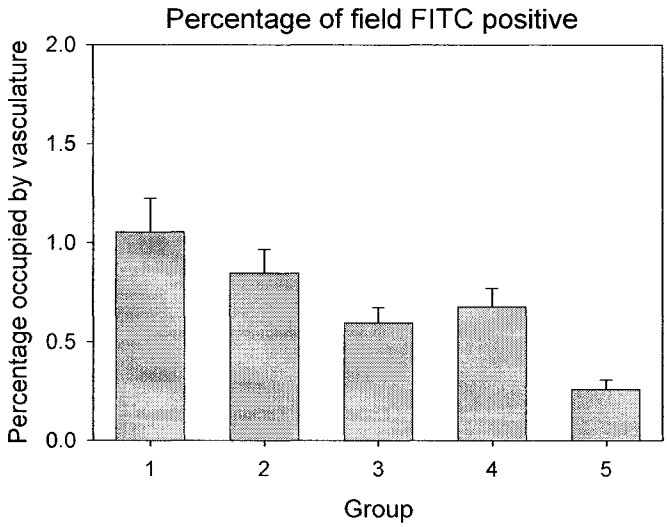

Figure 8b

Figure 8- AREA OCCUPIED BY FITC STAINING
The groups mentioned in the graphs are as follows- 1 – Normal saline injection, Control. Tumors collected at the same time as treatment group (five days post- HT); 2 – Ad LacZ + HT. 5 days post- HT; 3 – Ad *hsp* mIL-12, no HT. Same time as treatment group (5 days post- HT); 4 – Normal saline injection, HT only. 5 days post- HT; 5 – Ad *hsp* mIL-12+ HT. 5 days post- HT. Reduction in tumor vasculature was statistically significant ($p<0.05$) in Group 5 as compared to all other groups and for Group 3 when compared to Control group (Group 1).

Figure 8a. Expressed as pixels
Figure 8b. Same data expressed as a percentage of total area of the slide.

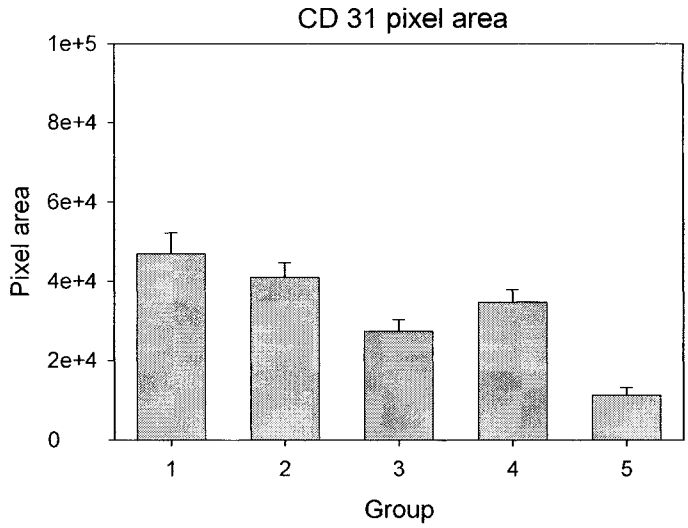

Figure 9a

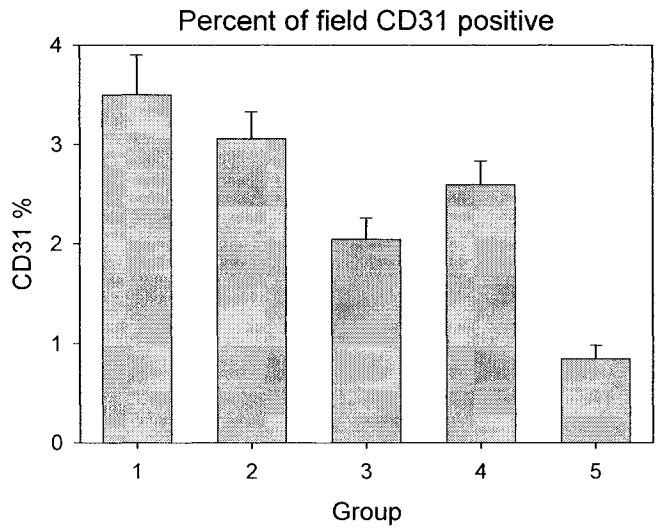

Figure 9b

Figure 9- AREA OCCUPIED BY CD31 STAINING
The groups mentioned in the graphs are as follows- 1 – Normal saline injection, Control. Tumors collected at the same time as treatment group (five days post- HT); 2 – Ad LacZ + HT. 5 days post- HT; 3 – Ad *hsp* mIL-12, no HT. Same time as treatment group (5 days post- HT); 4 – Normal saline injection, HT only. 5 days post- HT; 5 – Ad *hsp* mIL-12+ HT. 5 days post- HT. Reduction in tumor vasculature was statistically significant ($p<0.05$) in Group 5 as compared to all other groups and for Group 3 when compared to Control group (Group 1).
Figure 9a. Expressed as pixels
Figure 9b. Same data expressed as a percentage of total area of the slide.

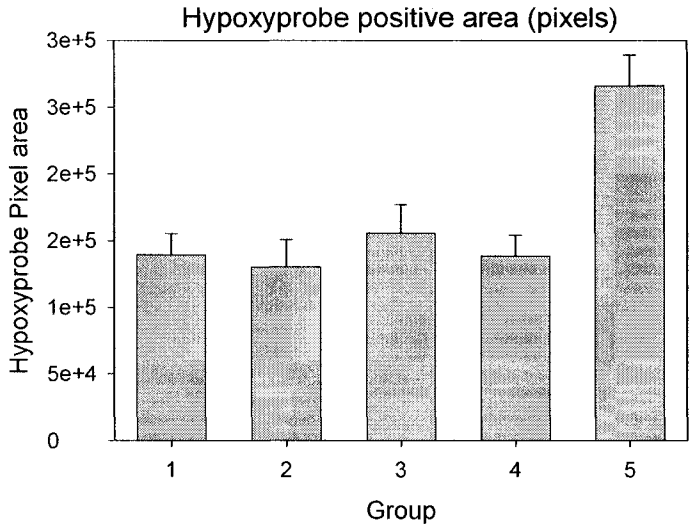

Figure 10a

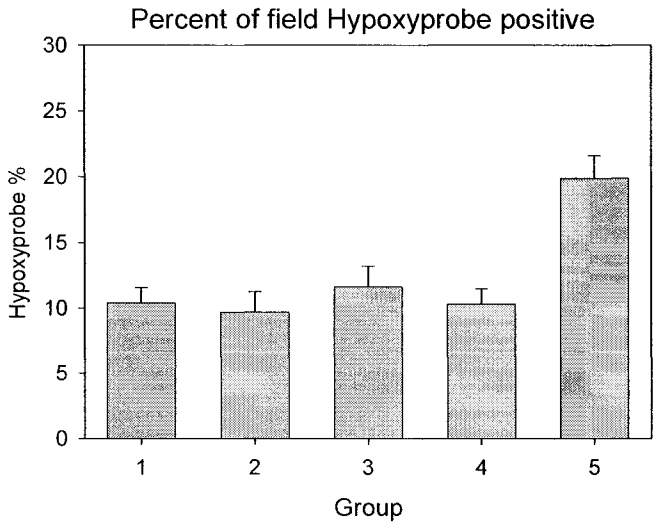

Figure 10b

Figure 10- AREA OCCUPIED BY HYPOXYPROBE STAINING
The groups mentioned in the graphs are as follows- 1 – Normal saline injection, Control. Tumors collected at the same time as treatment group (five days post- HT); 2 – Ad LacZ + HT. 5 days post- HT; 3 – Ad *hsp* mIL-12, no HT. Same time as treatment group (5 days post- HT); 4 – Normal saline injection, HT only. 5 days post- HT; 5 – Ad *hsp* mIL-12+ HT. 5 days post- HT. Increase in hypoxic fraction was statistically significant ($p<0.05$) in Group 5 as compared to all other groups.
Figure 10a. Expressed as pixels
Figure 10b. Same data expressed as a percentage of total area of the slide.

Cytokine staining- The pattern of interleukin-12 staining showed small patches distributed throughout the tumor section (Figure 11). A formal analysis of the area staining positive was not possible as the image analysis software could not differentiate between the colors on the slides. A rough estimate for the area staining positive for IL-12 was 5% to 10% for the tumors collected 24 hours post-HT and 10% to 20% for the tumors collected on the sixth day post- HT.

IP-10 staining (Figure 12) also showed a similar patchy distribution throughout the tumor section. However, it appeared to be more widely spread than IL-12.

Lung metastasis- Random sections of both lungs of 5 mice from the control group had a total of 9 metastases (Figure 13) while there were no lung metastases seen in the 5 mice from the Ad*hsp*fIL-12+HT group. Most lung metastases were just a few cells large. Only the two largest ones are shown in Figure 13.

Liver and spleen histology- Mice livers were examined for pathological changes reflective of IL-12 toxicity. There was no hepatic necrosis or any other pathology noted in livers from any of the groups.

The splenic histology in the IL-12 treated group revealed multiple coalescing large secondary follicles with large expanded germinal centers. These features were not present in the control group spleens (Figure 14).

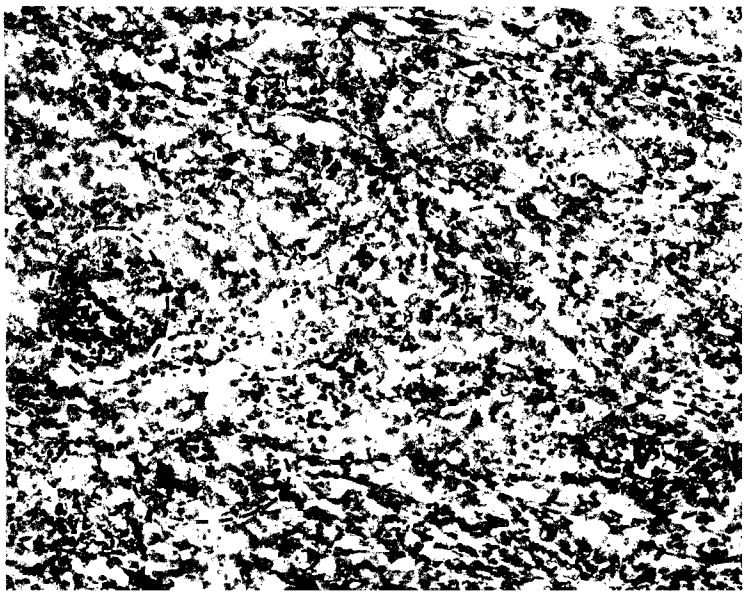

Figure 11a

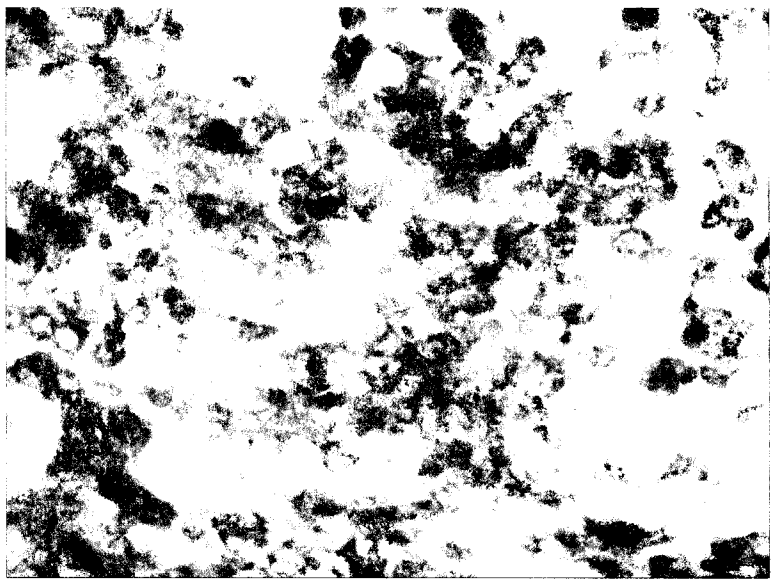

Figure 11b

Figure 11- INTERLEUKIN-12 STAINING
Figure 11a. The red circles outline so9me of the areas staining positive for IL-12 in a hematoxylin background. This image is from one of the tumors collected 6 days post HT. (100X)
Figure 11b. Another tumor section from same treatment group at 400X.

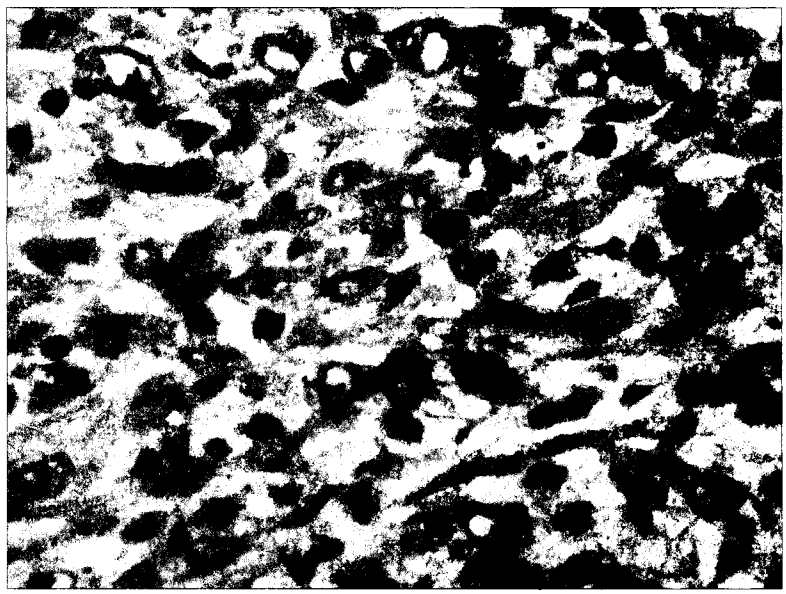

Figure 12a

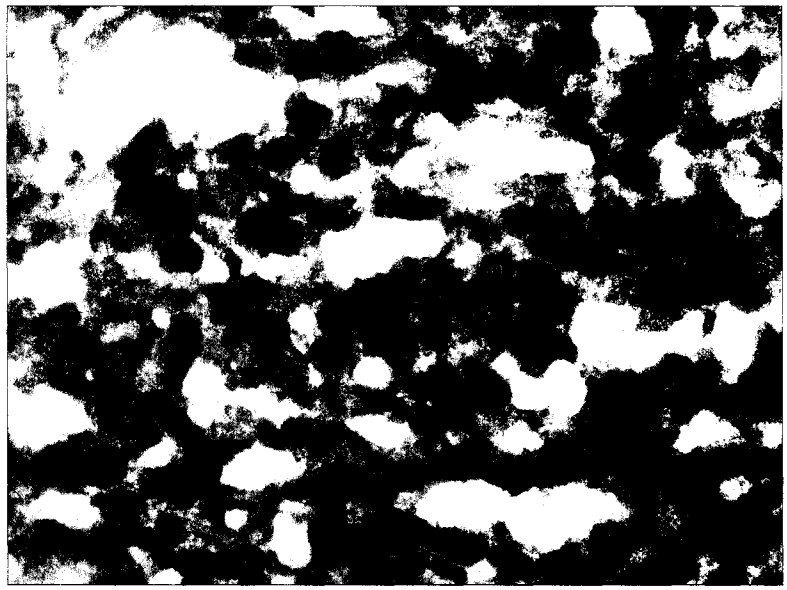

Figure 12b

Figure 12- IP-10 STAINING
Figure 12a- Tumor section from control group mouse stained for IP-10 (400X).
Figure 12b- Tumor section from IL-12 treated group collected on the 6th day post-HT stained for IP-10 (400X).

Tumor

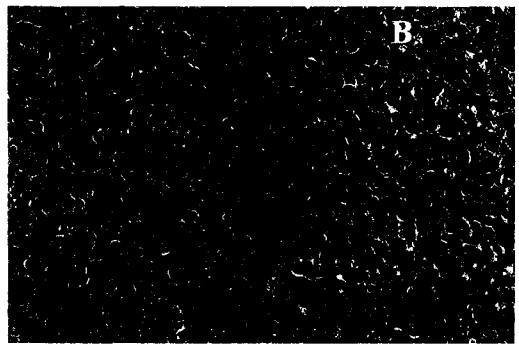

Lung Metastasis

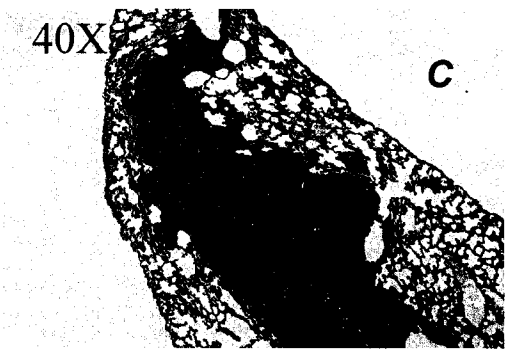

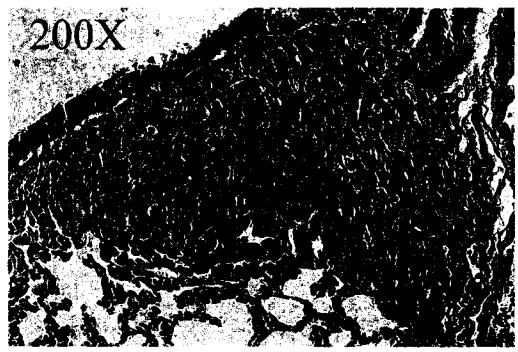

Figure 13- H&E IMAGES
Figure 13a. 100X image of 4T1 tumor
Figure 13b. 200X image of 4T1 tumor
Figure 13c. 40X image of 4T1 lung metastasis
Figure 13d. 200X image of 4T1 lung metastasis.

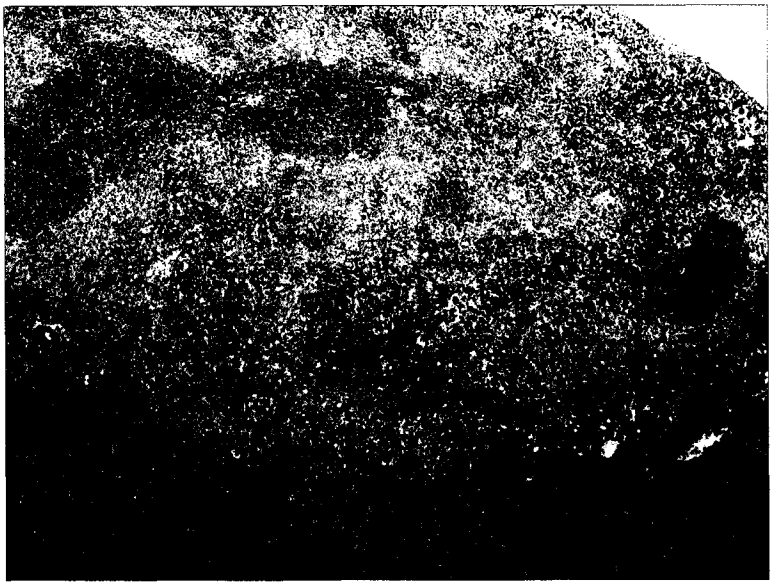

Figure 14a

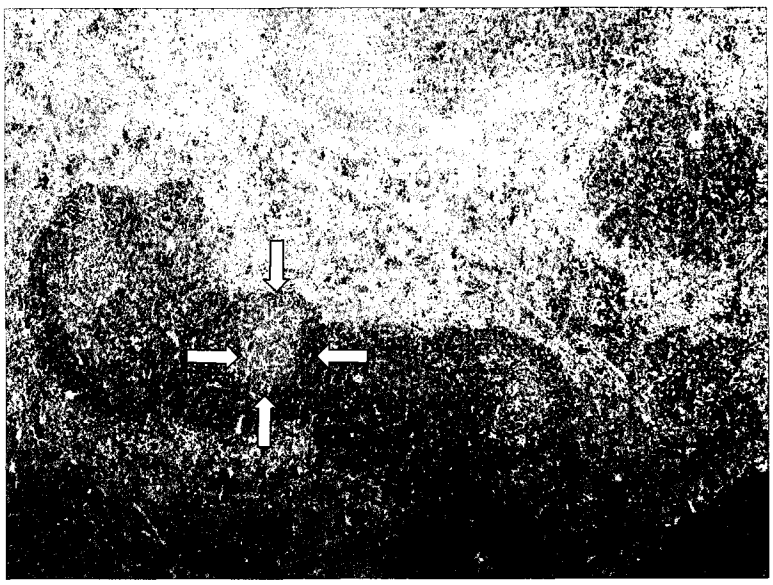

Figure 14b

Figure 14- SPLEEN HISTOLOGY

Figure 14a- Spleen from a control group mouse (40X).
Figure 14b- Spleen from a mouse euthanized on the 6th day post HT showing enlarged germinal centers (the yellow arrows outline one such germinal center). Many follicles appear to be coalescing together.

DISCUSSION

Interleukin-12 is a potent pro- inflammatory cytokine possessing anti- cancer properties[1]. Its anti- angiogenic properties are linked to its downstream proteins- interferon- γ and interferon- inducible protein 10 (IP-10)[12, 56]. Natural killer (NK) cells are also thought to be essential for IL-12 antiangiogenesis[9].We studied a hyperthermia- inducible gene construct to deliver interleukin-12 intratumorally. The murine IL-12 gene has been placed under control of inducible promoter *human heat shock promoter 70B* and replication-deficient adenovirus type 5 is employed as the vector for gene transfer to tumor cells. This construct has been designed to achieve a better spatial and temporal control over interleukin-12 expression. The aim is to have high tumor levels of the cytokines with limited systemic circulation to try and prevent generalized hematologic and hepatic toxicity. The gene- construct diluted in normal saline was injected into the tumor through a single injection site but multiple tracks were made to try and achieve a better physical distribution. Twenty- four hours were allowed for adenoviral infection of the tumor cells. This is the time required for maximum possible efficiency of infection[39, 57].

Hyperthermia (41°C for 60 minutes) was delivered to the tumor bearing leg using a water bath. This is a well- established technique described in various studies[38, 39, 58].

Real- time PCR was used to quantitatively study the mRNA expression of the genes of interest- IL-12, IFN-γ, IP-10, PAI-1 and VEGF. GAPDH was used as the housekeeping gene to serve as the loading control. The fold- increases in the mRNA levels in the treatment groups 2-5 were expressed normalized to the control group (group 1). Interleukin-12 induces production of IFN-γ from T-cells, NK cells, macrophages and

dendritic cells[59-61]. IFN-γ further leads to the secretion of IP-10 from endothelial cells, monocytes/ macrophages and other surrounding cells[9].

PAI-1 was found to be responsible for hyperthermia induced antiangiogenesis even at temperatures not directly cytotoxic to endothelial cells[41]. VEGF is a proangiogenic molecule[62].

Interleukin-12 mRNA levels have been reported to be maximally induced at 4 hours to 12 hours[63-65] after stimulation or induction. In our *in vitro* studies we had found the time point of maximal IL-12 mRNA levels to be 6 hours post- hyperthermia (Chapter 2). Hence this was one of the time points chosen in the Ad*hsp*fIL-12+HT group for tumor sample collection to measure cytokine levels. Based on our *in vitro* experiments and from data in literature[57, 58], the protein levels peak about 16-20 hours post induction, following the peak in the mRNA wave by a few hours. Based on that, the downstream cytokines of IL-12, IFN-γ and IP-10 would show their peak mRNA levels in the tumor sample collected 24 hours post- HT. That is what we found in our tumor tissue samples. The sixth day post- HT tumor sample had been collected mainly for IHC for antiangiogenesis studies. It was expected that the cytokine levels would reach close to baseline on the scale normalized to the control group. However, the IL-12 and IFN-γ mRNA levels were still about 1000-fold and 8-fold higher than baseline. The IP-10 mRNA levels had reached baseline though.

PAI-1 levels were maximally induced in the group receiving HT only (Group 4). Roca *et al*[41] studied the anti angiogenic properties of hyperthermia. They heated cultured human endothelial cells at 39°C, 41°C, 43°C and 45°C for 60 minutes and determined cell viability immediately and 16 hours after heating. cDNA expression array was used to

study the gene expression profile of endothelial cells after heat shock. One thousand one hundred and fifty human cancer related genes were evaluated. It was determined that hyperthermia activates a specific gene response involving the transcription of plasminogen activator inhibitor (PAI-1). This protein is a key regulator of the plasminogen activation pathway implicated in vascular thrombosis, metastasis diffusion, inflammation and angiogenesis. A dose- dependent inverse relationship between IFN-γ and PAI-1 has been reported[66] and our data also seems to support this finding.

An inverse relationship has also been found between IL-12 and VEGF[13, 14, 67]. Maximum IL-12 protein levels, which would be expected about 18-24 hours post-HT, coincide with the lowest VEGF mRNA levels in groups 5 a to c. Elevated levels of VEGF mRNA were seen in all the treatment groups. Any antiangiogenic measure such as hyperthermia[40] or interleukin-12 would possibly result in an increase in VEGF levels to attempt to counter the antiangiogenesis[68].

For tumor growth studies the 4T1 tumors growing in Balb/C mice were treated with HT alone or Ad*hsp*fIL-12+HT and compared with the control group. A statistically significant benefit was seen in the Ad*hsp*fIL-12+HT group. However, pairwise comparisons between controls and HT only and between HT only and Ad*hsp*fIL-12+HT did not show statistical significance. A similar study[39] using this construct in B16F10 melanoma cell line tumors had also shown a delayed tumor growth in the IL-12 treated group. The reduction in tumor vasculature in group 4, along with contribution from hyperthermia induced cytotoxicity, could be responsible for the delayed tumor growth. *In vitro* studies done on 4T1 cells did not show evidence of appreciable reduction in percentage of viable cells using the trypan blue dye exclusion test when heated at 39^0C to

42^0C. Only when heated at 43^0C the cell viability was reduced to approximately 75% (data not shown).

For studying patent functional vasculature FITC- conjugated *Lycopersicon esculentum* (Tomato plant) lectin was injected 3 minutes prior to euthanasia. Lectins are rapidly distributed through all vessels within a circulation period of about 60 seconds in mice[46]. They bind to the glycoproteins expressed on the endothelial cells[69]. CD31 staining, routinely used to study angiogenesis and antiangiogenesis in tissue sections, overestimates vascularity of a tumor[70-73] as it stains endothelial cells in the tumor sections even in the absence of functional vasculature. In our study, the area of the tumor section occupied by functional vasculature (~1%) was one- third of the area staining positive for CD31 antigen (~3%). CD31 positive area in the tumor have been reported as approximately 3.5% for A431 human squamous cell carcinomas and B16F10 melanomas[74] to approximately 6.5% to 7% for neuroblastomas[75] and LLC tumors[74].

The percentage vascularity of the treated group was 24% and 25% of the control group by CD31 and FITC studies respectively. These values are close to those reported in literature for IL-12 induced anti- angiogenesis in Balb/C and C57CL/6 mice using Matrigel assay[9] and in Balb/C mice in a breast carcinoma model[14]. A significant reduction in vascularity was also noted in Group 3 where the construct had been injected but hyperthermia had not been delivered. Approximately a 500- fold increase in IL-12 mRNA levels and a 20- fold and 16- fold increase in IFN-γ and IP-10 levels respectively were also seen. This suggested that some factor, other than HT, was leading to *hsp* induction in the tumor microenvironment. We have explored this phenomenon in our *in vitro* studies (Chapter 3).

Various methods to measure tumor hypoxia have been described in literature and the percentage of hypoxic cells have been found to range from 0% to 50% with most tumors having hypoxic areas between 10%-15%[76]. The level of hypoxia in 4T1 tumors, using Hypoxyprobe-1, was found to be 16± 7%[77]. In our tumor sections, using the same compound, the tumor hypoxic area was 9.7±7.6% to 11.6±7.3% for groups 1 to 4. However, in treatment group 5 (Ad*hsp*fIL-12+HT) the area had increased to 19.8±7.5%. This difference was statistically significant and reflective of the reduction in tumor vascularity.

Adenoviruses are efficient vectors for use in gene therapy protocols. *In vitro* they have been found to have high percentage infection of cells exposed[78, 79]. We found infection efficiencies of 90%-95% in our *in vitro* experiments (Chapter 2) using a GFP expressing adenoviral vector. However, the *in vivo* efficiencies are much lower. In malignant glioma cells Puumalainen *et al*[80] reported adenoviral infection as low as <0.01% to 11%. Adenoviral infections are highly dependent on the coxsackievirus and adenovirus receptor (CAR) status[81, 82]. Gu *et al*[83] found variations in CAR status among human musculoendothelial tumors. They found that CAR mRNA was expressed at highest levels in osteosarcoma, Ewing's sarcoma, neurofibroma, and schwannoma; at intermediate levels in exostosis, giant cell tumor, liposarcoma, synovial sarcoma, malignant peripheral nerve sheath tumor, and hemangioma; and at low levels in alveolar soft part sarcoma and desmoid. In our study also, immunohistochemical staining for IL-12 showed very sparse and patchy distribution suggestive of very low transfection efficiency *in vivo*. The distribution was more widespread on the sixth day post- HT as compared to 24 hours post-HT. Still, only about 10-15% of the cells seemed to be producing IL-12. IP-10, the

downstream cytokine, showed a comparatively larger distribution in the tumor sections. This could be because of the paracrine effects of IL-12 and IFN-γ.

It was surprising to find IL-12 protein in the tumors present and better distributed on the sixth day post- induction. The plasma half- life of IL-12 has been reported to be about 10 hours[84]. This is much longer than the half- lives of other cytokines that generally have $t_{1/2}$ of less than 30 minutes. Its persistence in the tumor for up to and possibly beyond six days may be due to (1) a reduced rate of clearance from the tumor, resulting in a longer effective half- life (2) setting up of a positive feedback loop for cytokine production.

The anti- metastatic properties of interleukin-12 have been extensively studied in literature[1] and are attributed to generalized immunostimulation and anti-angiogenic properties of IL-12[2, 9]. Rakhmilevich *et al*[85] delivered IL-12 using a gene-gun mediated approach and found a significant reduction in the number of lung metastases from 4T1 tumors with an increase in the survival time of the mice. In our treated group no metastases were detected in the lungs of the 5 mice examined as compared to a total of 9 individual metastases in 5 control mice. The number of metastases is much lower than those reported in other studies[86, 87] where a total of 30-40 individual metastases were counted 3-4 weeks after 4T1 cell line inoculation in the control group. In this study only one random H&E section of both lungs from each mouse was examined for metastases approximately 3 weeks post- inoculation and thus the number of metastases in both groups (control and treated) would be low.

Administration of recombinant IL-12 causes liver toxicity in the form of hepatic necrosis[88] or steatosis[89]. No liver pathology was noted using the localized method of delivery in this study. The spleens from the IL-12 treated group showed evidence for

generalized immunostimulation in the form of coalescing follicles with enlarged germinal centers. This feature was not observed in the spleens of the control mice.

In conclusion, using the Ad*hsp*mIL-12 construct we were able to deliver IL-12 intratumorally and demonstrate its potent anti- angiogenic effects and delayed tumor growth with limited systemic toxicity.

REFERENCES

1. Colombo MP, Trinchieri G. Interleukin-12 in anti-tumor immunity and immunotherapy. *Cytokine Growth Factor Rev* 2002;13:155-168.

2. Voest EE, Kenyon BM, O'Reilly MS, *et al.* Inhibition of angiogenesis in vivo by interleukin 12. *J Natl Cancer Inst* 1995;87:581-586.

3. Rutenfranz I, Kirchner H. Pharmacokinetics of recombinant murine interferon-gamma in mice. *J Interferon Res* 1988;8:573-580.

4. Brunda MJ, Sulich V, Bellantoni D. The anti-tumor effect of recombinant interferon alpha or gamma is influenced by tumor location. *Int J Cancer* 1987;40:807-810.

5. Luster AD, Unkeless JC, Ravetch JV. Gamma-interferon transcriptionally regulates an early-response gene containing homology to platelet proteins. *Nature* 1985;315:672-676.

6. Angiolillo AL, Sgadari C, Taub DD, *et al.* Human interferon-inducible protein 10 is a potent inhibitor of angiogenesis in vivo. *J Exp Med* 1995;182:155-162.

7. Sgadari C, Angiolillo AL, Tosato G. Inhibition of angiogenesis by interleukin-12 is mediated by the interferon-inducible protein 10. *Blood* 1996;87:3877-3882.

8. Tannenbaum CS, Tubbs R, Armstrong D, *et al.* The CXC chemokines IP-10 and Mig are necessary for IL-12-mediated regression of the mouse RENCA tumor. *J Immunol* 1998;161:927-932.

9. Yao L, Sgadari C, Furuke K, *et al.* Contribution of natural killer cells to inhibition of angiogenesis by interleukin-12. *Blood* 1999;93:1612-1621.

10. Gerber SA, Moran JP, Frelinger JG, *et al.* Mechanism of IL-12 mediated alterations in tumour blood vessel morphology: analysis using whole-tissue mounts. *Br J Cancer* 2003;88:1453-1461.

11. Moran JP, Gerber SA, Martin CA, *et al.* Transfection of the genes for interleukin-12 into the K1735 melanoma and the EMT6 mammary sarcoma murine cell lines reveals distinct mechanisms of antitumor activity. *Int J Cancer* 2003;106:690-698.

12. Cavallo F, Di Carlo E, Butera M, *et al.* Immune events associated with the cure of established tumors and spontaneous metastases by local and systemic interleukin 12. *Cancer Res* 1999;59:414-421.

13. Nakayama Y, Sako T, Shibao K, *et al.* Relationship between plasma levels of vascular endothelial growth factor and serum levels of interleukin-12 in patients with colorectal cancer. *Anticancer Res* 2000;20:4097-4102.

14. Dias S, Boyd R, Balkwill F. IL-12 regulates VEGF and MMPs in a murine breast cancer model. *Int J Cancer* 1998;78:361-365.

15. Nastala CL, Edington HD, McKinney TG, *et al.* Recombinant IL-12 administration induces tumor regression in association with IFN-gamma production. *J Immunol* 1994;153:1697-1706.

16. Rakhmilevich AL, Turner J, Ford MJ, *et al.* Gene gun-mediated skin transfection with interleukin 12 gene results in regression of established primary and metastatic murine tumors. *Proc Natl Acad Sci U S A* 1996;93:6291-6296.

17. Watanabe M, Fenton RG, Wigginton JM, *et al.* Intradermal delivery of IL-12 naked DNA induces systemic NK cell activation and Th1 response in vivo that is independent of endogenous IL-12 production. *J Immunol* 1999;163:1943-1950.

18. Tahara H, Zitvogel L, Storkus WJ, *et al.* Murine models of cancer cytokine gene therapy using interleukin-12. *Ann N Y Acad Sci* 1996;795:275-283.

19. Golab J, Zagozdzon R. Antitumor effects of interleukin-12 in pre-clinical and early clinical studies (Review). *Int J Mol Med* 1999;3:537-544.

20. Rook AH, Wood GS, Yoo EK, *et al.* Interleukin-12 therapy of cutaneous T-cell lymphoma induces lesion regression and cytotoxic T-cell responses. *Blood* 1999;94:902-908.

21. Car BD, Eng VM, Lipman JM, *et al.* The toxicology of interleukin-12: a review. *Toxicol Pathol* 1999;27:58-63.

22. Atkins MB, Robertson MJ, Gordon M, *et al.* Phase I evaluation of intravenous recombinant human interleukin 12 in patients with advanced malignancies. *Clin Cancer Res* 1997;3:409-417.

23. Halin C, Rondini S, Nilsson F, *et al.* Enhancement of the antitumor activity of interleukin-12 by targeted delivery to neovasculature. *Nat Biotechnol* 2002;20:264-269.

24. Koblish HK, Hunter CA, Wysocka M, *et al.* Immune suppression by recombinant interleukin (rIL)-12 involves interferon gamma induction of nitric oxide synthase 2 (iNOS) activity: inhibitors of NO generation reveal the extent of rIL-12 vaccine adjuvant effect. *J Exp Med* 1998;188:1603-1610.

25. Kurzawa H, Wysocka M, Aruga E, *et al.* Recombinant interleukin 12 enhances cellular immune responses to vaccination only after a period of suppression. *Cancer Res* 1998;58:491-499.

26. Saffran DC, Horton HM, Yankauckas MA, *et al.* Immunotherapy of established tumors in mice by intratumoral injection of interleukin-2 plasmid DNA: induction of CD8+ T-cell immunity. *Cancer Gene Ther* 1998;5:321-330.

27. Colombo MP, Vagliani M, Spreafico F, *et al.* Amount of interleukin 12 available at the tumor site is critical for tumor regression. *Cancer Res* 1996;56:2531-2534.

28. Rakhmilevich AL, Timmins JG, Janssen K, *et al.* Gene gun-mediated IL-12 gene therapy induces antitumor effects in the absence of toxicity: a direct comparison with systemic IL-12 protein therapy. *J Immunother* 1999;22:135-144.

29. Shi F, Rakhmilevich AL, Heise CP, *et al.* Intratumoral injection of interleukin-12 plasmid DNA, either naked or in complex with cationic lipid, results in similar tumor regression in a murine model. *Mol Cancer Ther* 2002;1:949-957.

30. Puisieux I, Odin L, Poujol D, *et al.* Canarypox virus-mediated interleukin 12 gene transfer into murine mammary adenocarcinoma induces tumor suppression and long-term antitumoral immunity. *Hum Gene Ther* 1998;9:2481-2492.

31. Seetharam S, Staba MJ, Schumm LP, *et al.* Enhanced eradication of local and distant tumors by genetically produced interleukin-12 and radiation. *Int J Oncol* 1999;15:769-773.

32. Putzer BM, Hitt M, Muller WJ, *et al.* Interleukin 12 and B7-1 costimulatory molecule expressed by an adenovirus vector act synergistically to facilitate tumor regression. *Proc Natl Acad Sci U S A* 1997;94:10889-10894.

33. Lohr F, Huang Q, Hu K, *et al.* Systemic vector leakage and transgene expression by intratumorally injected recombinant adenovirus vectors. *Clin Cancer Res* 2001;7:3625-3628.

34. Bramson JL, Hitt M, Gauldie J, *et al.* Pre-existing immunity to adenovirus does not prevent tumor regression following intratumoral administration of a vector expressing IL-12 but inhibits virus dissemination. *Gene Ther* 1997;4:1069-1076.

35. Zhang R, Straus FH, DeGroot LJ. Effective genetic therapy of established medullary thyroid carcinomas with murine interleukin-2: dissemination and cytotoxicity studies in a rat tumor model. *Endocrinology* 1999;140:2152-2158.

36. Nasu Y, Bangma CH, Hull GW, *et al.* Adenovirus-mediated interleukin-12 gene therapy for prostate cancer: suppression of orthotopic tumor growth and pre-established lung metastases in an orthotopic model. *Gene Ther* 1999;6:338-349.

37. Emtage PC, Wan Y, Hitt M, *et al.* Adenoviral vectors expressing lymphotactin and interleukin 2 or lymphotactin and interleukin 12 synergize to facilitate tumor regression in murine breast cancer models. *Hum Gene Ther* 1999;10:697-709.

38. Lohr F, Hu K, Huang Q, *et al.* Enhancement of radiotherapy by hyperthermia-regulated gene therapy. *Int J Radiat Oncol Biol Phys* 2000;48:1513-1518.

39. Huang Q, Hu JK, Lohr F, *et al.* Heat-induced gene expression as a novel targeted cancer gene therapy strategy. *Cancer Res* 2000;60:3435-3439.

40. Kanamori S, Nishimura Y, Okuno Y, *et al.* Induction of vascular endothelial growth factor (VEGF) by hyperthermia and/or an angiogenesis inhibitor. *Int J Hyperthermia* 1999;15:267-278.

41. Roca C, Primo L, Valdembri D, *et al.* Hyperthermia inhibits angiogenesis by a plasminogen activator inhibitor 1-dependent mechanism. *Cancer Res* 2003;63:1500-1507.

42. Fajardo LF, Prionas SD, Kowalski J, *et al.* Hyperthermia inhibits angiogenesis. *Radiat Res* 1988;114:297-306.

43. Lee JC, Kim DC, Gee MS, *et al.* Interleukin-12 inhibits angiogenesis and growth of transplanted but not in situ mouse mammary tumor virus-induced mammary carcinomas. *Cancer Res* 2002;62:747-755.

44. Miller FR, Miller BE, Heppner GH. Characterization of metastatic heterogeneity among subpopulations of a single mouse mammary tumor: heterogeneity in phenotypic stability. *Invasion Metastasis* 1983;3:22-31.

45. Aslakson CJ, Miller FR. Selective events in the metastatic process defined by analysis of the sequential dissemination of subpopulations of a mouse mammary tumor. *Cancer Res* 1992;52:1399-1405.

46. Debbage PL, Griebel J, Ried M, *et al.* Lectin intravital perfusion studies in tumor-bearing mice: micrometer-resolution, wide-area mapping of microvascular labeling, distinguishing efficiently and inefficiently perfused microregions in the tumor. *J Histochem Cytochem* 1998;46:627-639.

47. Bergers G, Song S, Meyer-Morse N, *et al.* Benefits of targeting both pericytes and endothelial cells in the tumor vasculature with kinase inhibitors. *J Clin Invest* 2003;111:1287-1295.

48. He TC, Zhou S, da Costa LT, *et al.* A simplified system for generating recombinant adenoviruses. *Proc Natl Acad Sci U S A* 1998;95:2509-2514.

49. Graham FL, Smiley J, Russell WC, *et al.* Characteristics of a human cell line transformed by DNA from human adenovirus type 5. *J Gen Virol* 1977;36:59-74.

50. Overbergh L, Valckx D, Waer M, *et al.* Quantification of murine cytokine mRNAs using real time quantitative reverse transcriptase PCR. *Cytokine* 1999;11:305-312.

51. Overbergh L, Giulietti A, Valckx D, *et al.* The use of real-time reverse transcriptase PCR for the quantification of cytokine gene expression. *J Biomol Tech* 2003;14:33-43.

52. Huang MC, Lee HY, Yeh CC, *et al.* Induction of protein growth factor systems in the ovaries of transgenic mice overexpressing human type 2 lysophosphatidic acid G protein-coupled receptor (LPA2). *Oncogene* 2004;23:122-129.

53. Gerber HP, Kowalski J, Sherman D, *et al.* Complete inhibition of rhabdomyosarcoma xenograft growth and neovascularization requires blockade of both tumor and host vascular endothelial growth factor. *Cancer Res* 2000;60:6253-6258.

54. Livak KJ, Schmittgen TD. Analysis of relative gene expression data using real-time quantitative PCR and the 2(-Delta Delta C(T)) Method. *Methods* 2001;25:402-408.

55. Pfaffl MW. A new mathematical model for relative quantification in real-time RT-PCR. *Nucleic Acids Res* 2001;29:e45.

56. Masiero L, Figg WD, Kohn EC. New anti-angiogenesis agents: review of the clinical experience with carboxyamido-triazole (CAI), thalidomide, TNP-470 and interleukin-12. *Angiogenesis* 1997;1:23-35.

57. Borrelli MJ, Schoenherr DM, Wong A, *et al.* Heat-activated transgene expression from adenovirus vectors infected into human prostate cancer cells. *Cancer Res* 2001;61:1113-1121.

58. Li GC, He F, Shao X, *et al.* Adenovirus-mediated heat-activated antisense Ku70 expression radiosensitizes tumor cells in vitro and in vivo. *Cancer Res* 2003;63:3268-3274.

59. Chan SH, Perussia B, Gupta JW, *et al.* Induction of interferon gamma production by natural killer cell stimulatory factor: characterization of the responder cells and synergy with other inducers. *J Exp Med* 1991;173:869-879.

60. Gately MK, Warrier RR, Honasoge S, *et al.* Administration of recombinant IL-12 to normal mice enhances cytolytic lymphocyte activity and induces production of IFN-gamma in vivo. *Int Immunol* 1994;6:157-167.

61. Frucht DM, Fukao T, Bogdan C, *et al.* IFN-gamma production by antigen-presenting cells: mechanisms emerge. *Trends Immunol* 2001;22:556-560.

62. Cross MJ, Claesson-Welsh L. FGF and VEGF function in angiogenesis: signalling pathways, biological responses and therapeutic inhibition. *Trends Pharmacol Sci* 2001;22:201-207.

63. Taoufik Y, Lantz O, Wallon C, *et al.* Human immunodeficiency virus gp120 inhibits interleukin-12 secretion by human monocytes: an indirect interleukin-10-mediated effect. *Blood* 1997;89:2842-2848.

64. Matsumoto H, Suzuki K, Tsuyuguchi K, *et al.* Interleukin-12 gene expression in human monocyte-derived macrophages stimulated with Mycobacterium bovis BCG: cytokine regulation and effect of NK cells. *Infect Immun* 1997;65:4405-4410.

65. Wittmann M, Larsson VA, Schmidt P, *et al.* Suppression of interleukin-12 production by human monocytes after preincubation with lipopolysaccharide. *Blood* 1999;94:1717-1726.

66. Gallicchio M, Hufnagl P, Wojta J, *et al.* IFN-gamma inhibits thrombin- and endotoxin-induced plasminogen activator inhibitor type 1 in human endothelial cells. *J Immunol* 1996;157:2610-2617.

67. Duda DG, Sunamura M, Lozonschi L, *et al.* Direct in vitro evidence and in vivo analysis of the antiangiogenesis effects of interleukin 12. *Cancer Res* 2000;60:1111-1116.

68. Bhujwalla ZM, Artemov D, Natarajan K, *et al.* Reduction of vascular and permeable regions in solid tumors detected by macromolecular contrast magnetic resonance imaging after treatment with antiangiogenic agent TNP-470. *Clin Cancer Res* 2003;9:355-362.

69. Roth J, Binder M, Gerhard UJ. Conjugation of lectins with fluorochromes: an approach to histochemical double labeling of carbohydrate components. *Histochemistry* 1978;56:265-273.

70. Huang J, Frischer JS, Serur A, *et al.* Regression of established tumors and metastases by potent vascular endothelial growth factor blockade. *Proc Natl Acad Sci U S A* 2003;100:7785-7790.

71. Hashizume H, Baluk P, Morikawa S, *et al.* Openings between defective endothelial cells explain tumor vessel leakiness. *Am J Pathol* 2000;156:1363-1380.

72. Gee MS, Procopio WN, Makonnen S, *et al.* Tumor vessel development and maturation impose limits on the effectiveness of anti-vascular therapy. *Am J Pathol* 2003;162:183-193.

73. McDonald DM, Choyke PL. Imaging of angiogenesis: from microscope to clinic. *Nat Med* 2003;9:713-725.

74. Streit M, Stephen AE, Hawighorst T, *et al.* Systemic inhibition of tumor growth and angiogenesis by thrombospondin-2 using cell-based antiangiogenic gene therapy. *Cancer Res* 2002;62:2004-2012.

75. Chantrain CF, DeClerck YA, Groshen S, *et al.* Computerized quantification of tissue vascularization using high-resolution slide scanning of whole tumor sections. *J Histochem Cytochem* 2003;51:151-158.

76. Hall EJ. Radiobiology for the radiologist. 5th ed. Philadelphia: Lippincott Williams & Wilkins; 2000.

77. Samoszuk M, Corwin MA. Mast cell inhibitor cromolyn increases blood clotting and hypoxia in murine breast cancer. *Int J Cancer* 2003;107:159-163.

78. Meeker TC, Lay LT, Wroblewski JM, *et al.* Adenoviral vectors efficiently target cell lines derived from selected lymphocytic malignancies, including anaplastic large cell lymphoma and Hodgkin's disease. *Clin Cancer Res* 1997;3:357-364.

79. Communal C, Huq F, Lebeche D, *et al.* Decreased efficiency of adenovirus-mediated gene transfer in aging cardiomyocytes. *Circulation* 2003;107:1170-1175.

80. Puumalainen AM, Vapalahti M, Agrawal RS, *et al.* Beta-galactosidase gene transfer to human malignant glioma in vivo using replication-deficient retroviruses and adenoviruses. *Hum Gene Ther* 1998;9:1769-1774.

81. Li D, Duan L, Freimuth P, *et al.* Variability of adenovirus receptor density influences gene transfer efficiency and therapeutic response in head and neck cancer. *Clin Cancer Res* 1999;5:4175-4181.

82. Douglas JT, Kim M, Sumerel LA, *et al.* Efficient oncolysis by a replicating adenovirus (ad) in vivo is critically dependent on tumor expression of primary ad receptors. *Cancer Res* 2001;61:813-817.

83. Gu W, Ogose A, Kawashima H, *et al.* High-level expression of the coxsackievirus and adenovirus receptor messenger RNA in osteosarcoma, Ewing's sarcoma, and benign neurogenic tumors among musculoskeletal tumors. *Clin Cancer Res* 2004;10:3831-3838.

84. Lauw FN, Dekkers PE, te Velde AA, *et al.* Interleukin-12 induces sustained activation of multiple host inflammatory mediator systems in chimpanzees. *J Infect Dis* 1999;179:646-652.

85. Rakhmilevich AL, Janssen K, Hao Z, *et al.* Interleukin-12 gene therapy of a weakly immunogenic mouse mammary carcinoma results in reduction of spontaneous lung metastases via a T-cell-independent mechanism. *Cancer Gene Ther* 2000;7:826-838.

86. Hiraga T, Williams PJ, Ueda A, *et al.* Zoledronic Acid Inhibits Visceral Metastases in the 4T1/luc Mouse Breast Cancer Model. *Clin Cancer Res* 2004;10:4559-4567.

87. Demaria S, Kawashima N, Yang AM, *et al.* Immune-Mediated Inhibition of Metastases after Treatment with Local Radiation and CTLA-4 Blockade in a Mouse Model of Breast Cancer. *Clin Cancer Res* 2005;11:728-734.

88. Dickerson EB, Akhtar N, Steinberg H, *et al.* Enhancement of the antiangiogenic activity of interleukin-12 by peptide targeted delivery of the cytokine to alphavbeta3 integrin. *Mol Cancer Res* 2004;2:663-673.

89. Kaneda M, Kashiwamura S, Ueda H, *et al.* Inflammatory liver steatosis caused by IL-12 and IL-18. *J Interferon Cytokine Res* 2003;23:155-162.

APPENDIX

A. CELL CULTURE MEDIA

For Crandall Feline Kidney Cells

DMEM stock→ DMEM Powder (Mediatech Cat # 50-003) 13.48g/ L + Sodium bicarbonate ($NaHCO_3$) 3.70 g/L

To make 100 mls

89 ml of DMEM stock

10 ml of fetal bovine serum

1 ml of Penicillin- Streptomycin

For Feline peripheral blood mononuclear cells (PBMCs)

RPMI 1640 stock→ RPMI 1640 Powder (Mediatech Cat # 50-020) 10.40 g/L + Sodium bicarbonate ($NaHCO_3$) 2.00 g/L

To make 100 mls

78.5 ml of RPMI 1640 stock

20 ml of fetal bovine serum

1 ml of Penicillin- Streptomycin

2.5 ml 2 Mercaptoethanol (Sigma, Cat. No. M-3148) (made up as 2.5 ml RPMI + 1.7µl 2ME)

For 4T1 cells

Modified RPMI 1640 medium (ATCC Cat # 30-2001)

To make 100 mls

90 ml of modified RPMI 1640

10 ml of fetal bovine serum

B. RNA EXTRACTION WITH TRIZOL REAGENT

Homogenization

1. Tissue samples- homogenize tissues in 1 ml of TRIzol reagent per 50-100 mg of tissue using a tissue homogenizer. First add about 200-300 µl of TRIzol and crush and homogenize tissue, then add remainder TRIzol or else it will spill out of the 1.5 ml tube.
2. Cells grown in monolayer- lyse cells directly in a culture dish by adding 1 ml TRIzol to a 35mm diameter dish and passing the lysate several times through the pipette. The amount of TRIzol reagent added is based on the area of the culture plate/ dish (1ml/ 10 cm^2) and not on the number of cells present. An insufficient amount of TRIzol reagent may result in contamination of the isolated RNA with DNA.

At this point the lysate can be frozen at –70°C for up to 1 month before use.

RNA Extraction

All equipment and reagents must be RNase free from this point on.

Phase separation- incubate homogenized samples for 5 minutes at 15-30°C to allow complete dissociation of the nucleoprotein complexes.

Add 200µl of Chloroform per mL of TRIzol and cap tubes (use 1.5 mL centrifuge tubes, tubes must be RNase free).

Shake tubes vigorously by hand for 15 seconds and incubate them at 15-30°C for 2-3 minutes.

Centrifuge the samples at no more than 12,000g for 15 minutes (11,500 rpm in the Beckman Coulter Microfuge® 18 Centrifuge) at 4°C.

The sample mixture separates into a lower red phenol- chloroform phase, an interphase and an upper aqueous phase (this phase should be about 60% of the original TRIzol volume, usually about 560 µl can be drawn- off).

RNA precipitation- Transfer the aqueous phase to a new 1.5mL RNase free tube.

Precipitate the RNA from the aqueous phase by mixing with isopropyl alcohol. Use 500µl isopropyl alcohol per mL of TRIzol used initially.

Incubate samples at 15-30°C for 10 minutes and centrifuge at no more than 12,000g (11,500 rpm in the Beckman Coulter Microfuge® 18 Centrifuge) for 10 minutes at 4°C.

The RNA precipitate forms a gel- like pellet at the side/ bottom of the tube.

Hint- In the centrifuge keep the hinged part of the tube to the outside for all samples. This makes it easier to locate the small amount of RNA isolated, which sometimes is not even visible.

RNA wash- Remove the supernatant.

Wash the RNA pellet with 75 % ethanol, adding at least 1mL of ethanol per mL of TRIzol used initially.

Mix the sample by vortexing (the samples can be stored at $-70^{\circ}C$ at this point for up to a year).

To sue immediately, centrifuge at 7500g (9500 rpm in the Beckman Coulter Microfuge® 18 Centrifuge) for 5 minutes at $4^{\circ}C$.

Redissolving the RNA- Dry the pellet by removing the supernatant and inverting the tube, leaving it for approximately 20 minutes (do not let pellet dry completely as it will decrease in solubility).

Dissolve RNA in 20 µl of RNase free water.

Incubate at $55^{\circ}C$ for 10 minutes.

Check optical density. Add about 5 µl of dissolved RNA in water and make sure $A_{260/280}$ >1.7.

DNase step- Add 1µl of DNase to each 20 µl of sample of dissolved RNA.

Incubate 20 minutes at $37^{\circ}C$.

Inactivate by heating for 5 minutes at $95^{\circ}C$.

Cool immediately on ice.

C. cDNA synthesis

Reagent	Concentration	Amount needed per reaction
First strand buffer	5X	4 μl
dNTP	10mM	1 μl
DTT	0.1M	1 μl
RNase out	40 U/ μl	0.25 μl
SuperScript II	200 U/ μl	0.25 μl
Random Hexamers	300 ng/ μl	2 μl
Water (RNase free)		1.5 μl

(Random hexamers: Stock solution is 3 μg/ μl, working solution is 300 ng/ μl, i.e. 1:10 dilution)

1. At all times, keep RNA, RT Mastermix and enzymes on ice.
2. Setup a 42^0C water bath and a 95^0C heat block.
3. Determine the number of reactions. 10 μl of RNA solution per reaction so one tube allows 2 reactions. Add 1-2 reactions to total to allow for pipetting errors.
4. Multiply number of reactions to amount needed for each reagent. Add each amount calculated to a single tube to create a single mastermix. (Keep on ice)
5. Spin down the mixture.

6. Prepare and label screw top (Fisher) tubes for each reaction. Distribute 10 µl of Mastermix to each tube and then distribute 10 µl of the RNA to each tube as well. (Keep on ice).
7. After finishing, incubate reaction at 42^0C for 50 minutes in the water bath.
8. After incubation, add 30 µl of pure water to each sample. Vortex and spin down.
9. Inactivate by placing in 95^0C heat block for 5 minutes. Retrieve some ice during this time.
10. After the 5 minutes, place immediately on ice. Store cDNA at –20°C.

D. RECONSTITUTION OF PRIMERS AND PROBE

1. Forward and reverse primers and primer with 5' FAM – 3' TAMRA are obtained from MWG Biotech in desiccated form.
2. Dissolve in 1X TE. Volume of 1X TE is ten times the amount of primer or probe as expressed in nmols. For example- if the MWG Biotech Oligo synthesis report says the amount is 47 nmol, dissolve in 470 µl of 1X TE.
3. This gives a concentration of 100 µM of both primers and probe.
4. Aliquot into 50 µl volumes and freeze at -20^0C.

For Primers: Dilute the 100 µM 1:5 to make a 20 µM concentration.

Add 200 µl of RNase free water to the 50 µl aliquot of both forward and reverse primers.

For Probe: Dilute the 100 µM 1:10 to make a 10 µM concentration.

Add 450 µl of RNase free water to the 50 µl aliquot of probe.

Each reaction uses 0.5 µl of forward and reverse primers and 0.2 µl of probe.

So, to make primers and probe mixture ready for use-

Forward primer- 250 µl

Reverse primer- 250 µl

Probe- 100 µl

TOTAL- 600 µl

For real time PCR, each 25 μl reaction is composed of the following-

Universal Mix- 12.5 μl

Primers + probe mix- 1.2 μl

H_2O- 6.3 μl

cDNA- 5 μl

E. CATALOG NUMBERS

Product	Company	Catalog no.
TRIzol reagent	Invitrogen	15596-018
TaqMan Universal PCR Master Mix	Applied Biosystems	4304437
96- well optical reaction plate	Applied Biosystems	4306737
Optical adhesive covers	Applied Biosystems	4311971
5X First strand buffer	Invitrogen	Y00146
dNTP	Invitrogen	18427-088
DTT	Invitrogen	Y00147
RNase out	Invitrogen	10777-019
SuperScript II reverse transcriptase	Invitrogen	18064-014
Random Hexamers	Invitrogen	48190-011

F. PRACTICAL TIPS FOR REAL- TIME PCR AND THE ABI PRISM 7000

1. Planning the experiment- Plan in advance the way in which wells in the 96- well PCR plate are to be utilized. Each sample should be run in triplicate. Use a planning sheet as shown below.

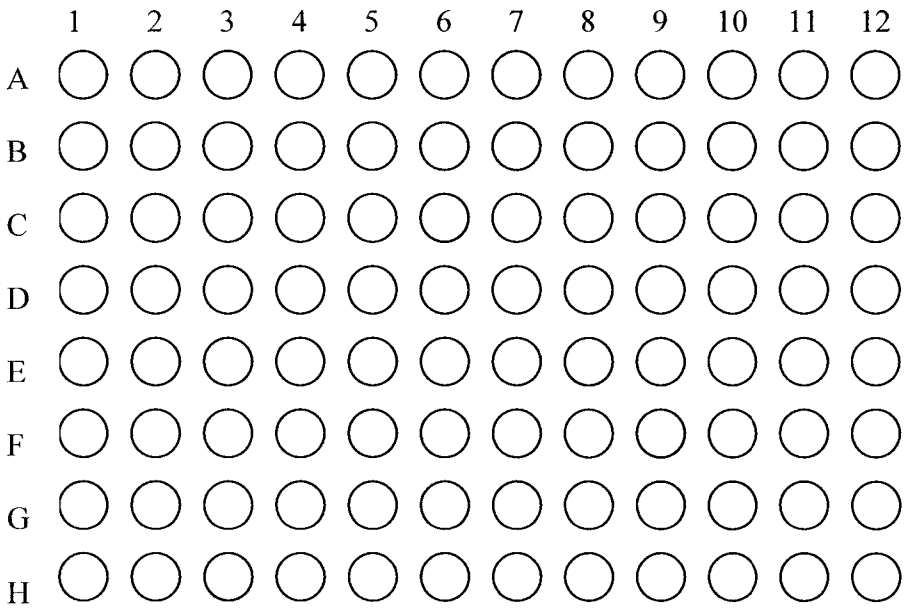

96 Well Template

2. Optical film- After loading the wells, carefully place the optical film on top, avoiding touching any of the surfaces of the film. Any grease or powder from the gloves can distort results. To handle the film touch only the corners of the perforated strips on the two ends. After placing the film, seal the plate by running the plastic wedge over the film a few times. Tear off the perforated strips on either ends.

3. Centrifugation- Centrifuge the plate at 1000 rpm (183 rcg) in the Beckman Microplus Carrier for about 5-6 seconds.

4. Compression pad- Place rubber compression pad on the plate. Even though there is no special recommendation for the use of the compression pad with the ABI Prism 7000, it is better to use it. Evaporation of the samples is seen in the peripheral wells of the plate if the pad is not used.

5. Using the ABI Prism 7000

    a. Turn on the instrument before turning the computer.
    b. Launch the ABI Prism 7000 SDS software.
    c. Remember to always to set the volume of reaction in each well in case you are using 25µl. (The default is set at 50 µl).
    d. Before running your plate it is advisable to do a background snapshot for all filters A to D. From the main toolbar click on "Instrument"→ "Calibrate"→ "Snapshot".

6. Always remember to remove the plate after the run is over and turn- off the instrument and computer. Do not leave the ABI Prism on.